Posted 665

GEORGIA INSTITUTE OF TECHNOLOGY
OFFICE OF RESEARCH ADMINISTRATION

RESEARCH PROJECT INITIATION

Date: March 3, 1975

Project Title: National Wind Energy Statistics for Large Arrays of Aerogenerators

Project No: E-16-665

Principal Investigator: Dr. C. G. Justus

Sponsor: National Science Foundation

Agreement Period: From 1/15/75 Until 6/30/76*

*12 month budget period plus 6 months for submission of required reports, etc.

Type Agreement: Grant No. AER75-00547

Amount: $65,700 NSF
3,475 GIT (E-15-354)
$69,175 Total

Reports Required: Annual Letter Technical, Final Report

Sponsor Contact Person (s):

Administrative Matters
thru ORA
Mr. Gaylord L. Ellis
Grants Officer
National Science Foundation
Washington, D. C. 20550
(202) 632-5965

Assigned to: Aerospace Engineering

COPIES TO:

- Principal Investigator
- School Director
- Dean of the College
- Director, Research Administration
- Director, Financial Affairs (2)
- Security-Reports-Property Office
- Patent Coordinator
- Library
- Rich Electronic Computer Center
- Photographic Laboratory
- Project File
- Other

RA—3 (6—71)

OFFICE OF CONTRACT ADMINISTRATION

SPONSORED PROJECT TERMINATION

Date: September 16, 1976

Project Title: Wind Energy Statistics for Large Arrays of Wind Turbines

Project No: E-16-665

Project Director: Dr. C. G. Justus

Sponsor: National Science Foundation

NSF Grant – No Property Actions @ HL

Effective Termination Date: 6/30/76

Clearance of Accounting Charges: 6/30/76

Grant/Contract Closeout Actions Remaining:

- _ Final Invoice and Closing Documents
- X Final Fiscal Report
- _ Final Report of Inventions
- _ Govt. Property Inventory & Related Certificate
- _ Classified Material Certificate
- _ Other _____

Assigned to: Aerospace Engineering (School/Laboratory)

COPIES TO:

- Project Director
- Division Chief (EES)
- School/Laboratory Director
- Dean/Director–EES
- Accounting Office
- Procurement Office
- ✓ Security Coordinator (OCA)
- Reports Coordinator (OCA)
- Library, Technical Reports Section
- Office of Computing Services
- Director, Physical Plant
- EES Information Office
- Project File (OCA)
- Project Code (GTRI)
- Other _____

CA–4 (3/76)

RANN DOCUMENT NO. NSF/RA-76-0191

ERDA/NSF-00547/76/1

UC-60

WIND ENERGY STATISTICS FOR LARGE ARRAYS OF WIND TURBINES (NEW ENGLAND AND CENTRAL U.S. REGIONS)

FINAL REPORT

C. G. Justus, Principal Investigator
School of Aerospace Engineering
Georgia Institute of Technology
Atlanta, GA 30332

August 1976

Prepared for

The National Science Foundation

Grant AER 75-00547

AS A PART OF THE FEDERAL WIND ENERGY PROGRAM

ADMINISTERED BY THE UNITED STATES ENERGY

RESEARCH AND DEVELOPMENT ADMINISTRATION

DIVISION OF SOLAR ENERGY

Abstract

The performance characteristics have been simulated for large dispersed arrays of 500 kW - 1500 kW wind turbines producing power and feeding it directly into the utility distribution grid in the New England - Middle Atlantic and the Central U.S. regions. These studies show that, in New England, arrays of 500 kW generators could produce (on an annual average basis) from 190 to 240 kW per generator, with Central U.S. average output being about 200 kW per 500 kW generator, annual average. Output from arrays of 1500 kW generators (similar in design to the new ERDA Mod 1 unit) would produce 240 to 340 kW per generator in New England and about 325 kW in the Central U.S. Best output was estimated from a 1125 kW design which had larger blades and lower cut-in and rated speed than the 1500 kW unit. The 1125 kW machine would average about 460 kW on an annual basis in the Central U.S.

Despite comparable wind regimes in coastal New England and in the Central U.S., wind power is potentially closer to being cost-effective as a fuel saver in New England. This is because of the heavy reliance on expensive fuels in New England as compared with the Central U.S. area. Details of cost-effectiveness as a fuel saver will depend on the reliability with which wind can displace the expensive peak load fuels. Dispersal of the wind turbines into large arrays enhances this reliability. Power levels of 200 kW per 1500 kW generator were found to have reliability (without storage) as high as 60% in New England and over 75% in the Central U.S. Power output reliability of 200 kW per generator for the 1125 kW wind turbines ranged seasonally from 77% to 93% in the Central U.S.

By array power return time analysis, it is estimated that 24 to 48 hours of storage would increase the power reliability of 200 kW per 1500 kW generator to about 95% in New England, and to better than 95% in the Central U.S. For the 1125 kW unit in the Central U.S., 24 hours storage would increase the reliability of 200 kW per generator to about 99%.

Preliminary analysis of diurnal cycles of monthly mean winds versus time of day shows that in both New England and the Central U.S., there is a strong summertime afternoon peak in available wind, which would correspond to the summertime peak air conditioning load. This correspondence of available wind power with peak load may mean that even better peak load displacement, reliability, and cost-effectiveness as a fuel saver might be achieved than indicated by the diurnally averaged results reported here.

TABLE OF CONTENTS

LIST OF FIGURES

LIST OF TABLES

DISCLAIMER

The purpose of this report is to study the expected performance of various designs of wind turbines and the influence of meteorological variability and spatial wind diversity on that performance. For purposes of the study, wind turbine designs which have been proposed by several commercial companies have been used. None of these wind turbine designs has been actually constructed, and so the performance results discussed here are only the analytically expected results, based on the respective power output curve characteristics of these machines. As a convenient method of referring to the various designs studied, which are specified in Table A-1, the wind turbines are designated by the company which proposed the design and the rated power of the wind turbine. These references to company names do not imply in any way that actual wind turbines which might be produced by one or the other of these companies would have either the costs or the performance characteristics used in this report. Furthermore, no statement in this report should be construed as a recommendation of one company's design over another, since all references in this report to company designs are merely used as a convenient method for specifying a wind turbine of the specific operating characteristics (cut-in speed, rated speed, etc.) as the designs given in Table A-1. It is hoped that the results in this report will be useful to all potential wind turbine manufacturers to improve their designs where possible in order to obtain optimum energy output performance.

When interpreting the results reported here it should also be kept in mind that the airport wind data locations were selected for easy data availability. They are not necessarily representative of the actual wind environments in which real wind turbines would be operated nor are they representative of the wind environments for which the machine designs were optimized.

1. INTRODUCTION

The purpose of this study is to evaluate and analyze the wind energy output statistics of realistically simulated arrays of wind turbines in various regions of the contiguous 48 states of the U.S. Two regions were selected for study: 1) the New England-Middle Atlantic area composed of Maine, New Hampshire, Vermont, Massachusetts, Connecticut, Rhode Island, New York, New Jersey, and Pennsylvania, and 2) the West Central area composed of Nebraska, Kansas, Missouri, Oklahoma, and Texas. National Weather Service tape data on wind speeds at three hour intervals have been obtained for 28 sites in the New England-Middle Atlantic area of study for the five years 1965-1969, and for 25 sites in the West Central area of study for the five years 1969-1973.

Appendix A describes how the data were processed and the method of analysis used. Briefly, time series of one minute average winds, measured once every three hours, were extrapolated to a uniform wind turbine hub height, and linear interpolation was used to fill in one or two observation gaps in the data.

Measured one minute average winds, adjusted to hub height, are used in power output curves (e.g. Figure A-1, Appendix A) to compute "instantaneous" power output from the simulated wind turbines. One minute average winds are preferable to hourly average because a one minute period more nearly represents the power output response time of the wind turbines being simulated. The one minute values every three hours are looked on as a more-or-less random sample of the wind data over the five year period of study. The power output curve characteristics were determined from parameters given in Table A-1. Simultaneous values of power output from a collection of National Weather Service sites were then combined at each time to simulate the power output of a widely dispersed array of wind turbines. All array power statistics are expressed in terms of power per array generator (see Appendix B). Hence, the simulated array can be considered as made up of wind energy "farms" of several wind turbines per site, with all generators at a given site being considered as 100% correlated.

For this particular study, the separate sites were each considered to have equal numbers of wind turbines, but this could easily be generalized (see Appendix B) to arrays made up of individual wind farms with unequal numbers of wind turbines at the separate farms.

The goals of this study are to determine and study:

- the operating statistics of single and arrayed wind turbines in the New England-Middle Atlantic and the Midwestern areas,
- the effects of locational and seasonal variations of average wind speed on wind turbine performance,
- the characteristics of inter-site correlations on the wind regime and the effects of these correlations on array performance for arrays of various sizes,
- the characteristics of time autocorrelations of wind speed, its influence by diurnal effects, its seasonal variations, its implications on adequacy of the three hour time spacing of data used,
- the mean values and seasonal variation of power output from several potential designs of wind turbines of the 500 kW to 1500 kW size, including their potential cost-effectiveness as fuel savers in the New England and Midwestern areas,
- the degree to which reliability of wind power can be increased (at various power output levels) by the use of large dispersed arrays of wind turbines (without resort to storage),
- the approximate amount of storage time required in order to reach 90% to 99% reliability of various power levels so that "credited power" can be provided by wind in the New England and Midwestern area.

The following two sections discuss separately the results of the studies in the New England-Middle Atlantic area and the Midwestern area. A final section discusses some general conclusions of the study.

2. NEW ENGLAND - MIDDLE ATLANTIC AREA

The New England and Middle Atlantic Federal Power Commission Regions include Maine, New Hampshire, Vermont, Massachusetts, Rhode Island, Connecticut, New York, Pennsylvania, and New Jersey. An area of study was selected which includes 28 sites, with some sites in each of these states, as shown in Figure 1, and listed in Table 1. Winds for the period 1965-1969 were analyzed as described in Appendix A. All winds were adjusted to a common wind turbine hub height of 42.7 m (140 ft), consistent with that designed for the majority of wind turbines studied. Power outputs from 5 different simulated wind turbine designs were evaluated and studied: the GE 500 kW, GE 1500 kW, Kaman 500 kW, Kaman 1500 kW, and Boeing 1000 kW designs (see Table A-1, Appendix A).

In addition to the full 28 site array, three sub-groups of sites were considered as smaller arrays: the New England inland array (13 sites shown as open circles in Figure 1), the Middle Atlantic inland array (8 sites shown as open triangles in Figure 1), and the coastal array (7 sites shown as solid dots in Figure 1).

Wind Statistics

Table 2 shows monthly mean wind speeds for each of the 28 New England-Middle Atlantic sites for the seasonal months of January, April, July and October. Mean speeds were evaluated by averaging over corresponding months for the five year period of record. Standard deviations in Table 2 are rms deviations of individual year monthly site mean speed from the 5 year average monthly

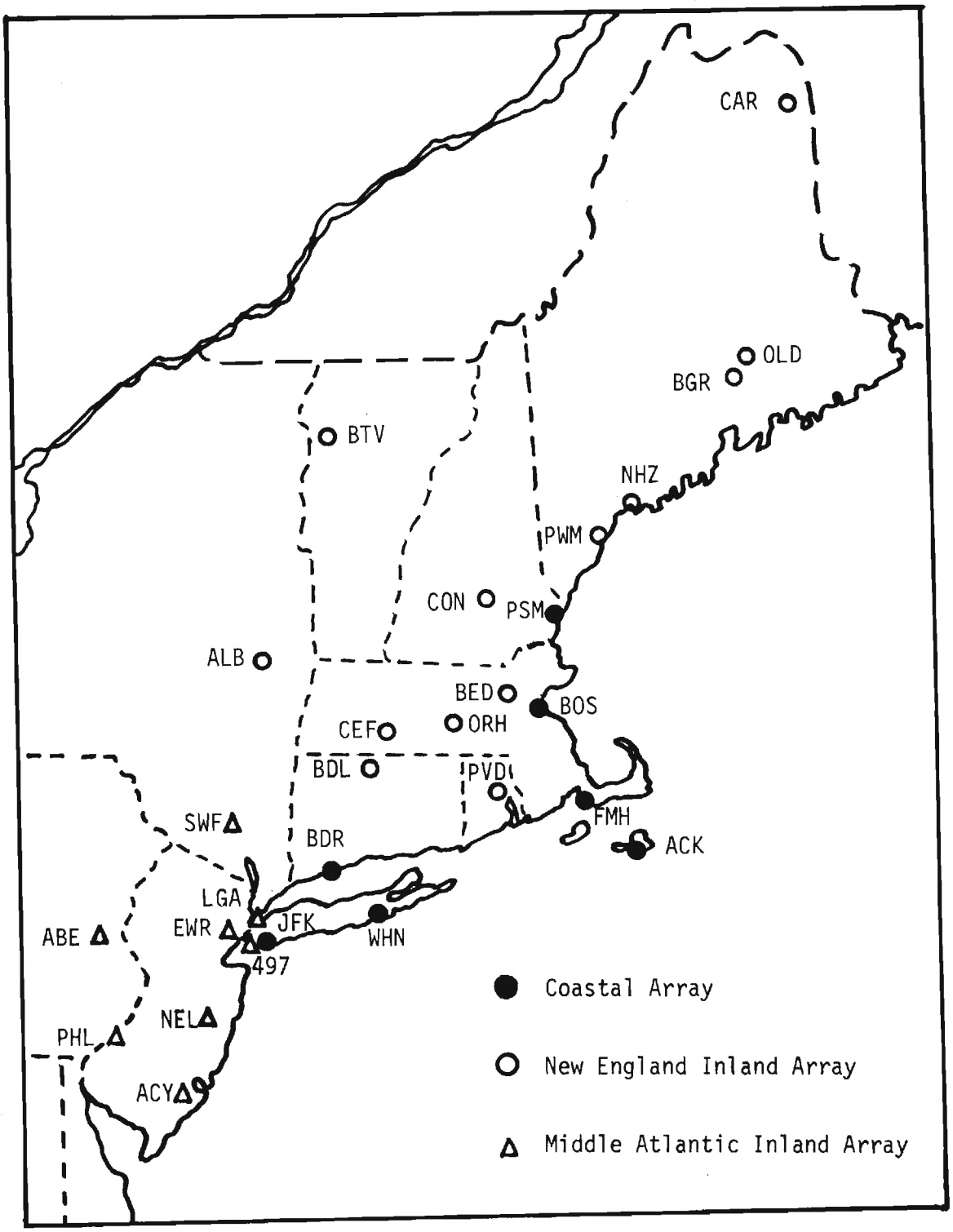

Figure 1 - Map of New England - Middle Atlantic Area Array Sites, Showing Three Sub-Group Arrays Studied Separately.

TABLE 1

Site Names for the New England - Middle Atlantic Area Sites

ABE	Allentown, PA	FMH	Falmouth, MA
ACK	Nantucket, MA	JFK	New York (J. F. Kennedy), NY
ACY	Atlantic City, NJ	LGA	New York (Laguardia), NY
ALB	Albany, NY	NEL	Lakehurst, NJ
BDL	Windsor Locks, CT	NHZ	Brunswick, ME
BDR	Bridgeport, CT	OLD	Oldtown, ME
BED	Bedford, MA	ORH	Worcester, MA
BGR	Bangor, ME	PHL	Philadelphia, PA
BOS	Boston, MA	PSM	Portsmouth, NH
BTV	Burlington, VT	PVD	Providence, RI
CAR	Caribou, ME	PWM	Portland, ME
CEF	Chicopee, MA	SWF	Newburgh, NY
CON	Concord, NH	WHN	Westhampton, NY
EWR	Newark, NJ	497	New York (Floyd Bennett), NY

TABLE 2

Mean wind speed $\bar{V}$ at the 43 m (140 ft) level. $\bar{v}$ is average over five years. σ is standard deviation of monthly averages about the five year monthly mean.

	JAN		APR		JUL		OCT	
Site	$\bar{V}$, m/s	σ, m/s	$\bar{V}$, m/s	σ, m/s	$\bar{V}$, m/s	σ, m/s	$\bar{V}$, m/s	σ, m/s
ABE	6.9	1.0	6.7	0.8	4.8	0.5	5.6	0.2
ACK	9.4	0.5	9.1	1.1	6.9	0.5	8.3	0.2
ACY	7.9	1.5	7.6	0.4	6.2	0.6	6.7	0.5
ALB	6.9	0.7	7.0	0.5	5.3	0.4	5.6	0.2
BDL	6.4	0.5	7.0	1.2	5.6	0.4	8.3	0.2
BDR	7.2	1.1	6.5	0.7	5.2	0.4	6.7	0.5
BED	5.7	0.8	5.7	0.5	4.4	0.5	5.9	0.8
BGR	5.6	0.9	6.0	0.7	4.7	0.8	5.9	0.4
BOS	9.3	0.6	9.3	1.4	8.1	0.4	6.4	0.7
BTV	6.2	0.8	6.4	0.6	5.7	0.6	4.6	0.2
CAR	7.1	0.6	7.1	0.4	6.4	0.7	4.8	0.4
CEF	5.1	0.8	5.6	1.0	3.8	0.6	8.3	0.6
CON	5.1	0.9	5.1	0.4	4.0	0.6	6.4	0.7
EWR	7.8	1.3	7.5	0.7	6.4	0.7	6.7	0.5
FMH	7.6	0.5	7.9	1.6	6.3	0.6	4.0	0.8
JFK	8.5	1.0	8.2	0.7	7.0	0.5	4.3	0.4
LGA	8.5	0.6	7.8	0.7	6.8	0.2	6.9	0.6
NEL	5.2	0.8	4.9	0.5	3.4	0.2	6.7	1.0
NHZ	5.0	1.0	5.9	0.4	4.7	0.1	7.6	0.4
OLD	4.2	0.5	5.0	0.6	3.7	0.1	7.4	0.2
ORH	7.9	1.0	7.2	0.7	5.7	0.5	3.7	0.6
PHL	7.2	1.2	7.1	0.3	5.6	0.3	4.5	0.4
PSM	6.2	0.9	6.2	0.9	5.3	0.6	4.0	0.2
PVD	7.6	0.9	8.0	0.7	6.4	0.3	6.5	0.7
PWM	5.5	0.9	5.9	0.4	4.9	0.5	6.2	0.4
SWF	5.0	1.0	5.2	0.7	3.9	0.8	4.6	0.8
WHN	7.2	1.1	6.7	0.6	5.5	0.9	5.6	0.5
497	6.8	0.7	6.6	0.6	5.6	0.2	5.7	0.6
AVG	6.8	0.8	6.8	0.6	5.5	0.3	5.9	0.4

mean speed. Table 2 shows the best sites of the 28 to be Boston (BOS) and Nantucket (ACK). In general the coastal array sites are better (i.e. windier) than those in the other two subgroups.

Table 3 and Figure 2 show data on the array average monthly mean speed (speeds averaged over all the sites in the array) for the full 28 site array and for the 7 site Coastal array. Standard deviations in Table 3 are the rms deviations of individual year monthly mean array wind speed from the 5 year average array mean wind speed. These results show similar seasonal variations for the full array and for the coastal array, with peak monthly mean winds in February and lowest monthly mean winds in August and September. The coastal array consistently has winds which average about 1 m/s higher on a monthly array average basis.

Time Autocorrelation

Examples of time autocorrelation functions, computed as described in Appendix A, are shown in Figures 3 and 4. There is a striking difference between these two figures, which show a strong influence of diurnal effects in July and almost complete lack of diurnal influence in January. The individual year curves in Figures 3 and 4 are remarkably consistent with each other in their indications of the degree of this diurnal influence. Examination of time autocorrelation for other months of the year (not shown) indicates intermediate degrees of diurnal influence, between the extremes indicated in Figures 3 and 4. The fact that time autocorrelations remain high (50% to 80%) over a time displacement of three hours is an indication that the three hour spacing of the input wind data is adequate to resolve the important diurnal variations, at least in a statistical average sense. Further study of this point is planned with selected sites of one hour time series data.

Spatial Cross Correlation

Meteorological studies of space and time correlation have tended to emphasize upper air levels (500 mb and higher) (Buell, 1960, 1972; Panchev and Syrakova,

TABLE 3

Five Year Monthly Mean Wind Speed $\bar{V}$ at the 43 m (140 ft) Level for Full Array and Coastal Array. σ is Standard Deviation of Monthly Averages about Five Year Monthly Mean.

Month	28 Site Full Array		7 Site Coastal Array	
	$\bar{V}$, m/s	σ, m/s	$\bar{V}$, m/s	σ, m/s
JAN	6.8	0.8	7.9	0.7
FEB	7.1	0.5	8.2	0.7
MAR	6.8	0.5	7.8	0.5
APR	6.8	0.6	7.7	0.9
MAY	6.5	0.5	7.4	0.5
JUN	5.7	0.1	6.8	0.3
JUL	5.5	0.3	6.3	0.4
AUG	5.4	0.2	6.3	0.3
SEP	5.4	0.5	6.3	0.4
OCT	5.9	0.4	6.9	0.4
NOV	6.2	0.3	7.3	0.5
DEC	6.6	0.7	7.7	0.8
---	---	---	---	---
ANN	6.2	0.6	7.2	0.7

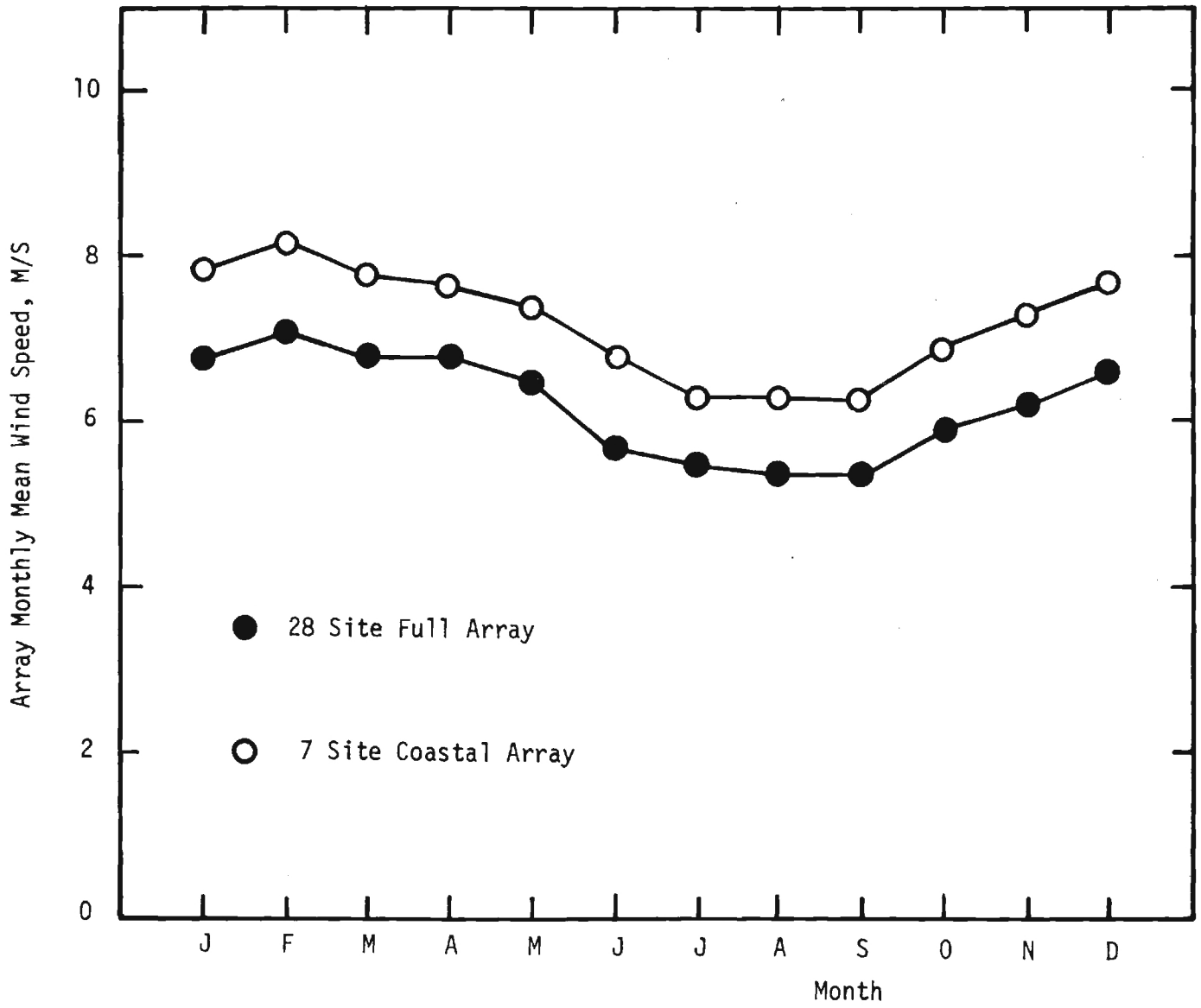

Figure 2 - Seasonal Variation of Array Average Mean Wind Speed at Wind Turbine Hub Height of 43 m (140 ft) for New England - Middle Atlantic Arrays.

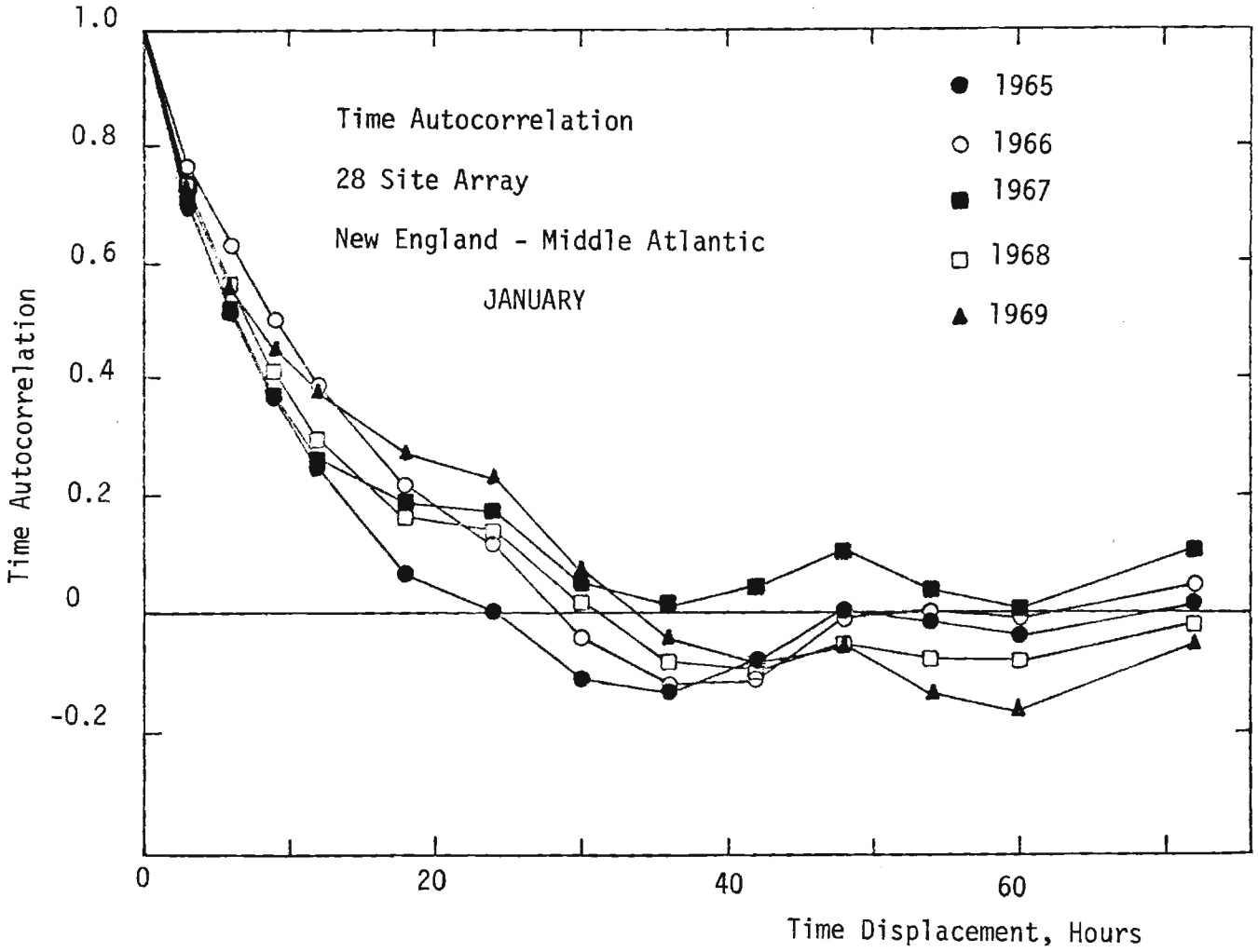

Figure 3 - Time Autocorrelation in January for the 28 Site Full Array (New England - Middle Atlantic Area)

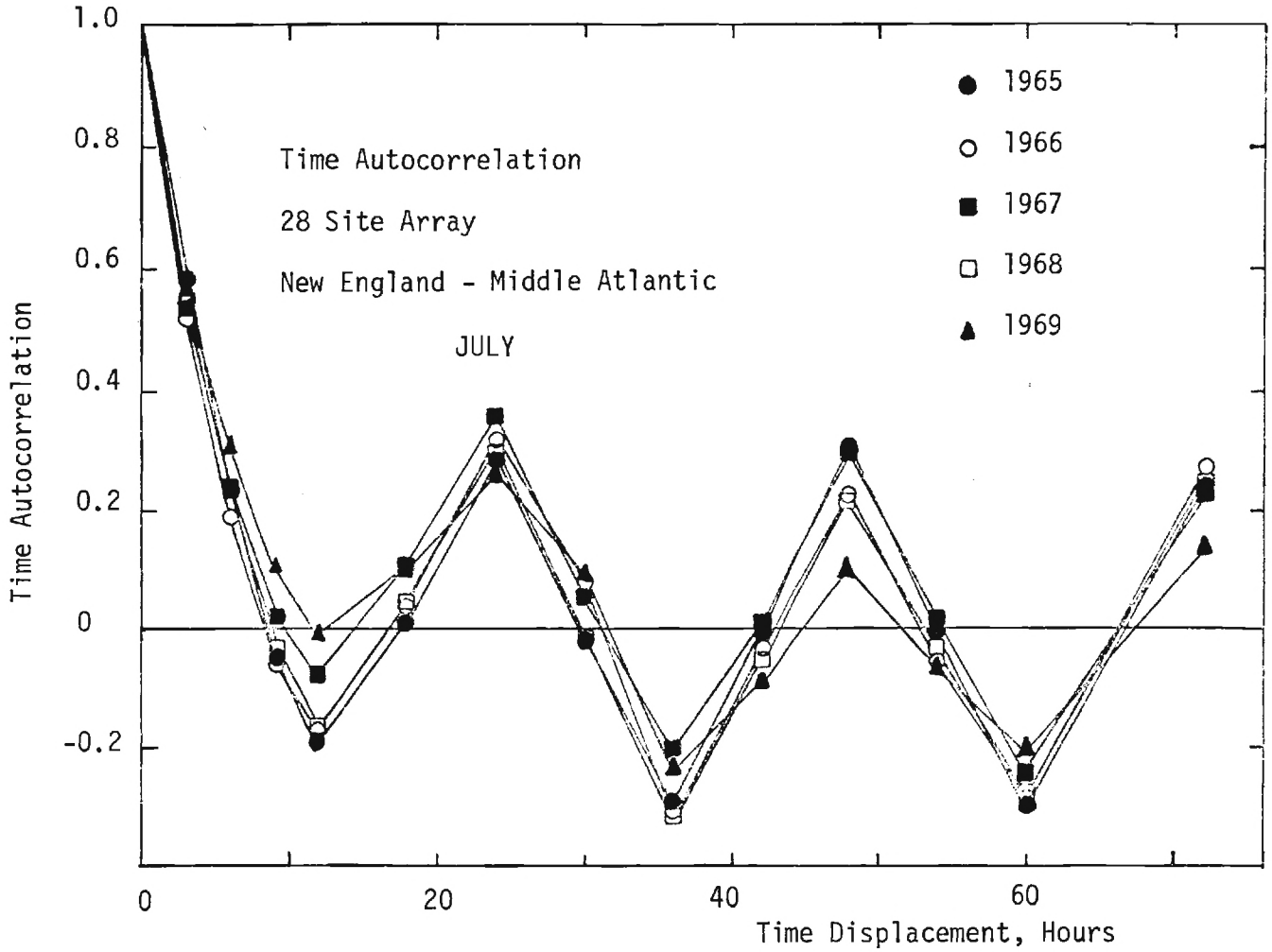

Figure 4 - Time Autocorrelation in July for the 28 Site Full Array (New England - Middle Atlantic Area)

1975; Seaman and Draudins, 1975). For the problem of space and time correlations relevant to wind power studies, namely correlation of wind speed residuals from mean speeds, only the spatial correlation work of Ballester (1961) is known to this author to be directly applicable.

Spatial cross correlation of wind speed departure from the monthly mean were computed as a function of inter-site separation, as described in Appendix A. Figures 5 and 6 show two examples of cross correlation as a function of separation for the full 28 site array. In these figures all correlation values were averaged together by intervals of 50 km in separation (i.e. all 0-50 km separations averaged, all 50-100 km separations averaged, etc.). The number of site pairs in the 0-50 km separation interval was 10, with 33 between 50 and 100 km, and 43 between 100 and 150 km. The number per 50 km interval then gradually decreased to 31 between 400 and 450 km, 17 between 450 and 500 km, and again decreased gradually to 7 between 750 and 800 km, with only 2 per 50 km interval beyond 800 km.

Figures 5 and 6 show correlations beginning well below one at the first separation interval, then gradually decreasing with separation. No zero or negative correlations are observed out to the maximum separation distances (1000 km). There is an indication of seasonal differences in correlation behavior in that the July curve (Figure 6) starts at lower correlation (65% at 25 km, versus 75% for January) and that the July correlations then decrease less rapidly with distance (the July average correlation remaining about 30% at 1000 km while the January curve falls to about 25% at 1000 km).

The average effective cross correlation for an array is found by averaging over all the individual site pair cross-correlations, regardless of separation. Table 4 and Figure 7 show that effective array correlations are higher for the smaller arrays, being highest for the Middle Atlantic inland array (average site separation 111 km) and lower as array average site separation increases, the correlation being lowest for the full 28 site array (average site separation 309 km). Average site separation is defined as the mean of the separation distances (magnitude only) between all site

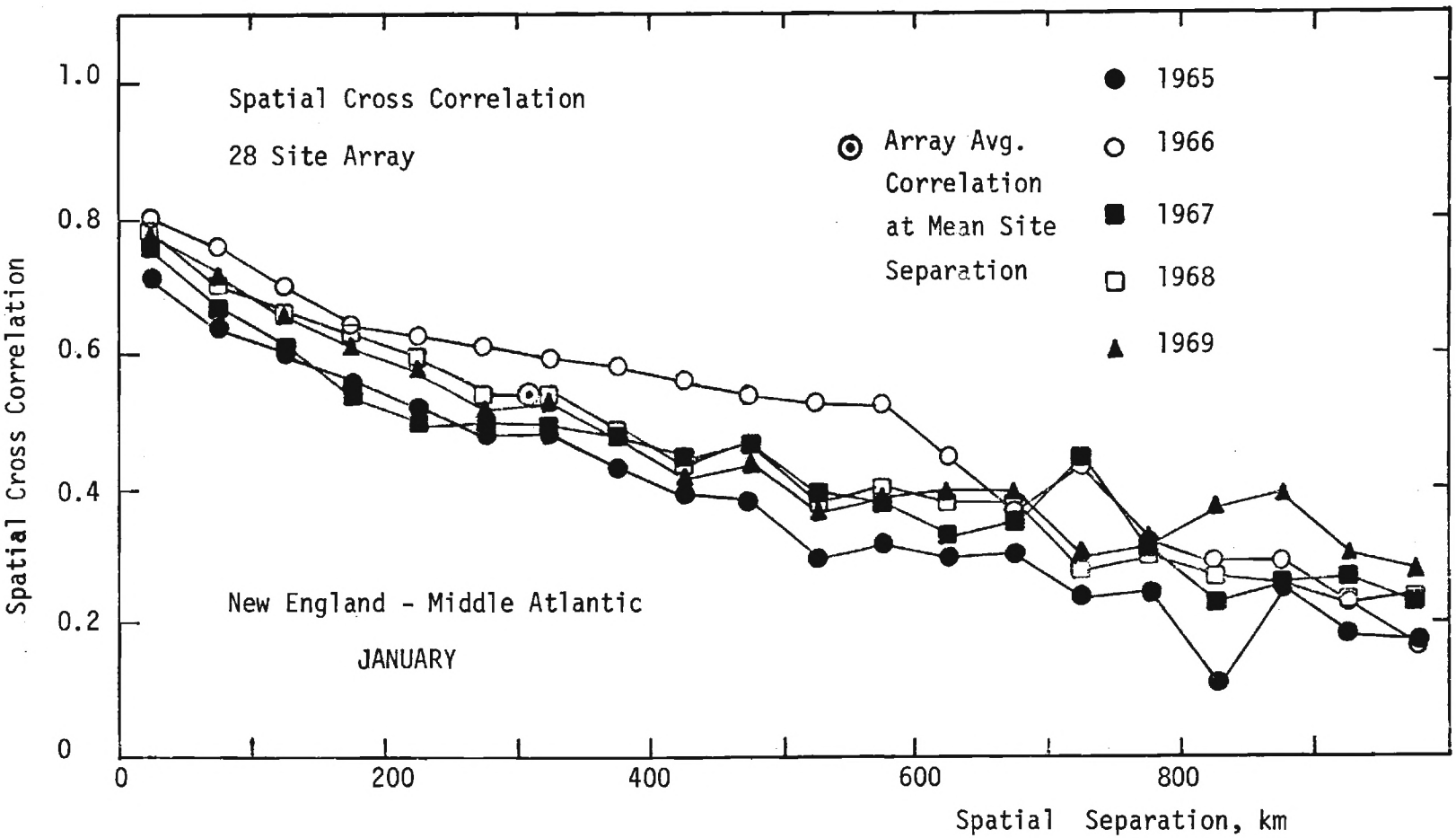

Figure 5 - Spatial Cross Correlation Versus Site Separation for 28 Sites New England - Middle Atlantic Array in January.

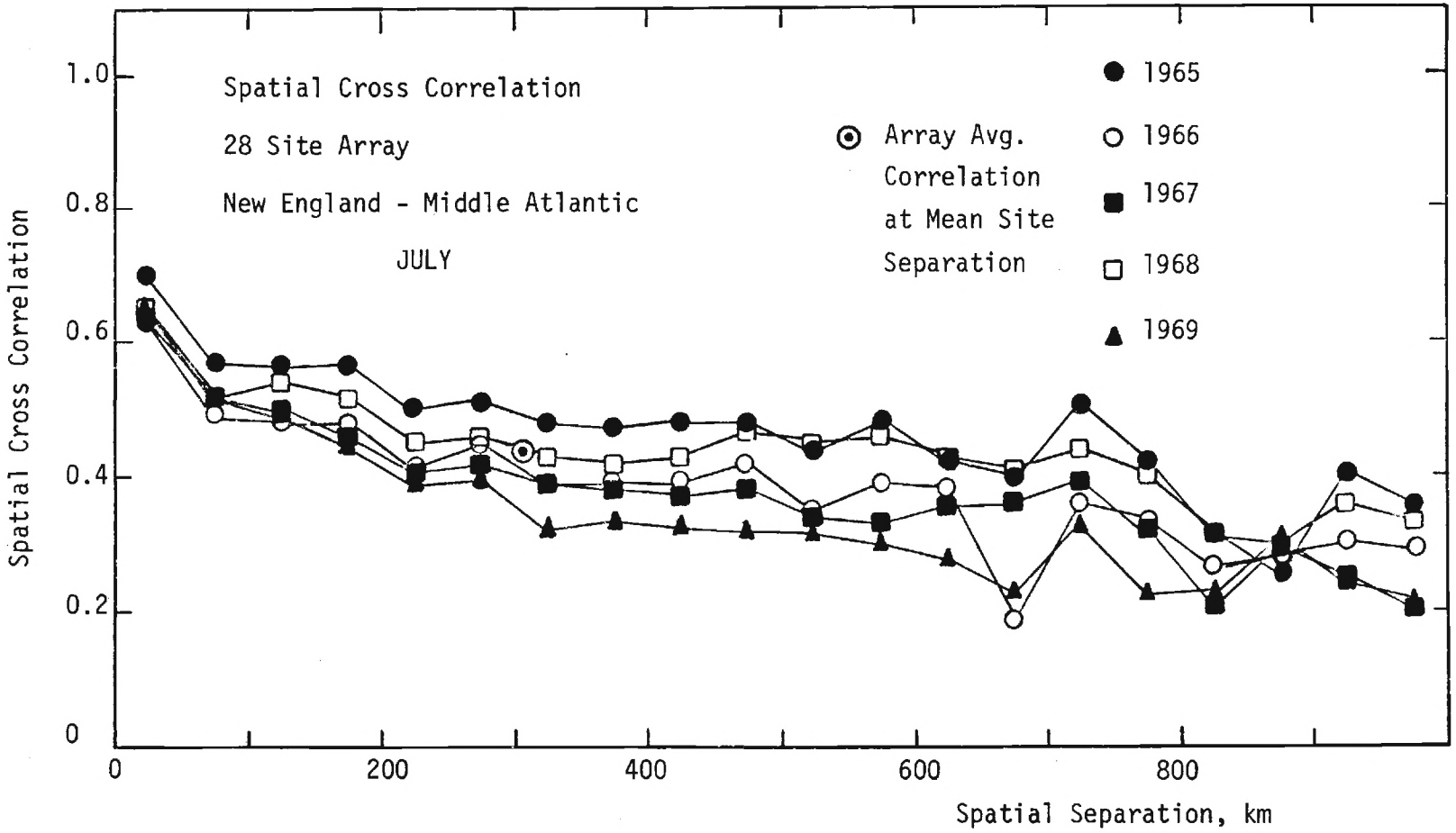

Figure 6 - Spatial Cross Correlation Versus Site Separation for 28 Site New England - Middle Atlantic Array in July.

TABLE 4

Average Cross Correlations for the four arrays. $\bar{\rho}$ is 5 year monthly average. σ is standard deviation of the monthly averages about the 5 year monthly mean. $\bar{r}$ is mean inter-site separation for the array.

Month	28 Site Full Array $\bar{r}$ = 309 km		13 Site New England Array $\bar{r}$ = 284 km		7 Site Coastal Array $\bar{r}$ = 198 km		8 Site Middle Atlantic Array $\bar{r}$ = 111 km	
	$\bar{\rho}$	σ	$\bar{\rho}$	σ	$\bar{\rho}$	σ	$\bar{\rho}$	σ
JAN	0.54	0.05	0.54	0.05	0.64	0.05	0.68	0.05
FEB	0.58	0.05	0.57	0.05	0.64	0.06	0.71	0.02
MAR	0.50	0.06	0.52	0.05	0.58	0.05	0.69	0.06
APR	0.48	0.05	0.51	0.05	0.53	0.05	0.62	0.05
MAY	0.45	0.08	0.49	0.05	0.51	0.10	0.59	0.06
JUN	0.43	0.04	0.44	0.05	0.48	0.05	0.54	0.03
JUL	0.45	0.05	0.49	0.04	0.47	0.05	0.51	0.03
AUG	0.45	0.04	0.48	0.03	0.48	0.06	0.53	0.03
SEP	0.47	0.04	0.50	0.01	0.53	0.05	0.61	0.06
OCT	0.53	0.05	0.53	0.04	0.59	0.06	0.65	0.03
NOV	0.54	0.01	0.54	0.01	0.60	0.02	0.69	0.03
DEC	0.53	0.06	0.52	0.05	0.61	0.06	0.69	0.06
ANN	0.50	0.05	0.51	0.03	0.56	0.06	0.63	0.07

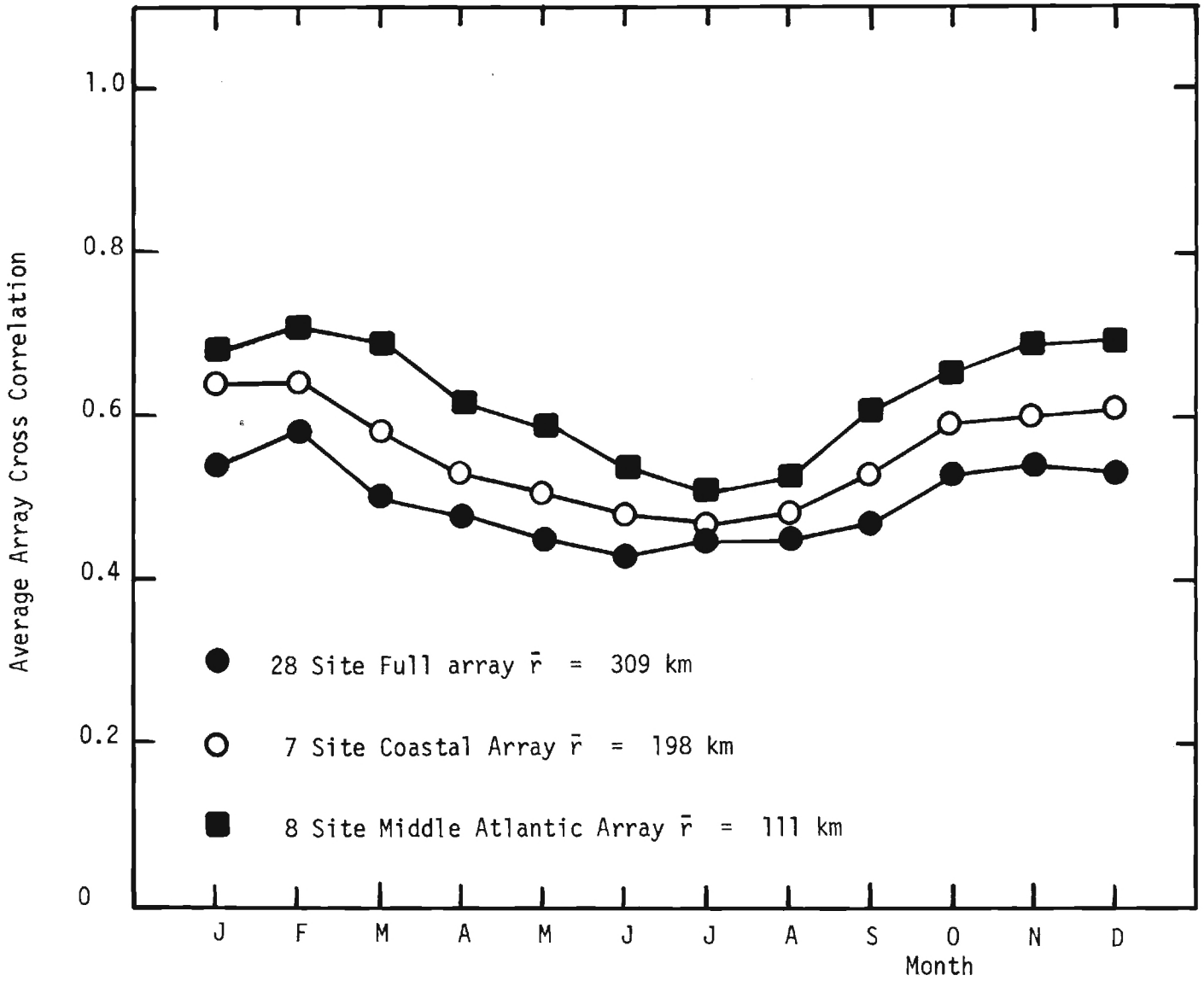

Figure 7 - Seasonal Variation of Average Array Cross Correlation for New England - Middle Atlantic Arrays.

pair combinations in the array. Table 4 and Figure 7 also show that there is considerable seasonal variation of array effective cross correlation. The phase of this seasonal variation corresponds approximately to the phase of the seasonal variation of the mean wind speed, with a maximum correlation in February (though the minimum correlation is in July, whereas the wind speed minimum is August or September). Since low cross correlations are desirable in order to maximize reliability (see Appendix B this coincident phase of winds and correlations mean, unfortunately, that higher winds are associated with higher (less favorable) correlations while lower (more favorable) correlations are associated with lower seasonal winds.

The apparent rapid fall-off of correlation over separations less than 25 km (apparent in Figures 5 and 6) is an interesting phenomenon which could have contributions from three effects: 1) anemometer measurement error such that two instruments side by side would not show full 100% correlation, 2) small scale turbulence (scale $\leq$ 100 to 1000 m), and 3) mesoscale wind variations (scale less than 25 km). It should be noted that, for one minute average winds, some of the turbulence will have been filtered out in the averaging process. If one calls the 25 km separation average correlation ρ_o, then the 5 year annual average value of ρ_o in the New England-Middle Atlantic area was found to be 72%, with a maximum ρ_o in February which averaged 78% over the 5 years, and a minimum ρ_o in July, of 65%. If the anemometer errors have an rms magnitude of σ_e, the turbulence (remaining after one minute average filtering) has an rms magnitude σ_t, and mesoscale (< 25 km) effects have an rms magnitude of σ_m, then the correlation at about 25 km should be

$$\rho_o = 1 - (\sigma_e^2 + \sigma_t^2 + \sigma_m^2)/\sigma_T^2 \qquad (1)$$

where σ_T is the total rms deviation of winds from the monthly mean. If we call σ_o the combined effect of error, turbulence, and mesoscale effects ($\sigma_o^2 = \sigma_e^2 + \sigma_t^2 + \sigma_m^2$), then the above mentioned correlation values ρ_o would imply an average February value for σ_o of 1.8 m/s, 1.5 m/s for July, and σ_o = 1.6 m/s on an annual average basis.

Clearly these values are too large to have been contributed completely from the error source, but they are reasonable values to have come from a combination of error and turbulence. Hence the contribution σ_m from mesoscale effects is relatively small (e.g. $\leq$ about 1 m/s). If the assumption of an rms error of σ_e = 0.5 m/s is made, and it is also assumed that σ_t is 15% of the monthly mean speed (i.e. $\sigma_t \simeq$ 1 m/s), then σ_m would be about 1.2 m/s, based on the observed values of ρ_o. These assumed values of σ_e and σ_t would imply that the spatial cross correlation remains about 97% for two anemometers side by side (error influence only). This estimate comes from the approximate relation

$$\rho_e = 1 - \sigma_e^2/\sigma_T^2 \qquad (2)$$

for correlation influenced only by error. The correlation would fall to about 88% over a separation of the order of 100 m (e.g. up to a few hundred meters) under the combined influence of error and turbulence. This comes from evaluation of the approximate relation

$$\rho_t = 1 - (\sigma_e^2 + \sigma_t^2)/\sigma_T^2 \qquad (3)$$

for correlation influenced by error and turbulence. The total rms magnitudes σ_T used in (2) and (3) were found to be a maximum (3.7 m/s) in February, and a minimum (2.6 m/s) in July, in phase with the seasonal variation in ρ_o and mean winds.

Comparison of the spatial correlations presented here with the results of Ballester (1961), show that the later indicate higher correlation (83 to 92%) in the separation regions 19 to 73 km. However, Ballester apparently correlated wind speed deviations from a continuous 50 or 54 month record. Hence, his results would still contain seasonal variations which would be highly correlated between sites. It is also not clear whether Ballester correlated "instantaneous" speeds, one minute average speeds, one hour average speeds or some other parameter.

Mean Output Wind Power

One minute average winds, adjusted to 42.7 m (140 ft) hub height, were used in power output curves (see Appendix A) to compute instantaneous output power from 5 different designs of wind turbine: GE 500 kW, GE 1500 kW, Kaman 500 kW, Kaman 1500 kW, and Boeing 1000 kW. Output power from these wind turbines was averaged over one month intervals, and corresponding months over 5 years (1965-1969) were averaged to yield monthly mean power output. Monthly mean power for each array - 28 site full array, 7 site coastal array, New England inland array, and Middle Atlantice inland array - were studied separately. Table 5 and Figure 8 show observed seasonal variation of monthly mean power output from the five wind turbines simulated, for the 28 site full array. Table 6 and Figure 9 show corresponding data for the coastal array - the best performance area of the array groups. In addition to monthly mean (5 year average) output power, Tables 5 and 6 also show standard deviations of individual year monthly average power about the 5 year mean, and the maximum and minimum individual year monthly mean out of the set of 5 years. The bottom lines in Tables 5 and 6 show annual average, standard deviation, maximum and minimum in kW and also expressed as capacity factor (i.e. relative to the rated power of the wind turbine). Figures 8 and 9 show that the seasonal variations in mean output power follow in phase with the annual variations in monthly mean wind. The Kaman 1500 and GE 1500 wind turbines are much more sensitive to seasonal variations because of the necessity of higher winds for effective operation of these larger rated power machines. Note, for example, that for 6 months out of the year in the coastal array (and 9 months out of the year for the full 28 site array) the Kaman 1500 kW rated wind turbine produces no more average power than does the GE 500 kW rated machine. Steadiest annual power output is provided by the 1000 kW wind turbine, which produces higher power levels than the 500 kW machines during good winds, and (because of the relatively low cut-in and rated speeds) is less sensitive to seasonal variations than the 1500 kW machines.

Figures 10 through 13 show, for each of the GE and Kaman wind turbines, plots of: a) individual site monthly mean output power as a function of

TABLE 5

Monthly Mean Power Output from 28 Site Full Array. CF is Annual Capacity Factor
$\bar{P}$, σ, MAX and MIN Powers are in kW while C.F. in Relative to Rated Power.

	GE 500				GE 1500				KAMAN 500				KAMAN 1500				BOEING 1000			
	$\bar{P}$	σ	MAX	MIN	$\bar{P}$	σ	MAX	MIN	$\bar{P}$	σ	MAX	MIN	$\bar{P}$	σ	MAX	MIN	$\bar{P}$	σ	MAX	MIN
JAN	219	37	272	177	320	83	449	232	144	28	185	113	236	68	344	164	330	49	395	277
FEB	235	25	258	194	356	60	414	262	161	17	178	136	263	50	317	187	357	38	407	302
MAR	222	26	259	193	311	63	386	245	146	23	177	122	225	51	281	171	342	40	407	303
APR	218	31	259	182	290	75	402	210	140	26	177	109	206	62	301	141	339	40	385	290
MAY	203	26	238	178	253	65	347	185	127	24	159	102	176	52	252	121	321	41	372	280
JUN	159	10	171	148	158	15	178	138	89	7	98	81	103	11	116	88	250	16	270	230
JUL	143	20	162	109	130	27	154	86	77	13	89	55	82	18	99	53	221	34	253	165
AUG	141	14	164	124	127	25	167	96	76	11	93	63	81	18	109	59	219	25	258	189
SEP	143	27	176	111	144	45	197	101	81	20	105	60	95	32	132	65	222	46	280	170
OCT	172	21	206	150	202	43	272	160	104	17	132	86	139	32	192	108	268	34	322	231
NOV	189	14	208	170	246	31	291	210	120	11	135	106	175	25	212	146	292	20	317	267
DEC	212	38	250	154	299	89	405	168	139	33	178	90	217	72	304	113	324	53	373	239
ANN	188	35	272	109	236	82	449	86	117	30	185	55	166	65	344	53	290	52	407	165
C.F.	0.38	0.07	0.54	0.22	0.16	0.05	0.30	0.06	0.23	0.06	0.37	0.11	0.11	0.04	0.23	0.04	0.29	0.05	0.41	0.17

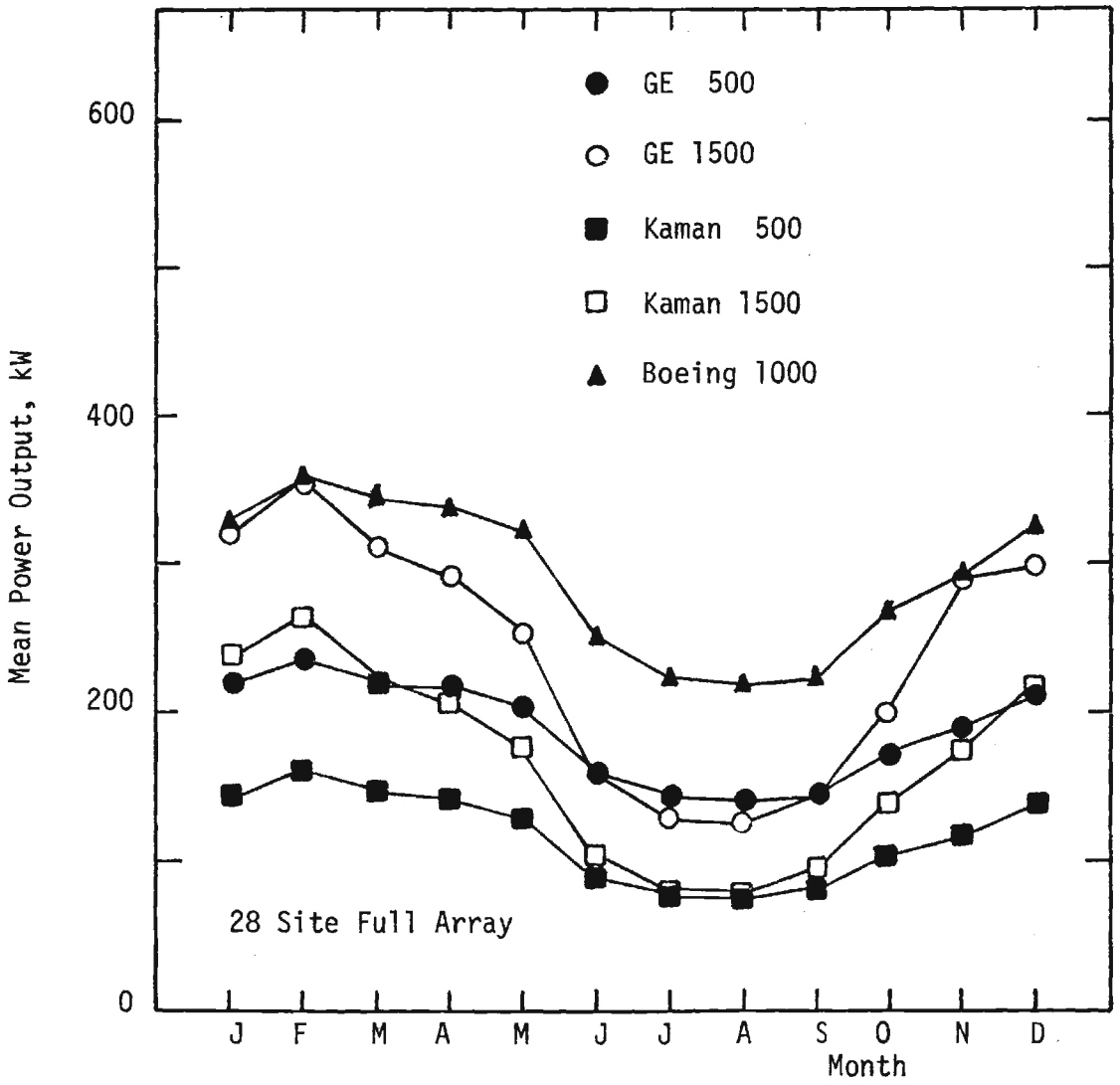

Figure 8 - Seasonal Variation of Monthly Mean Power Output for 28 Site Array in New England - Middle Atlantic Area.

TABLE 6

Monthly Mean Power Output from 7 Site Coastal Array. CF is Annual Capacity Factor.
$\bar{P}$, σ, MAX and MIN Powers in kW, while C.F. is Relative to Rated Power.

	GE 500				GE 1500				KAMAN 500				KAMAN 1500				BOEING 1000			
	$\bar{P}$	σ	MAX	MIN	$\bar{P}$	σ	MAX	MIN	$\bar{P}$	σ	MAX	MIN	$\bar{P}$	σ	MAX	MIN	$\bar{P}$	σ	MAX	MIN
JAN	274	35	313	233	437	91	544	341	187	28	224	157	329	78	428	247	406	42	471	361
FEB	290	34	317	231	489	97	588	337	206	29	231	158	372	85	470	242	411	51	486	363
MAR	271	22	304	249	415	63	499	360	186	19	215	168	307	54	374	260	410	34	427	382
APR	267	43	316	210	398	121	554	249	179	38	222	129	292	104	431	166	407	44	443	344
MAY	253	25	284	227	356	90	476	262	166	27	197	139	256	78	363	175	385	50	435	307
JUN	218	21	249	194	252	38	306	198	132	16	155	110	169	28	207	128	351	36	403	307
JUL	191	24	205	148	195	33	220	138	109	16	120	81	127	22	144	88	303	42	330	230
AUG	188	22	211	160	194	41	234	139	108	17	125	85	128	30	158	87	296	38	338	246
SEP	192	25	224	156	220	56	294	162	115	22	145	88	149	42	206	108	302	44	356	241
OCT	227	24	254	195	304	52	377	236	147	20	173	119	216	40	276	164	354	38	388	331
NOV	246	21	276	219	361	52	444	305	165	16	189	144	264	44	336	218	379	24	406	344
DEC	264	41	304	201	417	121	567	242	182	40	229	124	312	104	447	168	392	47	437	316
ANN	240	36	317	148	336	101	588	138	157	34	231	81	243	84	470	87	366	44	486	230
C.F.	0.48	0.07	0.63	0.30	0.22	0.07	0.39	0.09	0.31	0.07	0.46	0.16	0.16	0.06	0.31	0.06	0.37	0.04	0.49	0.23

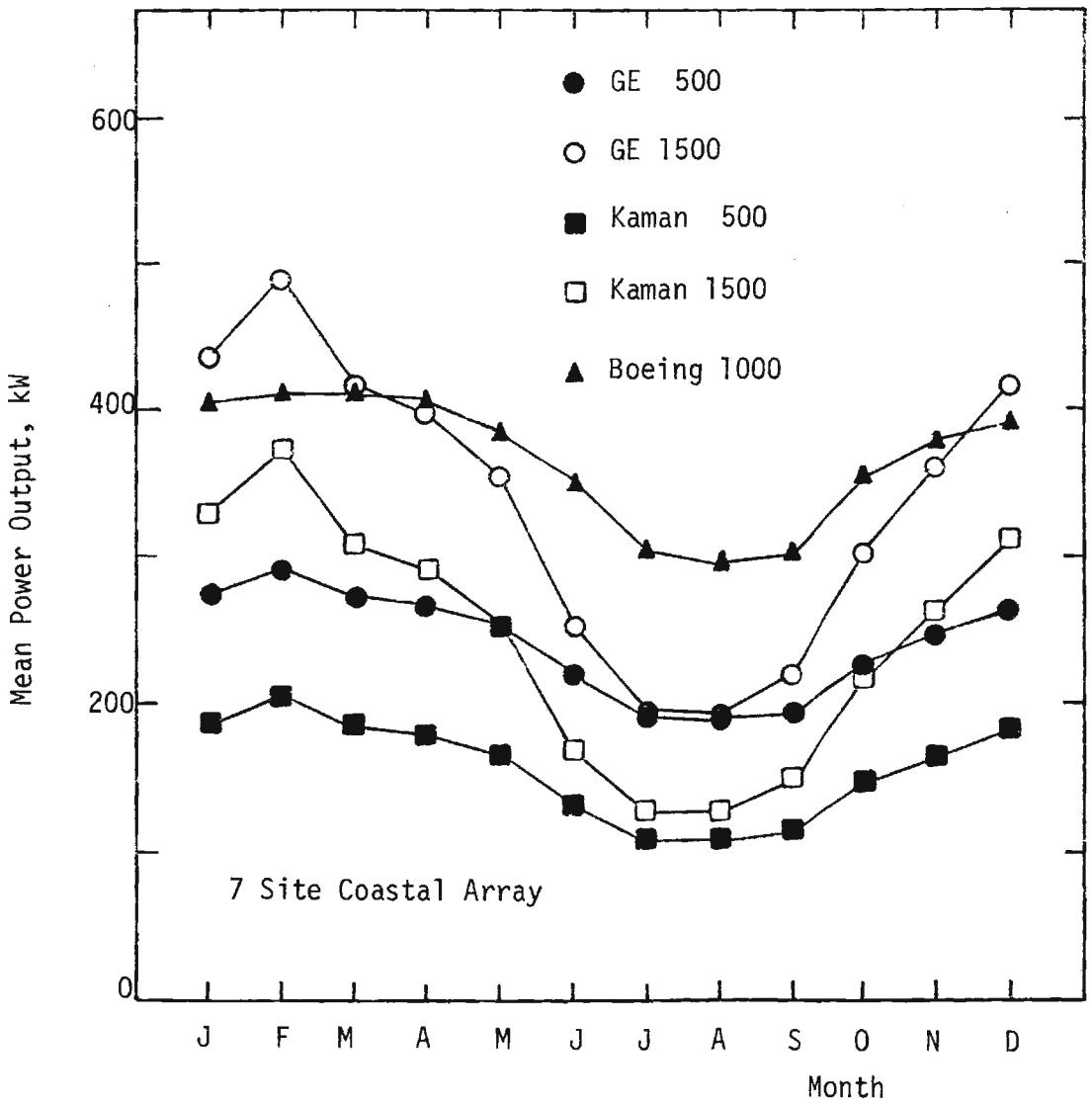

Figure 9 - Seasonal Variation of Monthly Mean Power Output for 7 Site Coastal Array.

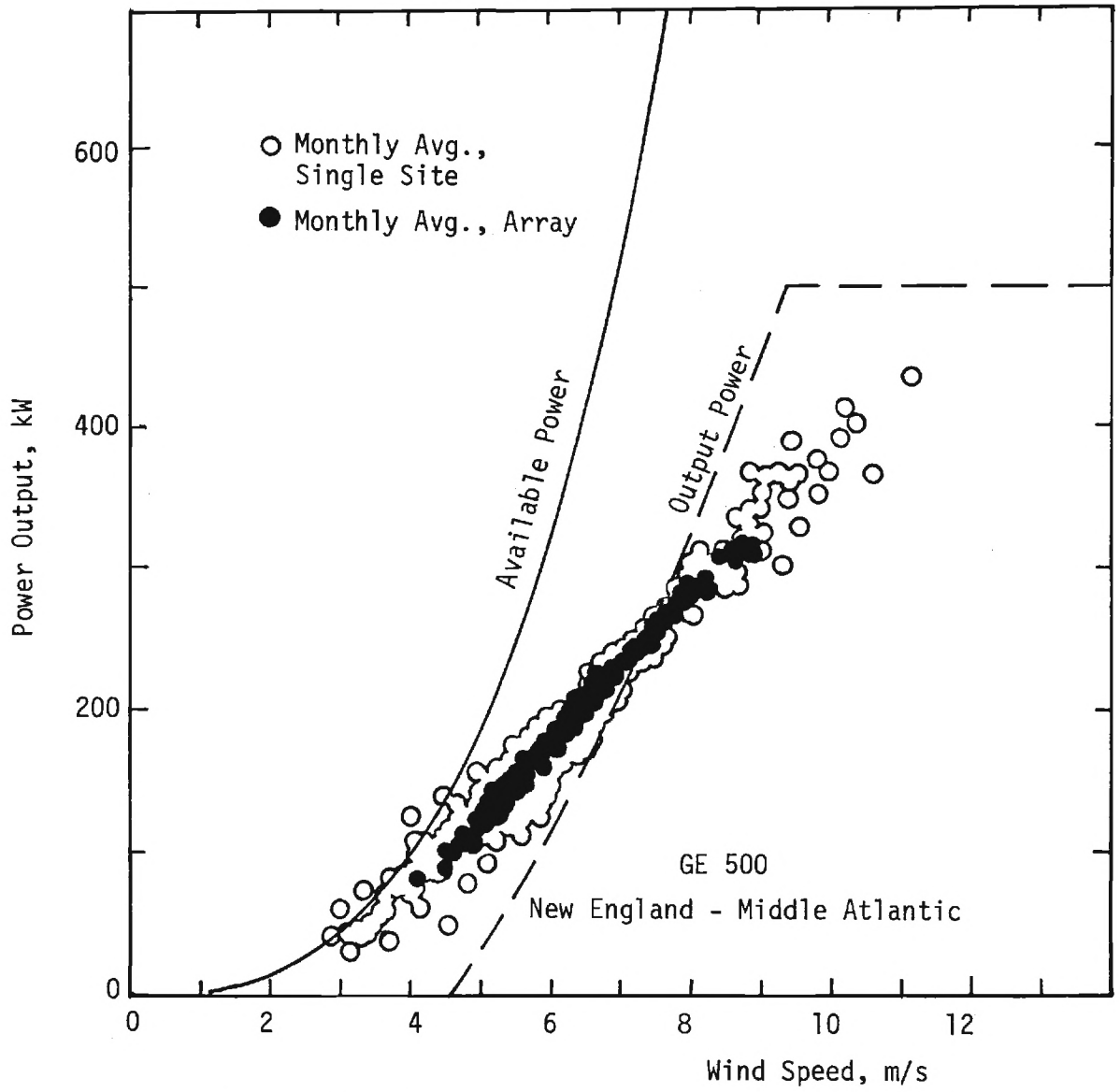

Figure 10 - Monthly Average Single Site and Array Output Power Versus Monthly Averaged Wind Speed for GE 500 kW Turbine. Solid Line is Instantaneous Theoretically Available Power. Dashed Line in Instantaneous Output Power Versus Instantaneous Wind. (Solid and Dashed Curves are Functions of Instantaneous Wind Speed, Data Points are Functions of Monthly Average Wind Speed).

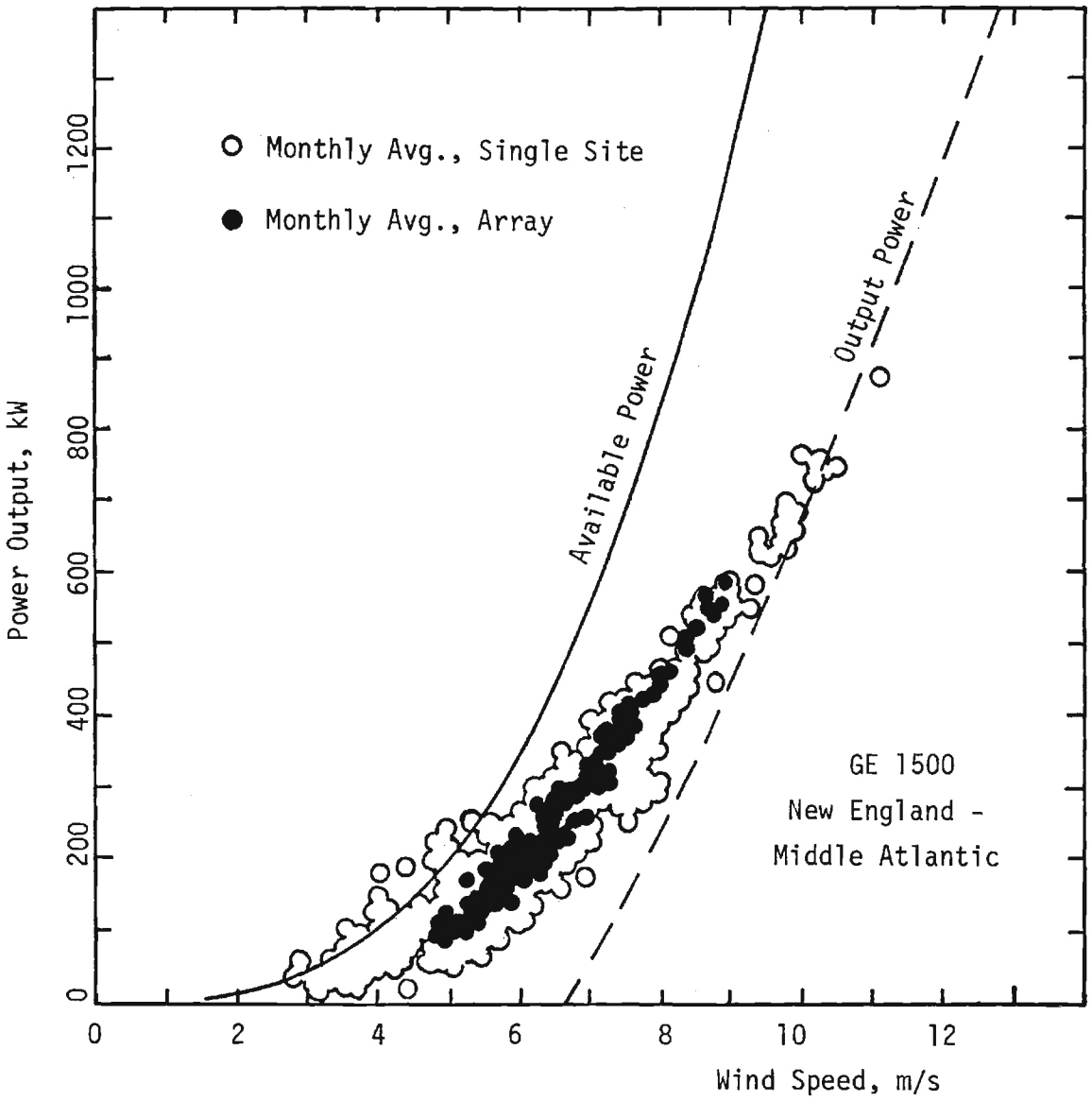

Figure 11 - As in Figure 9 for GE 1500 kW Turbine.

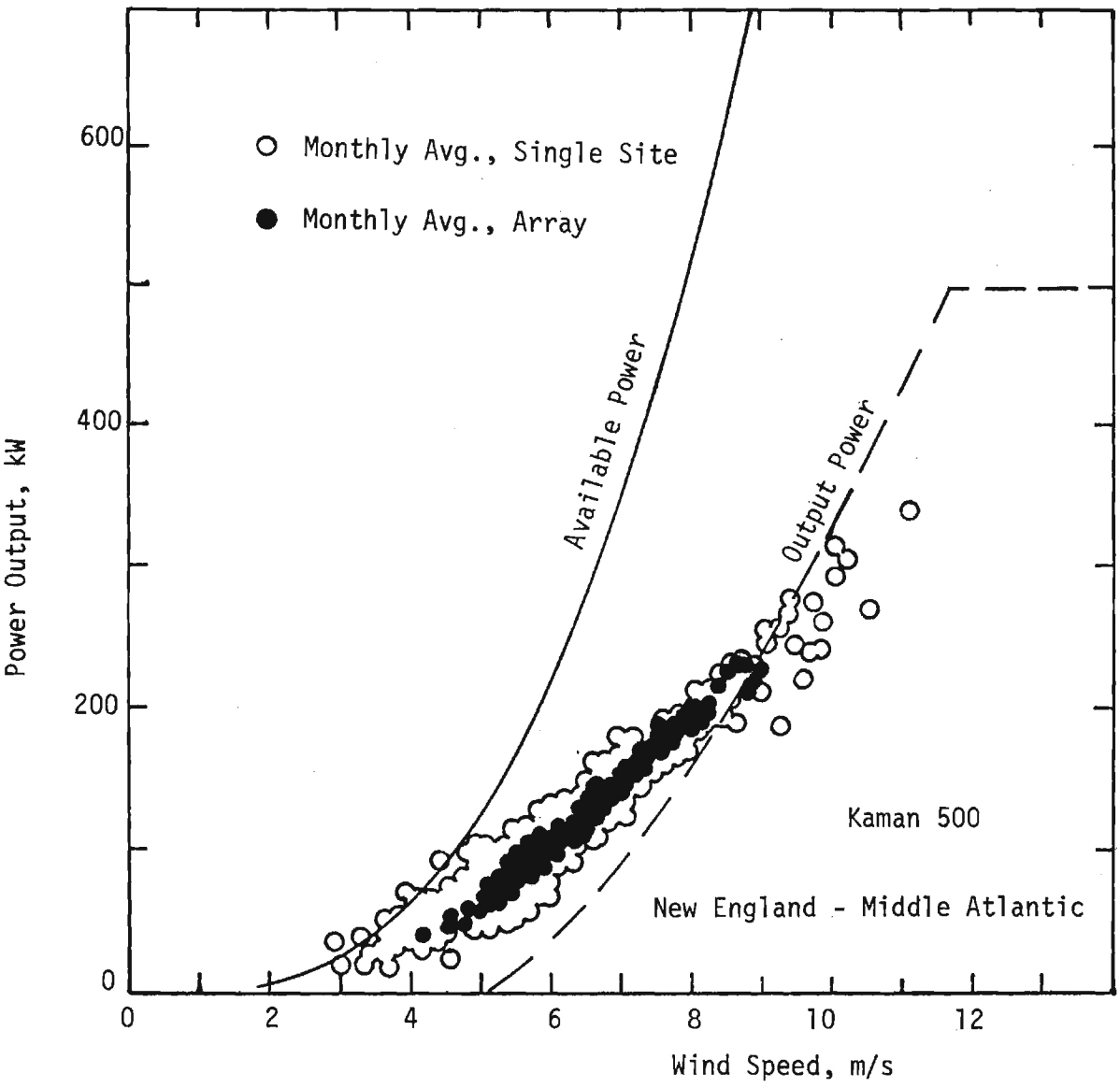

Figure 12 - As in Figure 9 for Kaman 500 kW Turbine.

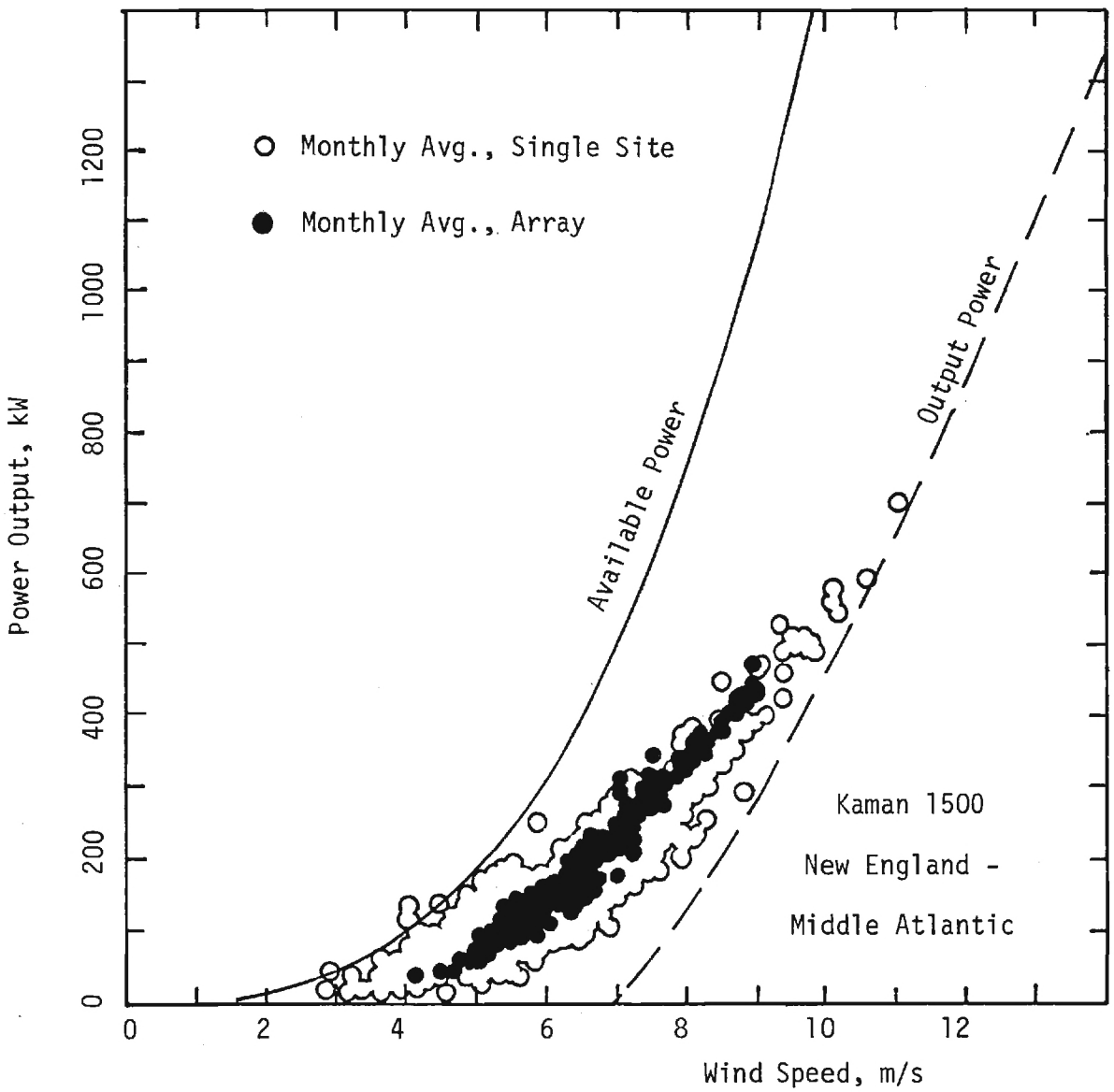

Figure 13 - As in Figure 9 for Kaman 1500 kW Turbine.

monthly mean wind speed, and b) array monthly mean output power as a function of array average monthly mean wind speed. Array output power versus array mean speed is seen to be approximately linear, following a line connecting points with 0 power at about 0.69 V_o and rated power at about 1.27 V_1, where V_o and V_1 are the cut-in and rated wind speeds, respectively. Individual site monthly mean output power versus monthly mean wind speed follows roughly the same linear relationship, although with much larger scatter of the individual data points (there is also some hint of curvature, rather than a strictly linear relationship, especially in the case of the 1500 kW rated power machines). For comparison purposes Figures 10-13 also plot the theoretically available power 0.5 ρ V^3 A and the actual power output curve of instantaneous power versus instantaneous wind speed. At low wind speeds, it is seen that the monthly mean power versus mean speed exceeds power available from the machines on an instantaneous basis (and, in some few cases, even exceed values of the theoretically available instantaneous power). This apparent anomaly is due to the effects of the non-linear power output curve on the monthly averaging of power values and wind speeds (the instantaneous and theoretically available power curves in Figures 10-13 being functions of instantaneous wind speed and the data on monthly average power being functions of monthly average wind speed).

The proposed linear relationship for monthly mean power (from zero power at 0.69 V_o to rated power at 1.27 V_1) should be useful at a first order estimate of monthly output power when monthly mean wind speed is known.

Cost Effectiveness as a Fuel Saver

From the annual mean power output, the cost effectiveness of the various wind turbine designs as a fuel saver can be evaluated. From Zimmer et al (1975), the break-even wind turbine cost, in dollars per rated kilowatt, can be evaluated under alternate assumptions (one optimistic, one pessimistic). Condition 1 (pessimistic) assumes that the amount of each type of fuel saved by the use

TABLE 7

Estimated Cost-Effectiveness of Various Wind Turbines Based on Five Year Average Capacity Factors at the 7 Site Coastal Array. Condition 1 Refers to Only Proportional Fuel Replacement (pessimistic). Condition 2 Refers to Only Most Expensive Fuel Replacement (optimistic). Ratios of Necessary to Actual $/kW Greater than 1 are Cost-Effective.

Wind Turbine	GE 500	GE 1500	Kaman 500	Kaman 1500	Boeing 1000
Annual Capacity Factor	0.48	0.22	0.31	0.16	0.37
Break-Even $/kW (Condition 1)	1000	458	646	333	771
Break-Even $/kW (Condition 2)	1500	807	1047	647	1207
Estimated Actual $/kW	974	449	841	498	600
Ratio Necessary to Actual (Condition 1)	1.03	1.02	0.77	0.67	1.29
Ratio Necessary to Actual (Condition 2)	1.54	1.80	1.24	1.30	2.01

of wind power is saved in proportion to the amount of fuel of that type presently used (i.e. if present fuel usage is 60% coal and 40% oil, then 60% of the fuel saved by wind power usage will be coal and 40% will be oil). This assumption implies that wind availability is so random that no better than this proportional replacement can be achieved. Condition 2 (optimistic) assumes that only the most expensive fuel (e.g. oil) will be replaced by wind power. This assumption implies that wind power is always available during times when the expensive fule is in use (generally during peak periods), which is an optimistic assumption. Actual conditions would be expected to fall somewhere between Condition 1 and Condition 2, with Condition 2 being more correct the better the reliability of available wind power.

Table 7 shows, for the Coastal array, the annual capacity factor (fraction of rated power actually available on an annual basis) for each of the five wind turbine designs. Necessary costs in $/kW in order to break-even as a fuel saver, under Condition 1 (proportional fuel replacement) and Condition 2 (most expensive fuel replacement) are shown, as taken from proportional adjustment of figures from Table 14.7 in Zimmer et al (1975). Table 7 also shows the estimated actual production costs in $/kW for the five wind turbines (General Electric, 1975; Kaman, 1975; Boeing from Honeywell, 1976). Note that although the analysis and data of Table 7 is done on a $/kW capital cost basis, the effects of fuel costs, discount rate, time horizon, installation rate, maintenance costs, and other factors, are accounted for by the use of nominal (base line) values for these parameters (as given in Table 14.5 of Zimmer et al (1975)). In order to be cost-effective as a fuel saver, the actual production cost $/kW must be less than the necessary break-even $/kW cost. As shown by the ratio of break-even to actual costs (which must be greater than one for cost-effectiveness), all of the wind turbine designs are cost-effective under the assumption of Condition 2 (only must expensive fuel replacement). However, both the 500 kW and 1500 kW Kaman

units are not cost-effective (ratios less than one) under the assumption of Condition 1 (proportional fuel replacement), and the GE 500 and 1500 kW wind turbines are just barely cost-effective under Condition 1.

Wind Power Frequency (Reliability Without Storage)

For some discussion of basic aspects of speed and power distributions and the relation of probability density functions (velocity frequency) to cumulative probability (velocity duration), the reader is referred to Appendix B. Frequency distributions of individual site output power were evaluated by direct "counting up" within power intervals of observed single site powers $P(V_i)$ for each time i, where $P(V_i)$ is the wind turbine output power as a function of the observed wind speed V_i (adjusted to hub height). Frequency distributions of array power were similarly evaluated counting up array power values in the various power intervals, where at each time i the array power $\bar{P}_i$ was evaluated by summing over the n individual sites in the array

$$\bar{P}_i = \sum_{j=1}^{n} P_j(V_i). \qquad (4)$$

Figures 14 through 17 show examples for the 5 year average January single site and array power output frequency distributions for the single site and array statistics. Tables 8 and 9 give observed cumulative frequencies of power levels within various power intervals for single sites and arrays, both for the 28 site full array and the 7 site coastal array.

As discussed in Appendix B, the frequency distribution curves (as in Figures 14 through 17 or Tables 8 - 9) can be used to determine the improvement in power output reliability which can be achieved by dispersing the wind turbines into arrays. For example, Figure 14 shows for the GE 500 kW turbine that a power output level of 200 kW per generator in the array is 65% reliable (45% cumulative probability), whereas the single site power output level of 200 kW per generator is only 56% reliable (54% cumulative probability). For a 100 kW per generator power level, the array produces 83% reliability versus only 64% reliability for

TABLE 8

5 Year Average Power Output Frequency for GE Wind Turbines. Cumulative Frequencies in Percent are Given for Power Output Intervals Shown.

	Output Power, KW	28 SITE FULL ARRAY								7 SITE COASTAL ARRAY							
		JAN		APR		JUL		OCT		JAN		APR		JUL		OCT	
		ARRAY	IND.	ARRAY	IND.	ARRAY	IND.	ARRAY	IND.	ARRAY	IND.	ARRAY	IND.	ARRAY	IND.	ARRAY	IND.
GE 500 KW	0 - 10	1.5	31.4	0.6	29.0	2.2	40.2	3.1	37.5	2.5	22.0	1.0	20.5	1.5	99.3	3.1	25.8
	10 - 100	25.3	44.4	24.3	43.2	42.8	58.2	37.2	53.0	17.1	35.6	17.3	33.8	30.3	46.5	25.4	40.9
	100 - 200	50.5	52.8	48.6	52.3	73.1	68.7	66.5	62.6	35.2	43.6	35.1	40.6	55.9	56.4	46.8	49.5
	200 - 500	99.8	75.1	100.0	77.4	100.0	91.2	100.0	84.8	92.7	70.4	96.8	68.5	99.6	85.5	96.0	76.0
GE 1500 KW	0 - 10	7.5	51.5	4.9	51.0	14.5	67.5	11.5	61.5	9.3	40.5	7.1	40.5	13.5	56.4	13.2	49.5
	10 - 100	31.6	57.4	31.2	57.5	57.9	74.3	46.9	67.7	24.9	46.4	26.3	47.1	44.1	63.7	36.9	55.8
	100 - 200	49.4	60.2	49.2	60.6	77.0	77.1	67.3	70.6	37.8	51.3	38.1	51.7	63.2	69.0	50.7	60.5
	200 - 5	76.9	75.1	79.8	77.3	96.5	91.2	87.7	84.7	65.0	67.2	65.0	68.5	90.3	85.5	78.2	76.0
	500 - 1000	94.4	87.8	97.5	90.5	100.0	98.0	98.4	94.3	87.7	83.3	93.4	84.4	99.8	96.1	94.8	89.6
	1000 - 1500	100.0	94.3	100.0	96.2	100.0	99.6	100.0	98.0	99.3	92.2	100.0	93.4	100.0	99.3	99.8	96.1

TABLE 9

5 Year Average Power Output Frequency for Kaman Wind Turbines. Cumulative Frequencies in Percent are Given for Power Output Intervals Shown.

	Output Power, KW	28 SITE FULL ARRAY								7 SITE COASTAL ARRAY							
		JAN		APR		JUL		OCT		JAN		APR		JUL		OCT	
		ARRAY	IND.	ARRAY	IND.	ARRAY	IND.	ARRAY	IND.	ARRAY	IND.	ARRAY	IND.	ARRAY	IND.	ARRAY	IND.
KAMAN 500 KW	0 - 10	6.6	38.7	4.2	36.1	10.4	49.2	9.1	45.2	6.2	26.7	4.3	27.2	8.0	36.9	9.0	32.9
	10 - 100	44.4	55.9	44.0	55.1	71.0	71.2	62.7	65.0	34.0	43.5	33.8	46.2	54.9	61.6	45.2	54.2
	100 - 200	71.9	70.8	72.5	72.1	92.6	87.2	83.4	80.3	57.7	56.8	56.8	62.5	83.5	79.4	70.5	70.2
	200 - 500	100.0	91.1	100.0	93.1	100.0	98.8	100.0	95.8	99.9	81.4	99.8	88.7	100.0	97.6	99.5	92.2
KAMAN 1500 KW	0 - 10	10.7	55.0	9.7	54.7	23.2	71.2	17.1	64.9	12.3	43.3	10.8	45.3	20.2	61.6	19.0	54.0
	10 - 100	42.7	60.2	42.0	60.6	71.6	77.1	61.6	70.6	33.8	49.0	34.2	51.7	58.1	69.0	46.4	60.5
	100 - 200	60.8	67.8	61.1	69.2	88.2	84.9	77.2	78.1	49.7	55.3	48.9	59.4	77.1	77.6	62.3	68.0
	200 - 500	85.4	81.1	90.3	83.7	99.7	95.0	93.5	89.5	76.0	71.7	79.3	77.1	96.9	92.0	86.9	83.2
	500 - 1000	97.4	92.6	98.9	94.8	100.0	99.3	99.7	97.0	92.5	86.6	97.4	90.7	100.0	98.6	97.5	94.3
	1000 - 1500	100.0	97.2	100.0	98.4	100.0	99.9	100.0	99.3	99.9	94.0	100.0	97.0	100.0	99.9	100.0	98.5

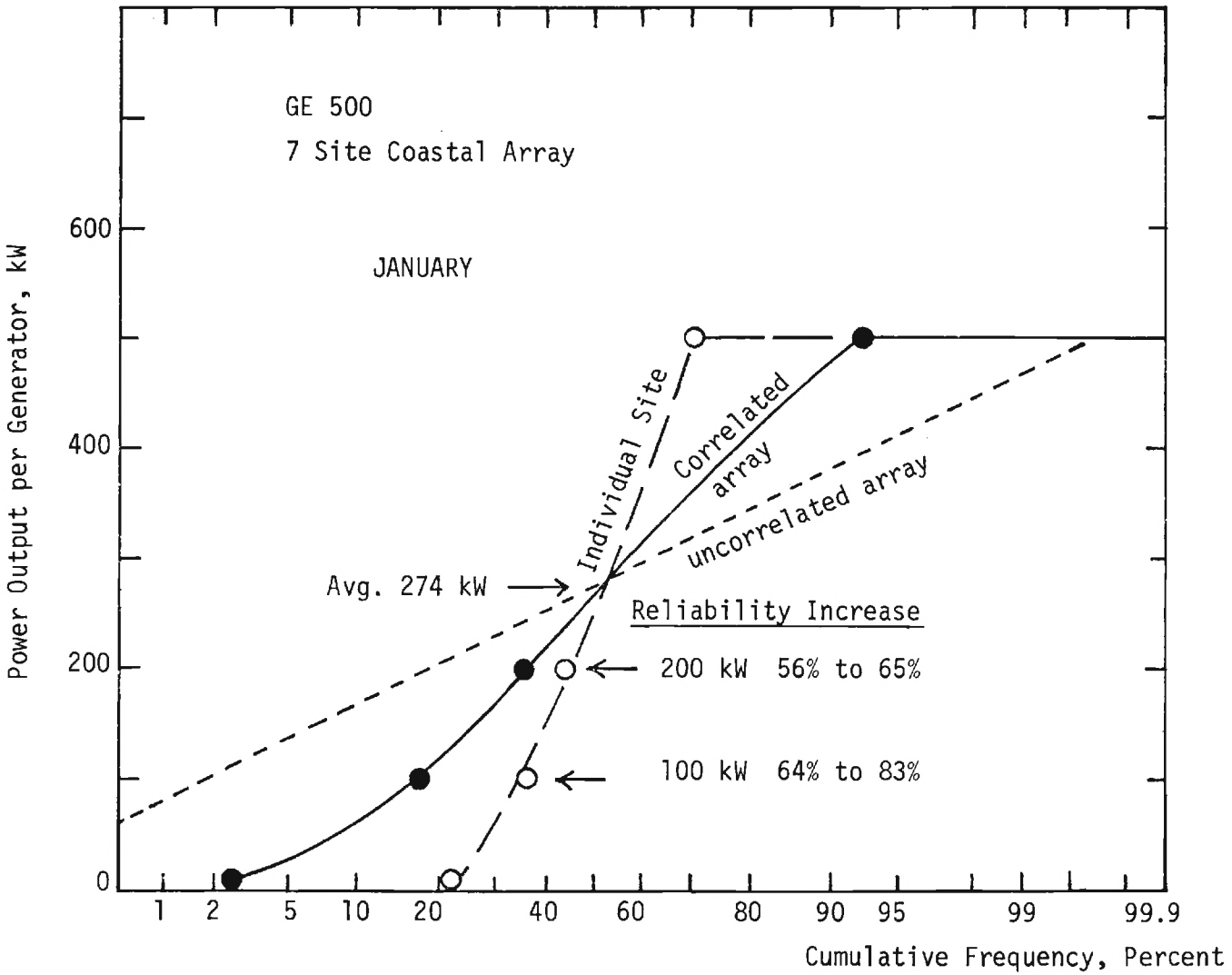

Figure 14 - Power Output Frequency Distribution for GE 500 kW Wind Turbines, 7 Site Coastal Array in January. (See Appendix B for Discussion of Interpretation)

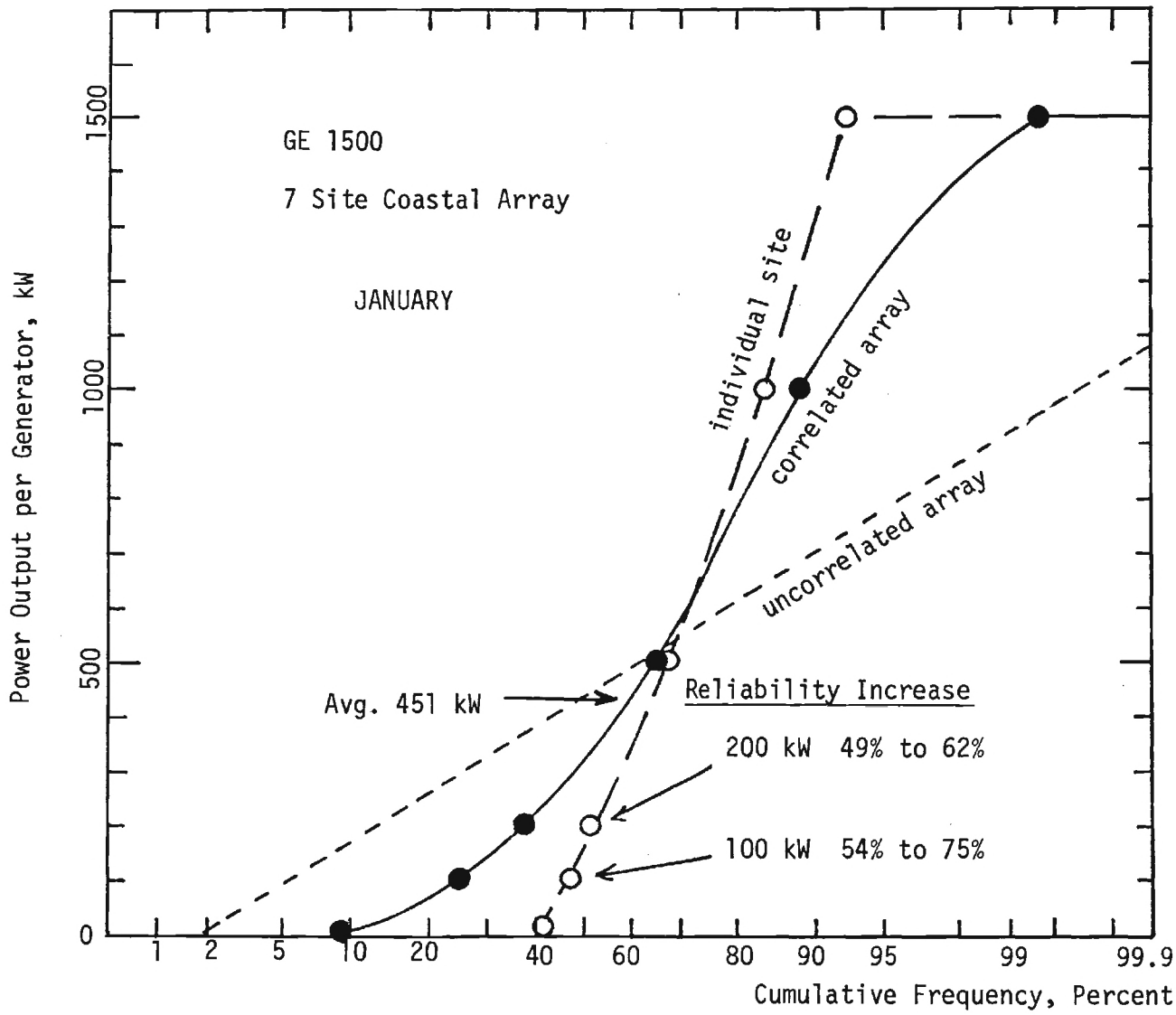

Figure 15 - As in Figure 14 for GE 1500 kW Turbine.

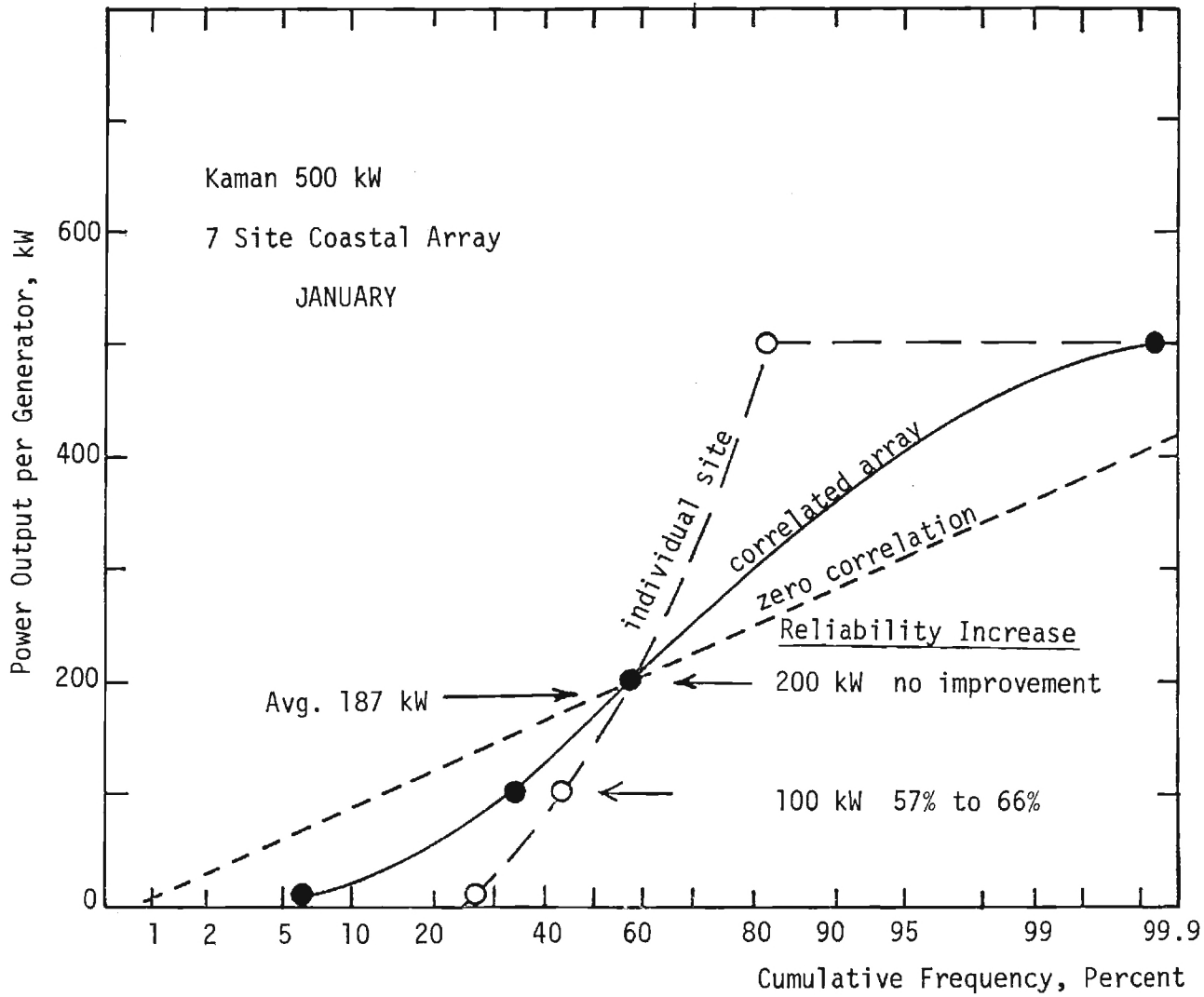

Figure 16 - As in Figure 14 for Kaman 500 kW Turbine.

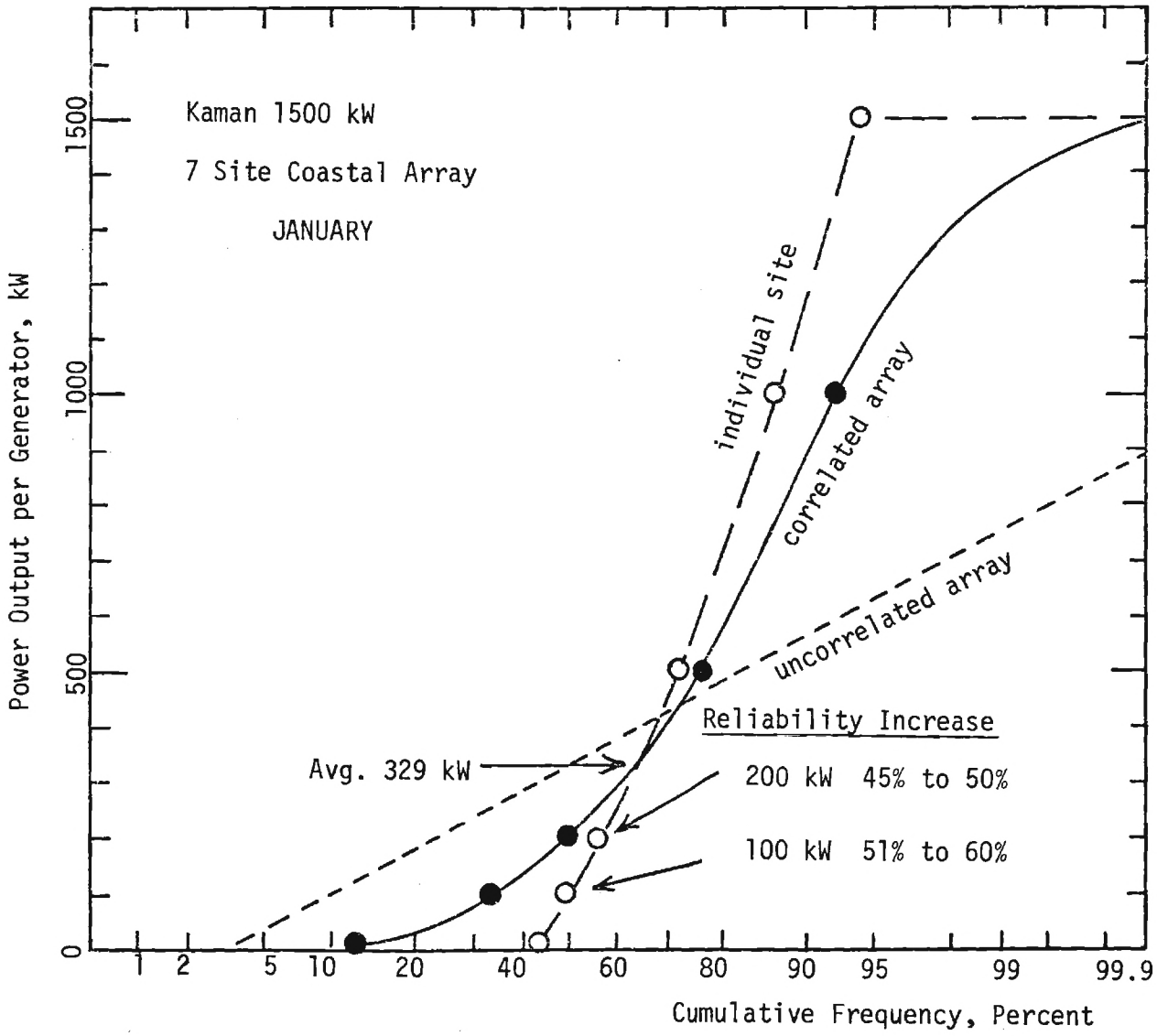

Figure 17 - As in Figure 14 for Kaman 1500 kW Turbine.

that power level in single site configuration.

As shown by the dotted curves for zero correlation arrays in Figures 14-17, increased reliability could be obtained from arrays which had lower than the observed spatial correlation (observed to average roughly 50% - See Table 4). See Appendix B for the method of evaluating zero correlation array power distributions. One way the array correlation could, of course, be made lower would be by spreading the array over larger spatial area (again see Table 4). Note that the actual (approximately 50% correlated) array output power distribution curves fall roughly halfway between the curves for single site (100% correlation) and the zero correlation array curves. This suggests that interpolation between these two curves (single site and zero correlation curves) would be appropriate given knowledge of only the effective array correlation value.

Note, also from the discussion in Appendix B, that improved array output power reliability could also be achieved by going to a larger number of sites (since σ_n for an uncorrelated n site array decreases as $1/\sqrt{n}$, and makes the slope less steep for the zero correlation array). Even with non-zero correlation, the increase in number of sites would still improve the power reliability to some extent.

Return Times for Array Power (Reliability with Storage)

For an approximate analysis of array power reliability with storage, the statistics of array power return times were evaluated at two power levels (100 kW and 200 kW per generator). An array power return time for a given power level is defined as the time required after array power goes below the given power level until the array power returns above that level. Table 10 shows average, standard deviation, maximum and minimum return times in hours for the 7 site coastal array for the months of January, April, July and October, for

TABLE 10

Average and Maximum Return Times for Seven Site Coastal Array. $\bar{T}$ and σ are Mean Return Time and Standard Deviation in Hours. $\bar{T}_{MAX}$ and σ_{MAX} are Mean Maximum and Standard Deviation in Hours. T_{MAX} is Highest Maximum from 5 Year Data Set, in Hours.

	WIND TURBINE	JAN					APR					JUL					OCT				
		$\bar{T}$	σ	$\bar{T}_{MAX}$	σ_{MAX}	T_{MAX}	$\bar{T}$	σ	$\bar{T}_{MAX}$	σ_{MAX}	T_{MAX}	$\bar{T}$	σ	$\bar{T}_{MAX}$	σ_{MAX}	T_{MAX}	$\bar{T}$	σ	$\bar{T}_{MAX}$	σ_{MAX}	T_{MAX}
100 KW RETURN TIME	GE 500	10	1	27	6	33	8	1	18	4	24	9	1	19	3	24	10	1	32	9	42
	GE 1500	10	2	34	11	48	9	2	19	3	24	12	3	31	13	45	13	2	50	18	69
	Kaman 500	14	2	43	8	51	11	2	26	10	39	15	5	52	40	117	17	3	64	11	75
	Kaman 1500	13	3	44	12	54	11	2	27	13	45	15	5	56	37	117	17	3	63	11	75
200 KW RETURN TIME	GE 500	14	2	45	15	66	11	3	24	9	39	16	5	50	28	93	16	3	60	16	78
	GE 1500	14	2	55	27	102	13	3	32	20	63	18	6	77	42	141	18	4	91	21	111
	Kaman 500	23	3	74	30	117	18	5	52	24	93	38	10	118	47	189	27	7	132	31	162
	Kaman 1500	19	4	65	26	105	17	6	46	19	78	27	9	92	38	141	23	4	118	25	159

array power output levels of 100 and 200 kW per generator. The standard deviation in return time is the rms deviation of the individual year monthly means about the 5 year monthly mean. $\bar{T}_{MAX}$ is the average of the 5 maximums for the 5 individual monthly time periods in the 5 year series. σ_{MAX} is the rms deviation of the individual year monthly maximum about the 5 year monthly maximum. T_{MAX} is the absolute maximum return time observed for any given month out of the 5 year data set.

Table 11 shows the observed frequency distribution (cumulative probability) for return times of various durations. Figure 18 shows a sample of the distribution data from Table 11, in graphical form. From Figure 18 it can be seen that, by interpolation, the GE 500 kW wind turbine, for example, would have 90% reliable 200 kW per generator power output if there were a storage system with about 29 hours of power storage (i.e. 5800 kW-hours storage capacity per generator, 200 kW x 29 hours). Similarly the GE 500 kW wind turbine in Figure 18 would have 95% reliable 200 kW per generator power if about 37 hours of storage were available.

Comparison of Power Reliability With and Without Storage

Power reliability data, without storage, from the power frequency distribution information (Tables 8 and 9) can be combined with power reliability data, with storage, from the return time analyses (Table 11), to compare the wind power reliability with and without storage. Results for the 7 site coastal array in January, April, July and October are shown in Table 12. The reliability levels of 10 kW power per generator are compared for single sites versus arrays without storage only. These data show that the improved statistics of arrays mean that some small amount of power (e.g. 10 kW per generator) is virtually always available with the array configuration.

TABLE 11

Return Time Probability Distributions for 7 Site Coastal Array.
Cumulative Frequencies are Given in Percent for Return Times Within Intervals Shown.

	Time Interval, Hours	100 KW RETURN TIME								200 KW RETURN TIME							
		GE				KAMAN				GE				KAMAN			
		JAN	APR	JUL	OCT	JAN	APR	JUL	OCT	JAN	APR	JUL	OCT	JAN	APR	JUL	OCT
Rated Power = 500 KW	0 - 4	33.8	33.8	23.3	35.5	24.4	16.7	18.7	20.0	26.1	19.8	15.0	20.8	18.7	18.3	4.0	20.7
	4 - 8	52.3	50.0	37.1	49.5	44.4	29.6	25.9	30.0	39.8	33.0	23.3	30.7	24.2	29.4	5.3	30.4
	8 - 16	84.6	95.9	93.1	86.0	68.9	75.9	67.6	68.2	65.9	80.2	64.7	69.3	47.3	57.8	32.0	55.4
	16 - 32	96.9	100.0	100.0	96.8	91.1	92.6	95.0	89.1	92.0	98.1	92.5	85.1	74.7	83.5	54.7	75.0
	32 - 64	100.0	100.0	100.0	100.0	100.0	100.0	99.3	97.3	98.9	100.0	99.2	97.0	93.4	97.2	84.0	89.1
	64 - 128	100.0	100.0	100.0	100.0	100.0	100.0	100.0	100.0	100.0	100.0	100.0	100.0	100.0	100.0	97.3	96.7
Rated Power = 1500 KW	0 - 4	38.6	24.5	20.7	30.6	27.2	23.4	18.6	21.7	25.0	20.8	14.2	23.3	21.6	21.2	10.4	19.4
	4 - 8	51.1	43.9	31.9	41.7	46.7	35.5	28.6	31.1	50.0	32.1	25.4	32.0	36.1	30.8	18.9	30.6
	8 - 16	78.4	86.7	75.6	78.7	72.8	80.4	65.7	67.9	72.1	78.3	64.2	68.9	60.8	62.5	48.1	59.2
	16 - 32	96.6	100.0	97.8	91.7	90.2	97.2	93.6	87.7	92.3	94.3	89.6	84.5	80.4	85.6	70.8	79.6
	32 - 64	100.0	100.0	100.0	98.1	100.0	100.0	99.3	94.3	99.0	100.0	97.0	98.1	95.9	97.1	93.4	91.8
	64 - 128	100.0	100.0	100.0	100.0	100.0	100.0	100.0	100.0	100.0	100.0	99.3	100.0	100.0	100.0	99.1	99.0

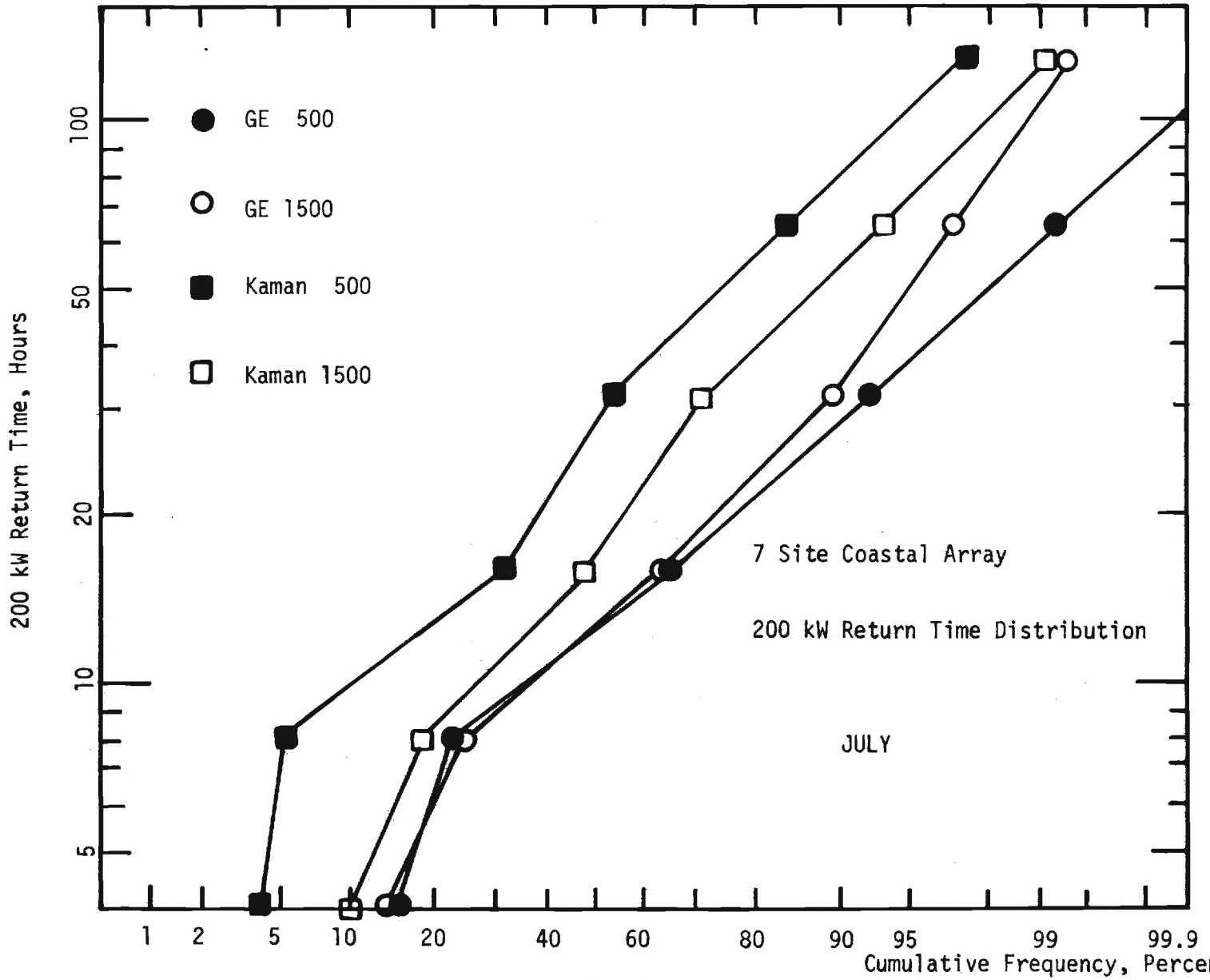

Figure 18 - Frequency Distribution of 200 kW Return Times for 7 Site Coastal Array in July.

TABLE 12

Reliability of Power Levels of 10, 100, and 200 KW per Generator, With and Without Storage. 7 Site Coastal Array or Individual Site. T is Storage Time in Hours. R is Reliability in Percent. T = 0 Indicates No Storage.

		JAN								APR								JUL								OCT							
		GE				KAMAN				GE				KAMAN				GE				KAMAN				GE				Kaman			
		500				1500				500				1500				500				1500				500				1500			
		T hrs.		R %		T hrs.		R %		T hrs.		R %		T hrs.		R %		T hrs.		R %		T hrs.		R %		T hrs.		R %		T hrs.		R %	
10 KW/GEN.	IND.	0		78		0		60		0		73		0		57		0		80		0		60		0		73		0		55	
	ARRAY	0		98		0		91		0		94		0		57		0		99		0		93		0		96		0		89	
100 KW/GEN.	IND	0		64		0		54		0		57		0		51		0		66		0		53		0		54		0		48	
	↑	0		83		0		75		0		66		0		66		0		83		0		74		0		66		0		66	
	ARRAY	20		90		22		90		31		90		32		90		13		90		17		90		27		90		21		90	
	↓	27		95		28		95		36		95		36		95		15		95		19		95		35		95		27		95	
		47		99		44		99		46		99		46		99		20		99		23		99		45		99		40		99	
200 KW/GEN.	IND.	0		56		0		49		0		43		0		45		0		59		0		48		0		38		0		41	
	↑	0		65		0		62		0		42		0		50		0		65		0		62		0		43		0		51	
	ARRAY	29		90		28		90		53		90		45		90		20		90		25		90		40		90		38		90	
	↓	39		95		38		95		68		95		59		95		25		95		33		95		53		95		52		95	
		66		99		64		99		88		99		83		99		37		99		43		99		79		99		79		99	

		JUL								OCT							
		GE				KAMAN				GE				Kaman			
		500				1500				500				1500			
		T hrs.		R %		T hrs.		R %		T hrs.		R %		T hrs.		R %	
10 KW/GEN.	IND.	0		72		0		44		0		63		0		38	
	ARRAY	0		99		0		87		0		92		0		80	
100 KW/GEN.	IND	0		54		0		36		0		38		0		31	
	↑	0		70		0		56		0		35		0		42	
	ARRAY	15		90		22		90		26		90		28		90	
	↓	17		95		26		95		32		95		35		95	
		22		99		36		99		57		99		58		99	
200 KW/GEN.	IND.	0		44		0		31		0		21		0		22	
	↑	0		44		0		37		0		17		0		23	
	ARRAY	29		90		33		90		79		90		54		90	
	↓	37		95		49		95		104		95		71		95	
		60		99		110		99		124		99		124		99	

		OCT							
		GE				Kaman			
		500				1500			
		T hrs.		R %		T hrs.		R %	
10 KW/GEN.	IND.	0		74		0		51	
	ARRAY	0		97		0		87	
100 KW/GEN.	IND	0		59		0		44	
	↑	0		75		0		63	
	ARRAY	19		90		28		90	
	↓	27		95		42		95	
		49		99		82		99	
200 KW/GEN.	IND.	0		51		0		40	
	↑	0		53		0		49	
	ARRAY	39		90		38		90	
	↓	53		95		48		95	
		80		99		74		99	

		OCT							
		Kaman							
		500				1500			
		T hrs.		R %		T hrs.		R %	
10 KW/GEN.	IND.	0		67		0		46	
	ARRAY	0		91		0		81	
100 KW/GEN.	IND	0		46		0		40	
	↑	0		55		0		54	
	ARRAY	34		90		39		90	
	↓	48		95		66		95	
		79		99		87		99	
200 KW/GEN.	IND.	0		30		0		32	
	↑	0		30		0		38	
	ARRAY	68		90		56		90	
	↓	103		95		77		95	
		162		99		128		99	

For 100 kW per generator and 200 kW per generator, Table 12 compares reliabilities in percent for individual sites and arrays without storage (T = 0), and the storage time, in hours, required to produce the given array power levels with 90%, 95%, and 99% reliability. Note that in good wind months, the array configuration always improves the reliability of 100 kW and 200 kW per generator power levels. However, for poor wind cases and low generator capacities (i.e. Kaman 500 kW generator in July and October for 200 kW per generator) the array configuration will not offer improved reliability (in these cases the 200 kW per generator is at or above the average power, hence little or no improvement is gained from the array - see Appendix B for further interpretation).

3. CENTRAL U.S. AREA

The West North Central Federal Power Commission Region includes the States of North and South Dakota, Nebraska, Kansas, Minnesota, Iowa, and Missouri. The West South Central Region includes the States of Texas, Oklahoma, Arkansas, and Louisiana. From the wind power potential studies of Zimmer et al (1975), the best wind areas within these two regions were determined to be in Nebraska, Kansas, Oklahoma, north Texas, and western Missouri. Wind data from the 25 sites shown in Figure 19 and listed in Table 13 were analyzed, by the methods described in Appendix A for the 5 year period 1969-1973. Power outputs from three simulated wind turbine designs were evaluated and studied: the GE 500 kW, GE 1500 kW and Boeing 1125 kW designs (see Table A-1, Appendix A). The Kaman 500 kW and 1500 kW designs were not studied in the Central U. S. area. The Boeing 1125 kW design is slightly modi-

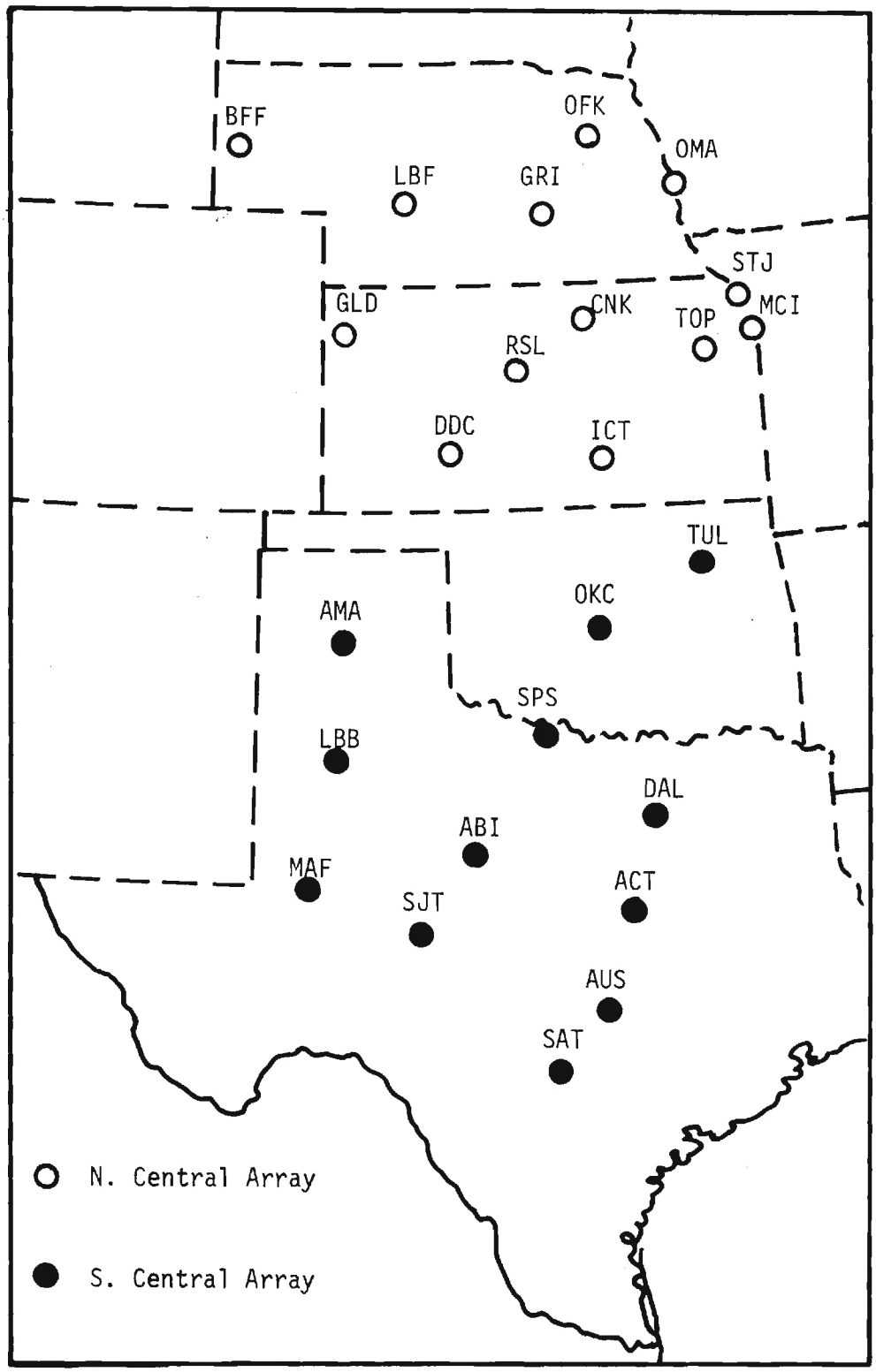

Figure 19 - Map of Central U.S. Array Sites, Showing Two Sub-Group Arrays Studied Separately.

TABLE 13

Site Names for the Central U.S. Area Sites

ABI	Abilene, TX	MAF	Midland, TX
ACT	Waco, TX	MCI	Kansas City (Intnl.), MD
AMA	Amarillo, TX	OFK	Norfolk, NB
AUS	Austin, TX	OKC	Oklahoma City, OK
BFF	Scottsbluff, NB	OMA	Omaha, NB
CNK	Concordia, KS	RSL	Russell, KS
DAL	Dallas (Love), TX	SAT	San Antonio (Intnl.), TX
DDC	Dodge City, KS	SJT	San Angelo, TX
GLD	Goodland, KS	SPS	Wichita Falls, TX
GRI	Grand Island, NB	STJ	St. Joseph, MO
ICT	Wichita, KS	TOP	Topeka, KS
LBB	Lubbock, TX	TVL	Tulsa (Intnl.), OK
LBF	North Platte, NB		

fied from the original preliminary 1000 kW design (Wiesner and Kisovec, 1976).

In addition to the full 25 site array, two sub-groups of sites were studied as smaller arrays: the 13 site North Central Array (Nebraska, Kansas, and Missouri sites), and the 12 site South Central Array (Oklahoma and north Texas sites). Thes are shown, respectively, as the open circles and the solid dots in Figure 19.

Wind Statistics

Table 14 shows the monthly mean wind speeds, projected to a simulated hub height of 43 m (100 ft), for each of the 25 Central U.S. sites, for the seasonal months of January, April, July, and October. Mean speeds were evaluated by averaging over corresponding months for the five year 1969 - 1973 period of record. Standard deviations in Table 14 are rms deviations of individual year monthly site mean wind speeds from the five year average. Table 14 shows the two best sites to be Amarillo, Texas (AMA) and Goodland, Kansas (GLD). As a whole, the North Central Sites are approximately equal in mean wind speed to the South Central sites, with perhaps a slight advantage to the South Central array. Comparison of Table 14 and Table 2 indicates the 25 site Central U.S. sites to be much better on the whole than the 28 site New England - Middle Atlantic sites. However, the 7 site Coastal Array sites are approximately comparable to the Central U.S. sites in terms of mean speed.

Table 15 and Figure 20 show data on the array average monthly mean speed (speeds averaged over all sites in the array) for the full 25 site Central U.S. Array and the North Central and South Central sub-groups. Standard deviations in Table 15 are rms deviations of individual year monthly means about the five year average. Seasonal variations are similar, both in magnitude and seasonal phase, for the North Central and the South Central sites,

TABLE 14

Means wind speed $\bar{V}$ at the 43 m (140 ft) level. σ is rms deviation of individual year monthly mean speed about five year average.

	JAN		APR		JUL		OCT	
Site	$\bar{V}$, m/s	σ, m/s	$\bar{V}$, m/s	σ, m/s	$\bar{V}$, m/s	σ, m/s	$\bar{V}$, m/s	σ, m/s
ABI	7.91	0.32	8.94	0.63	7.57	0.57	7.59	0.33
ACT	7.31	0.58	8.16	0.64	6.86	0.45	6.38	0.56
AMA	8.39	0.73	9.82	0.72	8.10	0.55	8.62	0.23
AUS	6.76	0.46	7.18	0.35	5.92	0.45	5.83	0.55
BFF	7.68	1.17	7.98	0.95	5.92	0.58	6.41	0.75
CNK	8.23	0.37	9.02	0.54	7.64	0.45	7.88	0.37
DAL	7.25	0.57	8.26	0.57	6.85	0.45	6.76	0.29
DDC	8.09	0.44	9.29	0.29	7.99	0.34	8.21	0.32
GLD	8.32	0.28	9.47	0.27	7.95	0.52	8.20	0.15
GRI	7.99	0.36	9.10	0.83	6.96	0.53	7.71	0.17
ICT	7.77	0.37	8.85	0.35	7.32	0.49	7.48	0.22
LBB	7.18	0.56	8.57	0.41	6.58	0.55	6.59	0.25
LBF	6.18	0.30	8.28	0.47	6.15	0.24	6.40	0.43
MAF	7.26	0.60	8.44	0.55	7.44	0.77	7.09	0.38
MCI	7.30	0.61	7.39	0.28	6.08	0.60	6.34	0.25
OFK	6.93	0.88	8.04	0.52	5.48	0.58	6.13	0.25
OKC	7.50	1.09	8.83	0.95	7.46	0.52	7.69	0.90
OMA	7.32	0.49	7.78	1.01	5.90	0.30	6.18	0.52
RSL	8.15	0.52	8.56	1.05	8.16	0.52	8.05	0.61
SAT	5.98	0.24	6.96	0.19	6.10	0.33	5.86	0.50
SJT	7.35	0.63	7.80	0.89	7.09	0.78	6.61	0.83
SPS	7.77	0.29	9.00	0.94	7.80	0.90	7.54	0.48
STJ	6.60	0.35	7.60	0.56	5.34	0.40	5.43	0.22
TOP	6.76	0.27	7.60	0.80	5.61	0.50	5.84	0.22
TUL	6.30	0.46	7.37	0.34	6.43	0.57	6.24	0.39
AVG	7.36	0.19	8.33	0.27	6.82	0.26	6.91	0.19

TABLE 15

Five Year Average Array Monthly Mean Speed $\bar{V}$ at the 43 m (140 ft) Level. σ is rms deviation of Individual Year Array Monthly Mean Speed about the Five Year Average.

	25 Site Full Array		13 Site North Central		12 Site South Central	
	$\bar{V}$, m/s	σ, m/s	$\bar{V}$, m/s	σ, m/s	$\bar{V}$, m/s	σ, m/s
JAN	7.36	0.19	7.48	0.19	7.25	0.28
FEB	7.47	0.50	7.41	0.40	7.53	0.69
MAR	8.18	0.48	7.96	0.40	8.40	0.60
APR	8.33	0.27	8.36	0.43	8.29	0.44
MAY	7.52	0.47	7.52	0.26	7.52	0.71
JUN	7.40	0.37	7.22	0.40	7.60	0.41
JUL	6.82	0.26	6.63	0.25	7.02	0.39
AUG	6.39	0.30	6.43	0.26	6.35	0.40
SEP	6.83	0.47	6.82	0.36	6.84	0.65
OCT	6.91	0.19	6.92	0.11	6.90	0.30
NOV	7.20	0.59	7.07	0.53	7.34	0.66
DEC	7.12	0.56	6.97	0.61	7.27	0.54
ANN	7.29	0.56	7.23	0.55	7.36	0.58

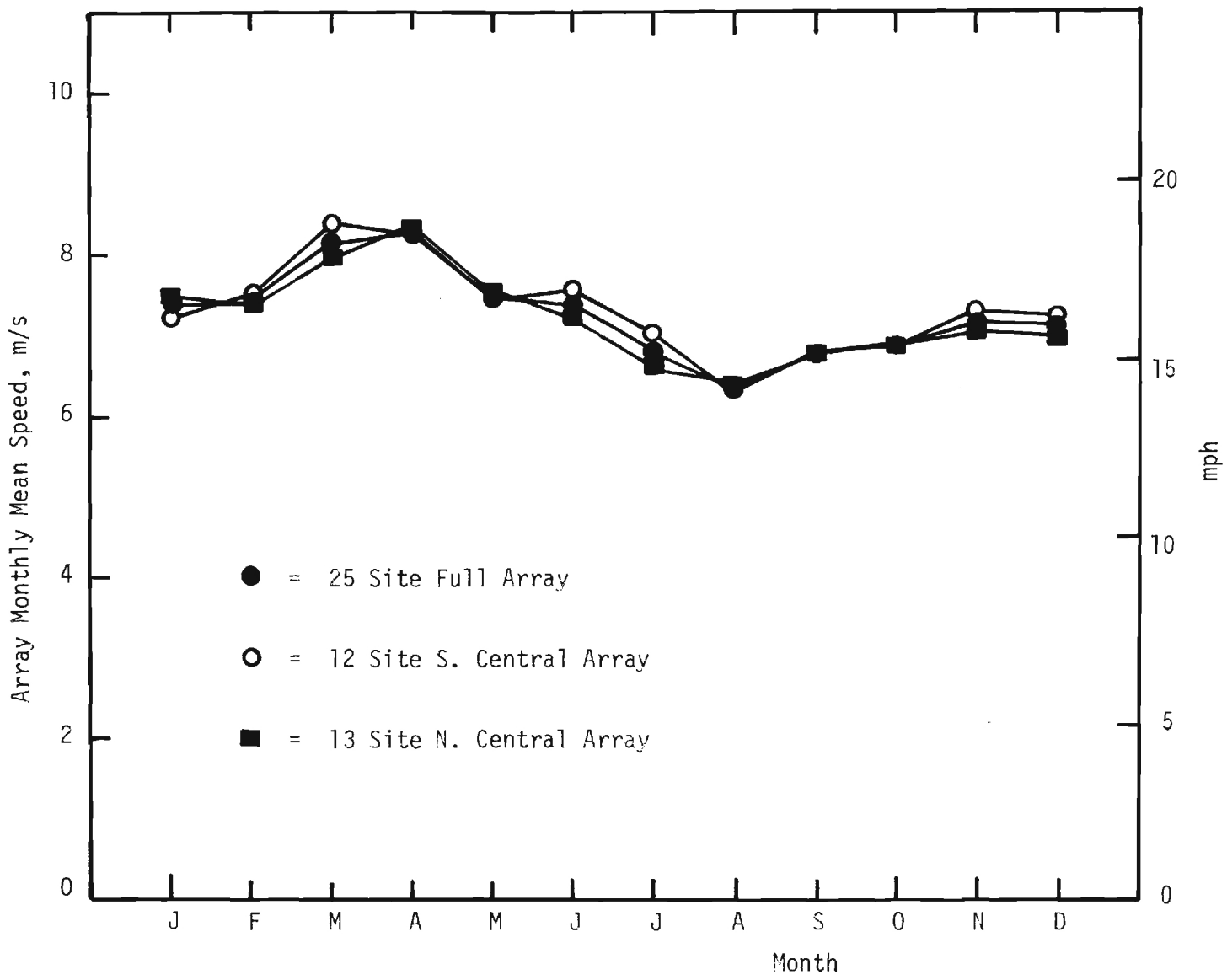

Figure 20 - Seasonal Variation of Array Average Mean Wind Speed at Wind Turbine Hub Height of 43 m (140 ft) for Central U.S. Arrays.

both having maximum monthly mean wind speeds in March and April, with minimums in August. This seasonal variation is somewhat out of phase with the New England - Middle Atlantic area, which peaked in February and had minumuns in August and September.

Time Autocorrelation

Example time autocorrelation curves for the full 25 site Central U.S. array in January and July and the South Central array in July are shown in Figures 21 - 23. Behavior of the Central U.S. area time autocorrelation curves is similar to that found in the New England - Middle Atlantic area - strong diurnal influence in July, and very little diurnal influence in January (with intermediate degrees of diurnal influence in the intervening months). It can be hypothesized that strong summertime insolation is responsible for the dominant diurnal influence in the summer months. This hypothesis is supported by the observation that the South Central sites (Figure 23) have stronger diurnal influence than the full array (Figure 22), which includes the weaker insolation North Central sites. However, strong insolation must not be the only controling influence because Figure 4 shows stronger diurnal influence on the New England - Middle Atlantic sites, despite their more northerly latitude and lesser insolation than the Central U.S. array. One possibility for enhanced diurnal effect on the New England sites, at least in the Coastal areas, is an enhanced land-sea breeze circulation in the summer months.

Spatial Cross Correlations

Figures 24 and 25 show examples of the average spatial cross correlation for the 25 site Central U.S. array. In these figures all correlation values were averaged together by intervals of 50 km in site separation. The number

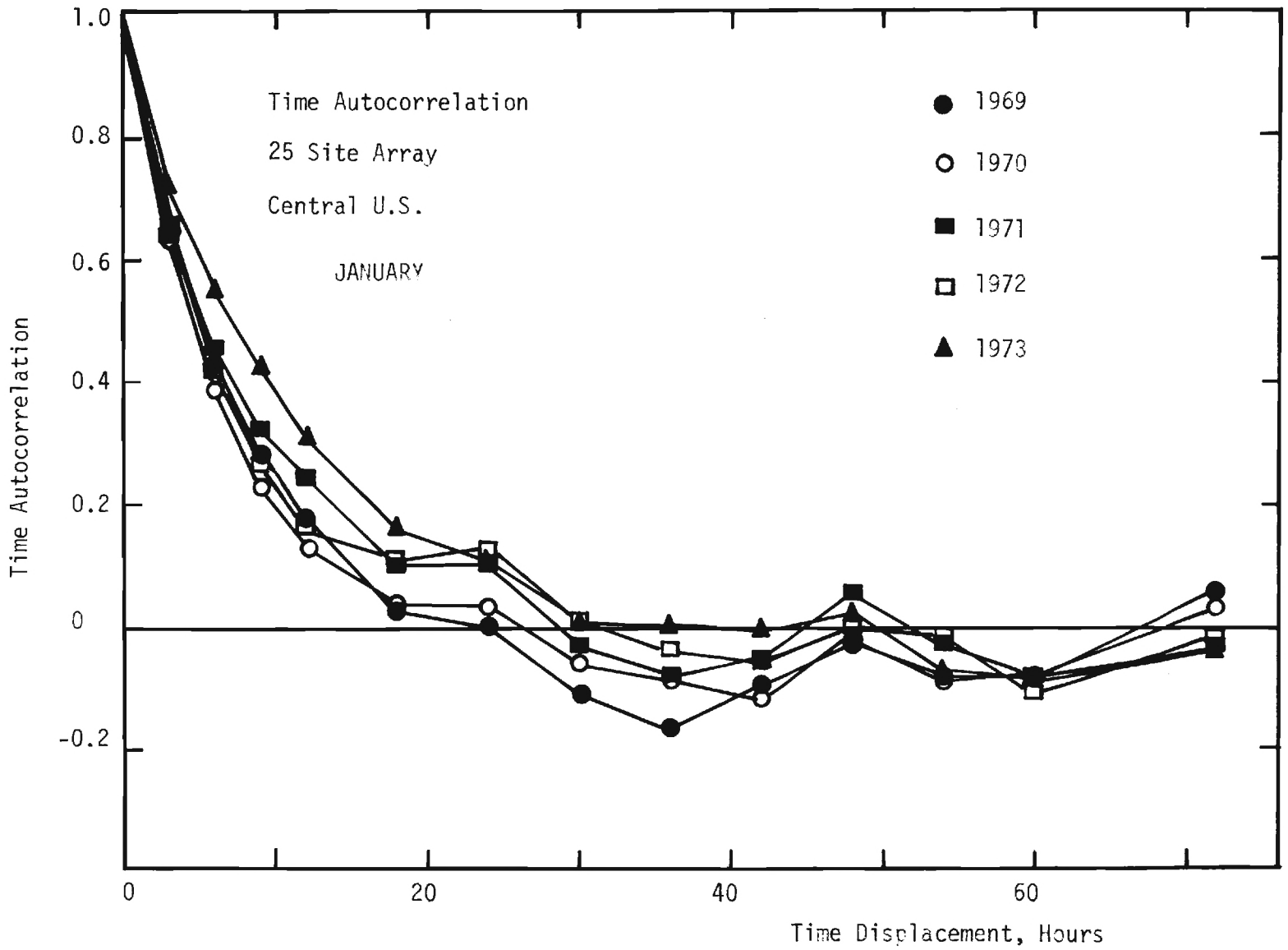

Figure 21 - Time Autocorrelation in January for 25 Site Full Array in Central U.S.

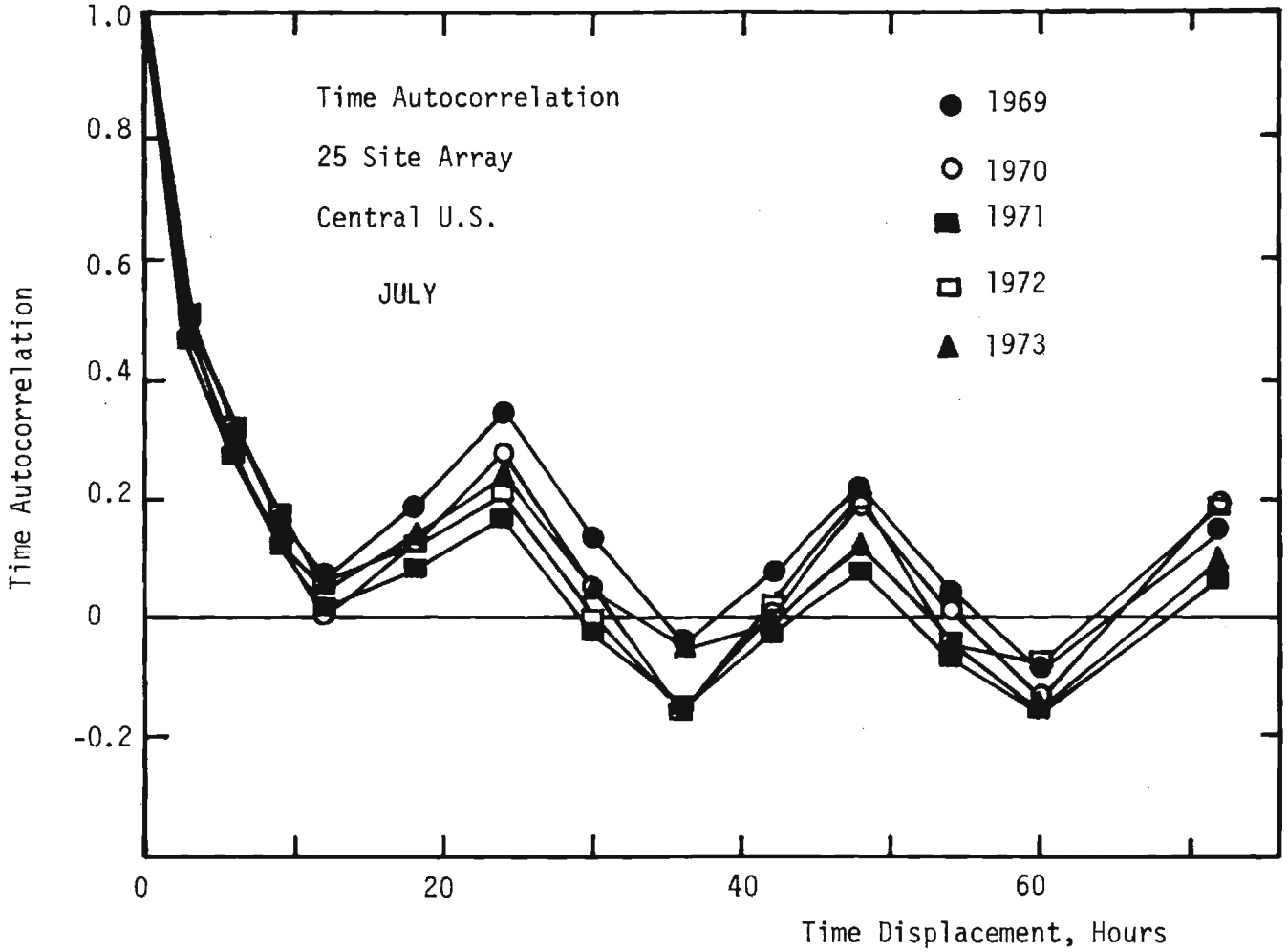

Figure 22 - Time Autocorrelation in July for Full 25 Site Array in Central U.S.

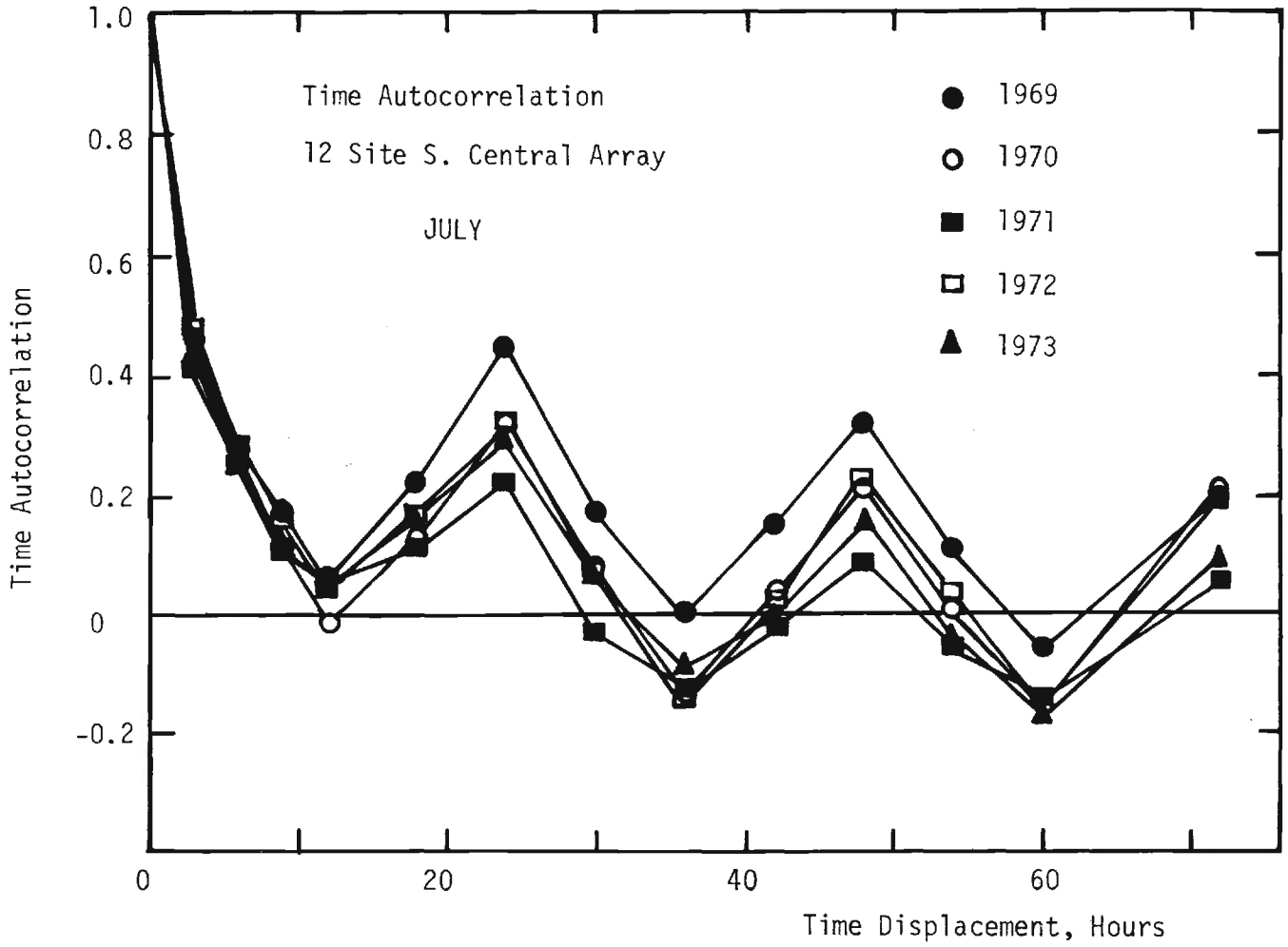

Figure 23 - Time Autocorrelation in July for 12 Site S. Central Array.

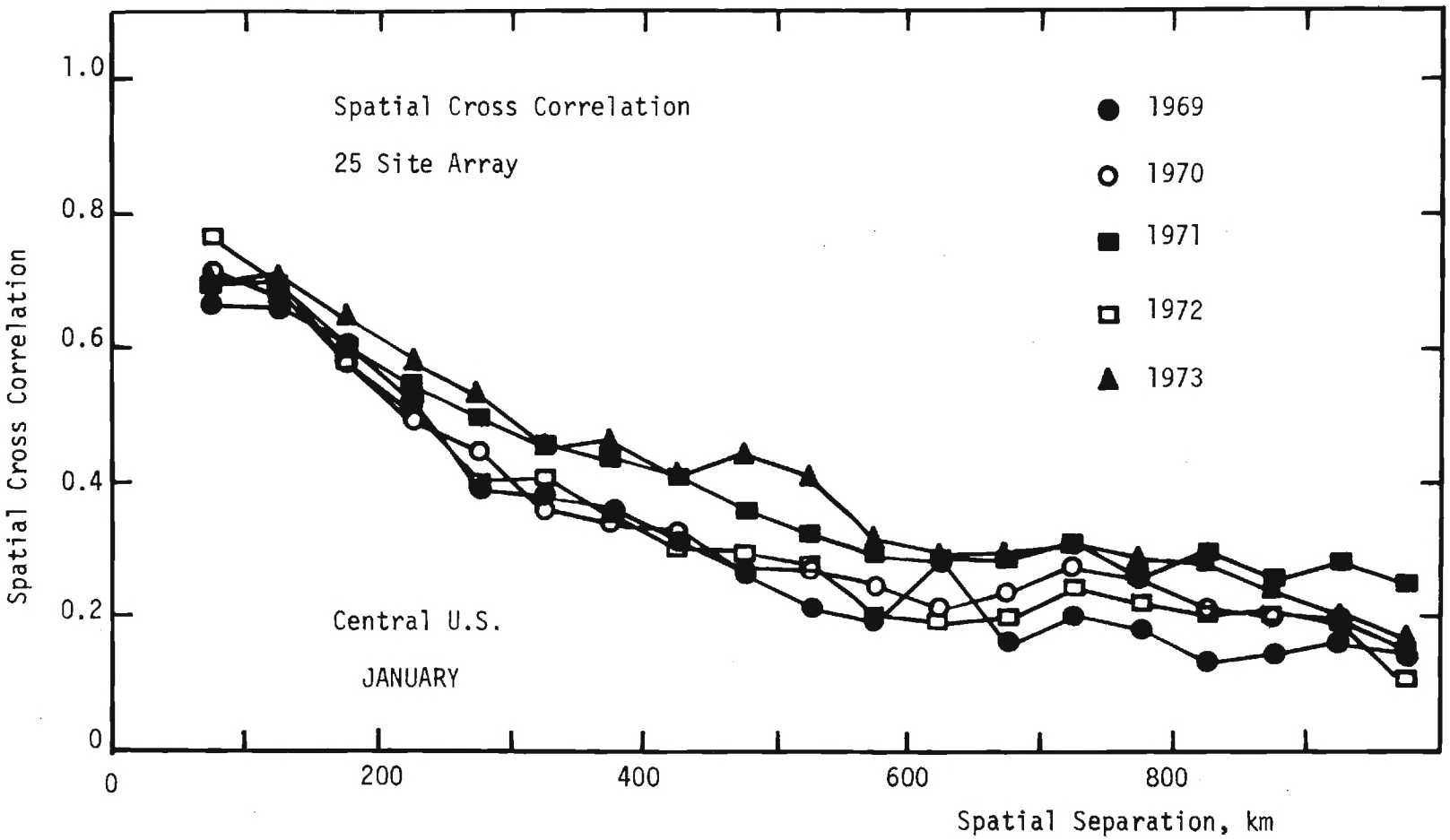

Figure 24 - Spatial Cross Correlation Versus Site Separation for 25 Site Central U.S. Array in January.

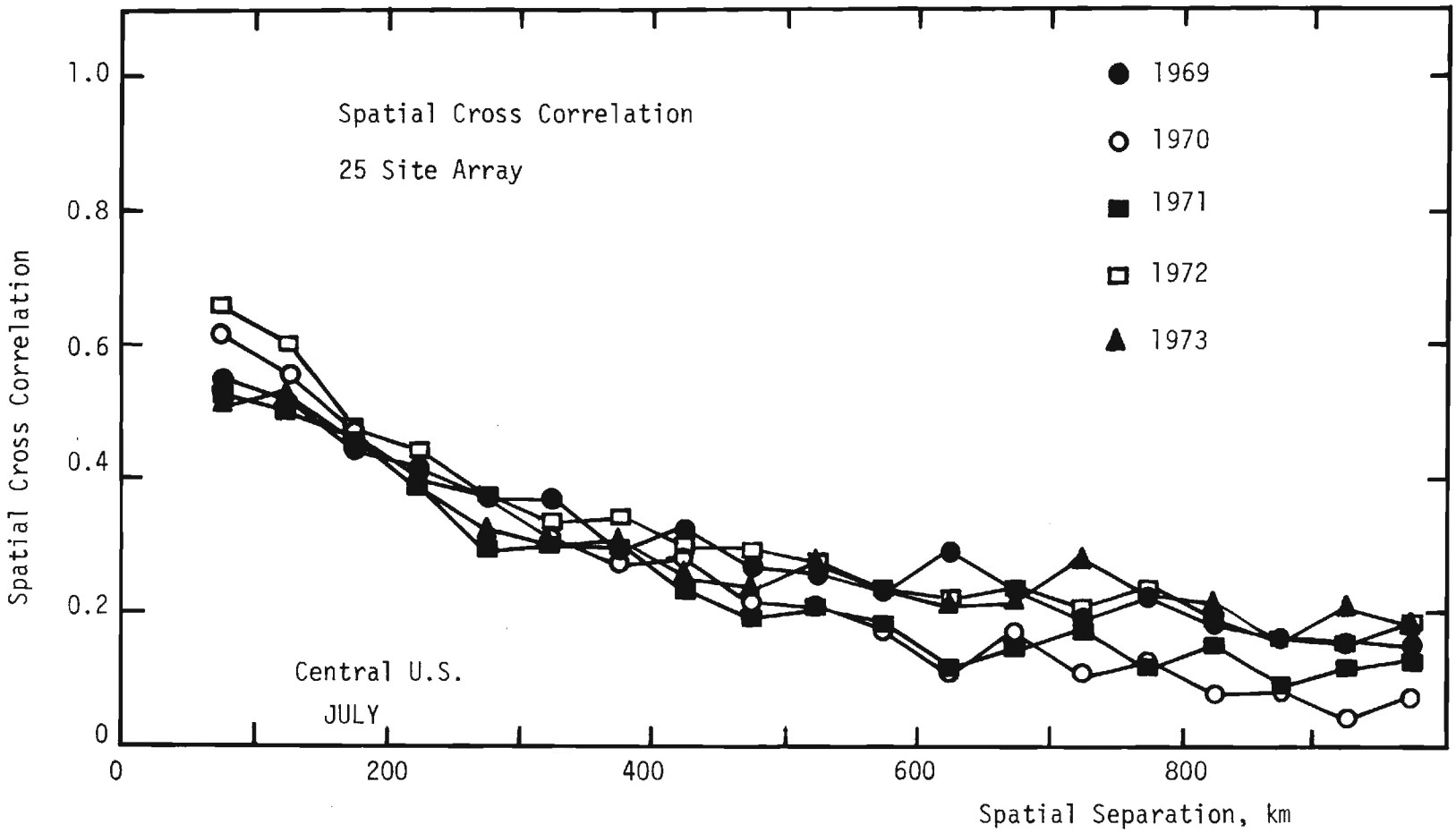

Figure 25 - Spatial Cross Correlation Versus Site Separation for 25 Site Central U.S. Array in July.

of site pairs was zero for the 0-50 km separation interval, 2 for the 50-100 km interval, 6 in the 100-150 km interval. The number per 50 km interval then remained fairly constant at between 9 and 20, out to 950 km separation. There were 54 site pairs with separations greater than 950 km (all averaged together and plotted at the 975 km abscissa in Figures 24 and 25).

As with the New England sites, the Central U.S. spatial cross correlations begin well below one and gradually decrease with separation. No zero or negative values of average cross correlation are seen out to the maximum separation distances (1460 km). However, certain individual sites (notably Scottsbluff, Nebraska (BFF) and Amarillo, Texas (AMA), and, to a lesser extent Goodland, Kansas (GLD), and Lubbock, Texas (LBB)) did, on occasional months, have very low correlations with surrounding sites. Since there sites are on more rolling terrain, approaching the Rocky Mountains (Scottsbluff and Goodland) or the Sacramento Mountains (Amarillo and Lubbock), this unusual and sporadic behavior may be a terrain influence. The sporadic nature of it may be due to prevailing winds differing from month to month (and even year to year for the same month). A similar spradic low correlation was observed for Burlington, Vermont in the New England - Middle Atlantic area. Since Burlington is separated from the other sites by the White Mountains, this could easily be terrain influence also. However, the Burlington effect also occurred only sporadically, somewhat more frequent in December and January, but not occurring in each of the five years studied. At this time, all that can be concluded is that there may be terrain effects which can occasionally cause low correlations between adjacent sites, but the details of this effect are not well understood.

The array average spatial cross correlations, shown in Table 16 and

TABLE 16

Five year Average Array Cross Correlation. σ is rms Deviation of Individual Year Monthly Average about the Five Year Average. $\bar{r}$ is Mean Inter-Site Separation for the Array.

	25 Site Full Array $\bar{r}$ = 618 km		13 Site N. Central $\bar{r}$ = 374 km		12 Site S. Central $\bar{r}$ = 389 km	
	$\bar{\rho}$	σ	$\bar{\rho}$	σ	$\bar{\rho}$	σ
JAN	0.32	0.05	0.39	0.06	0.42	0.06
FEB	0.33	0.04	0.44	0.05	0.41	0.05
MAR	0.37	0.07	0.47	0.09	0.44	0.07
APR	0.35	0.03	0.45	0.05	0.39	0.05
MAY	0.34	0.03	0.43	0.05	0.38	0.07
JUN	0.33	0.09	0.39	0.09	0.41	0.09
JUL	0.25	0.03	0.31	0.04	0.33	0.02
AUG	0.28	0.03	0.36	0.06	0.33	0.08
SEP	0.31	0.03	0.40	0.05	0.39	0.06
OCT	0.35	0.04	0.43	0.05	0.44	0.03
NOV	0.37	0.07	0.45	0.06	0.46	0.05
DEC	0.28	0.06	0.36	0.05	0.42	0.07
AVG	0.32	0.04	0.41	0.05	0.40	0.04

Figure 26, show significant seasonal variation, in phase with the seasonal variation of monthly mean speed (i.e. maximums in March and April, minimums in July and August). Array average correlations for the Central U.S. arrays are consistently smaller than for the New England - Middle Atlantic arrays, because of their larger spatial extent.

The rapid fall-off in spatial cross-correlation is evident for the Central U.S. sites, but because there were no site pairs with separations less than 50 km, no good data on correlations from closely spaced sites was obtained. The correlations for the 50-100 km separation averaged 67%, with a maximum in March of 76% and a minimum in August of 55% (in seasonal phase with the mean winds). As with the New England - Middle Atlantic sites, values of correlation this low cannot be accounted for by anemometer error alone, and must be explained by some additional contributions from small scale turbulence (remaining after one minute averaging) and mesoscale (< 50 km) motions.

Mean Output Wind Power

One minute average winds, adjusted to 43 m (140 ft) hub height, were used in power output curves (see Appendix A) to compute instantaneous output power from 3 different wind turbine designs: GE 500 kW, GE 1500 kW, and Boeing 1125 kW. Output power values from these wind turbines were averaged over one month intervals, and corresponding months over the 5 years (1969 - 1973) were averaged to yield monthly mean power output. Table 17 and Figure 27 show the computed seasonal variation of monthly mean power output for the three wind turbines simulated, for the 25 site Central U.S. array. Table 18 and Figure 28 show corresponding data for the 12 site South Central array. Tables 17 and 18 also show standard deviations of individual year monthly average power about the 5 year mean, and the maximum and minimum individual year monthly mean out

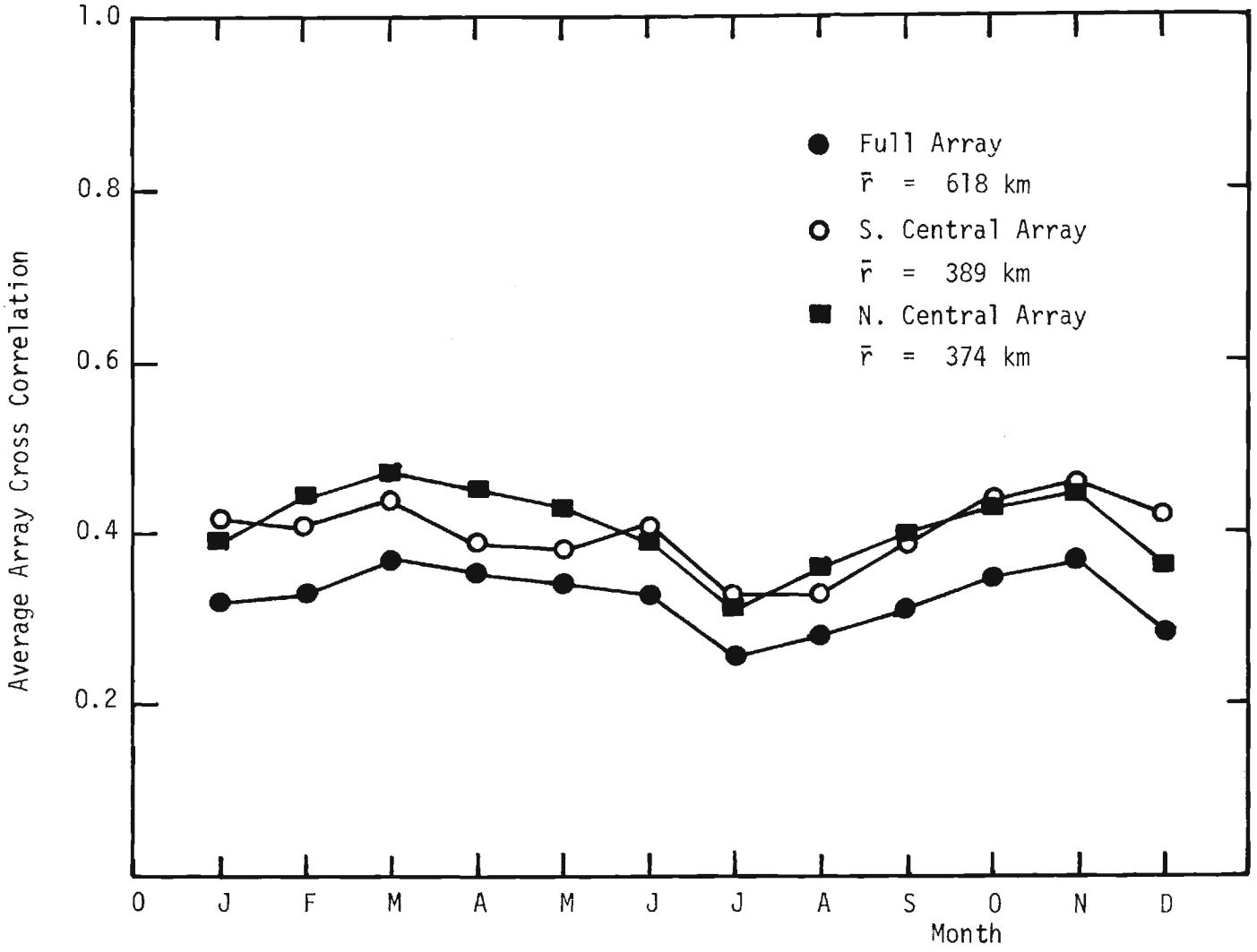

Figure 26 - Seasonal Variation of Average Array Cross Correlation for Central U.S. Arrays.

TABLE 17

Monthly mean power output from 25 site central U.S. array. C.F. is annual capacity factor. $\bar{P}$, σ, MAX and MIN powers are in kW, while C.F. is relative to rated power.

	GE 500				GE 1500				BOEING 1125			
Month	$\bar{P}$	σ	MAX	MIN	$\bar{P}$	σ	MAX	MIN	$\bar{P}$	σ	MAX	MIN
JAN	242.2	11.1	253.2	229.2	334.0	22.3	360.5	304.5	470.1	22.3	491.7	444.4
FEB	247.9	25.1	291.1	228.4	351.6	71.6	476.3	298.9	483.6	57.8	583.9	440.0
MAR	287.6	22.4	311.1	262.4	450.6	71.6	541.2	372.1	572.6	53.2	631.9	515.3
APR	297.4	12.5	309.6	278.4	471.3	37.4	515.8	415.8	593.6	28.6	624.1	550.2
MAY	254.1	27.0	293.1	222.6	356.0	69.4	453.2	267.3	496.2	61.0	583.0	421.6
JUN	251.3	21.8	269.0	216.0	333.2	57.4	390.0	240.5	485.1	49.4	527.8	405.1
JUL	215.1	17.1	236.5	194.8	237.4	31.5	279.8	201.0	401.5	35.0	446.9	361.2
AUG	186.9	20.2	212.7	156.7	192.0	35.3	243.1	145.0	345.8	41.3	400.9	285.9
SEP	213.9	29.1	247.7	169.8	262.8	66.9	342.8	166.7	407.4	63.0	481.4	312.8
OCT	219.8	12.0	238.7	208.3	283.8	23.8	313.1	262.0	423.3	25.1	461.9	399.1
NOV	232.6	33.6	282.5	191.6	320.8	79.3	454.7	248.4	448.8	73.4	566.3	369.9
DEC	228.9	30.6	263.1	190.0	306.0	71.2	394.6	222.3	441.9	66.4	518.9	359.8
ANN	239.8	31.1	311.1	156.7	325.0	79.9	541.2	145.0	464.2	70.0	631.9	285.9
CF	0.48	0.06	0.62	0.31	0.22	0.05	0.36	0.10	0.41	0.06	0.56	0.25

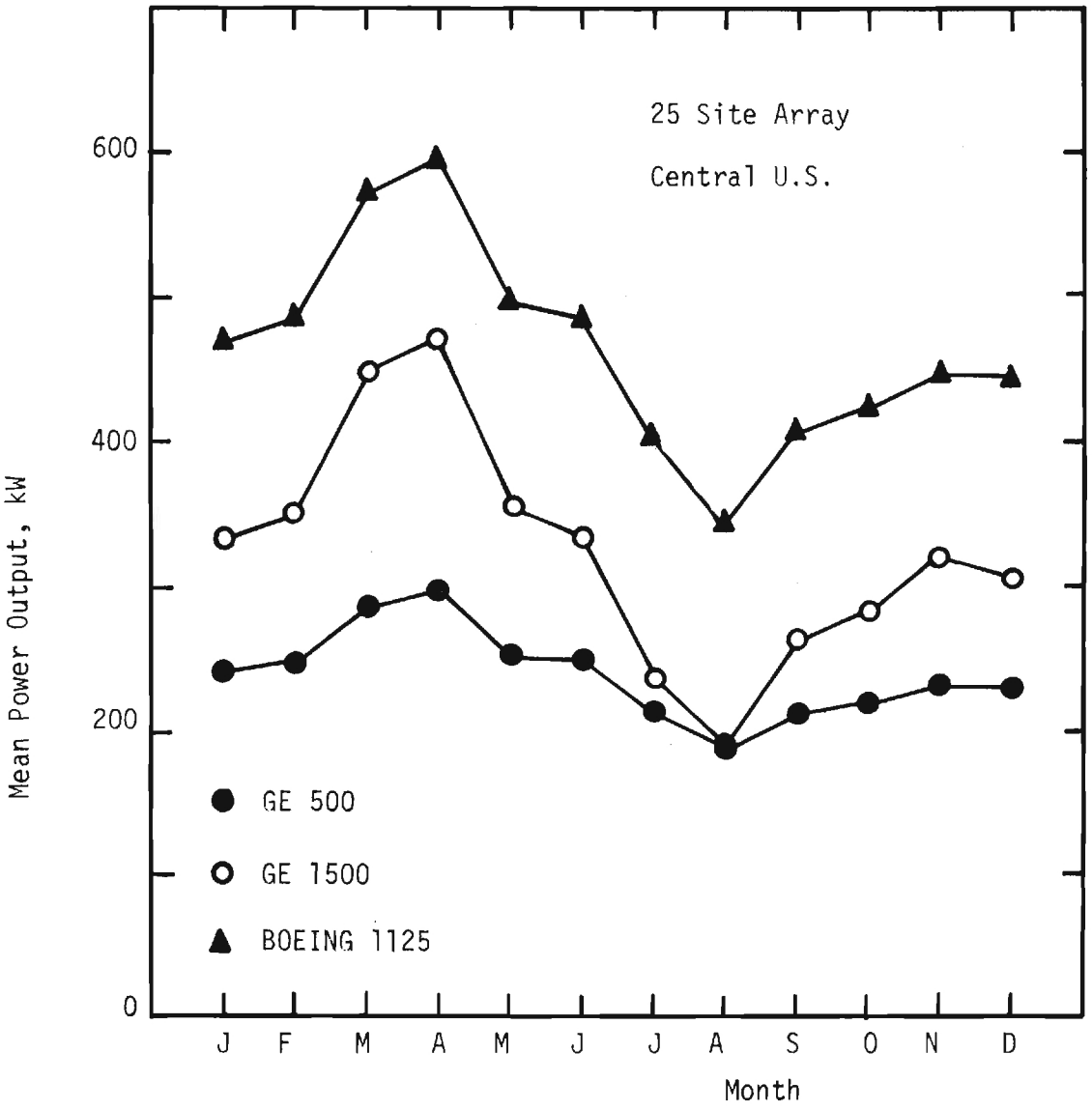

Figure 27 - Seasonal Variation of Monthly Mean Power Output for 25 Site Full Array in Central U.S.

TABLE 18

As in Table 17 for 12 Site South Central Array

Month	GE 500				GE 1500				BOEING 1125			
	$\bar{P}$	σ	MAX	MIN	$\bar{P}$	σ	MAX	MIN	$\bar{P}$	σ	MAX	MIN
JAN	233.2	17.0	249.6	204.6	316.7	26.0	337.2	272.3	451.0	32.2	480.6	396.6
FEB	248.9	37.0	310.8	22.4	355.1	97.0	521.8	283.6	485.9	83.6	627.6	424.3
MAR	299.8	27.4	336.8	268.4	475.0	92.7	605.5	375.8	596.7	65.4	684.1	522.4
APR	295.6	24.3	329.1	273.0	456.4	68.5	548.5	383.0	586.3	55.8	664.1	531.8
MAY	252.2	41.1	311.8	207.7	347.7	102.1	501.3	227.6	490.4	91.6	624.4	387.1
JUN	264.1	25.4	296.7	227.7	343.9	59.1	406.0	251.3	507.1	55.7	576.6	425.4
JUL	227.2	26.3	268.4	203.3	237.6	49.5	319.1	198.5	418.8	54.2	505.8	373.2
AUG	181.4	27.5	205.5	138.2	171.1	41.2	209.4	111.8	330.4	53.4	377.5	248.1
SEP	213.8	42.4	260.9	145.9	252.6	81.1	342.7	124.7	403.8	88.1	502.2	263.2
OCT	217.3	17.3	245.9	202.3	270.1	35.1	317.8	242.5	414.6	37.0	470.5	384.4
NOV	237.8	38.6	292.3	218.2	330.7	88.1	474.3	242.4	461.9	83.1	586.3	362.2
DEC	235.0	30.6	271.0	188.6	319.0	65.6	407.2	233.3	454.7	64.4	533.5	360.9
ANN	242.2	33.4	336.8	138.2	323.0	85.9	605.5	111.8	466.8	74.9	685.1	248.1
CF	0.48	0.07	0.67	0.28	0.22	0.06	0.40	0.07	0.41	0.07	0.61	0.22

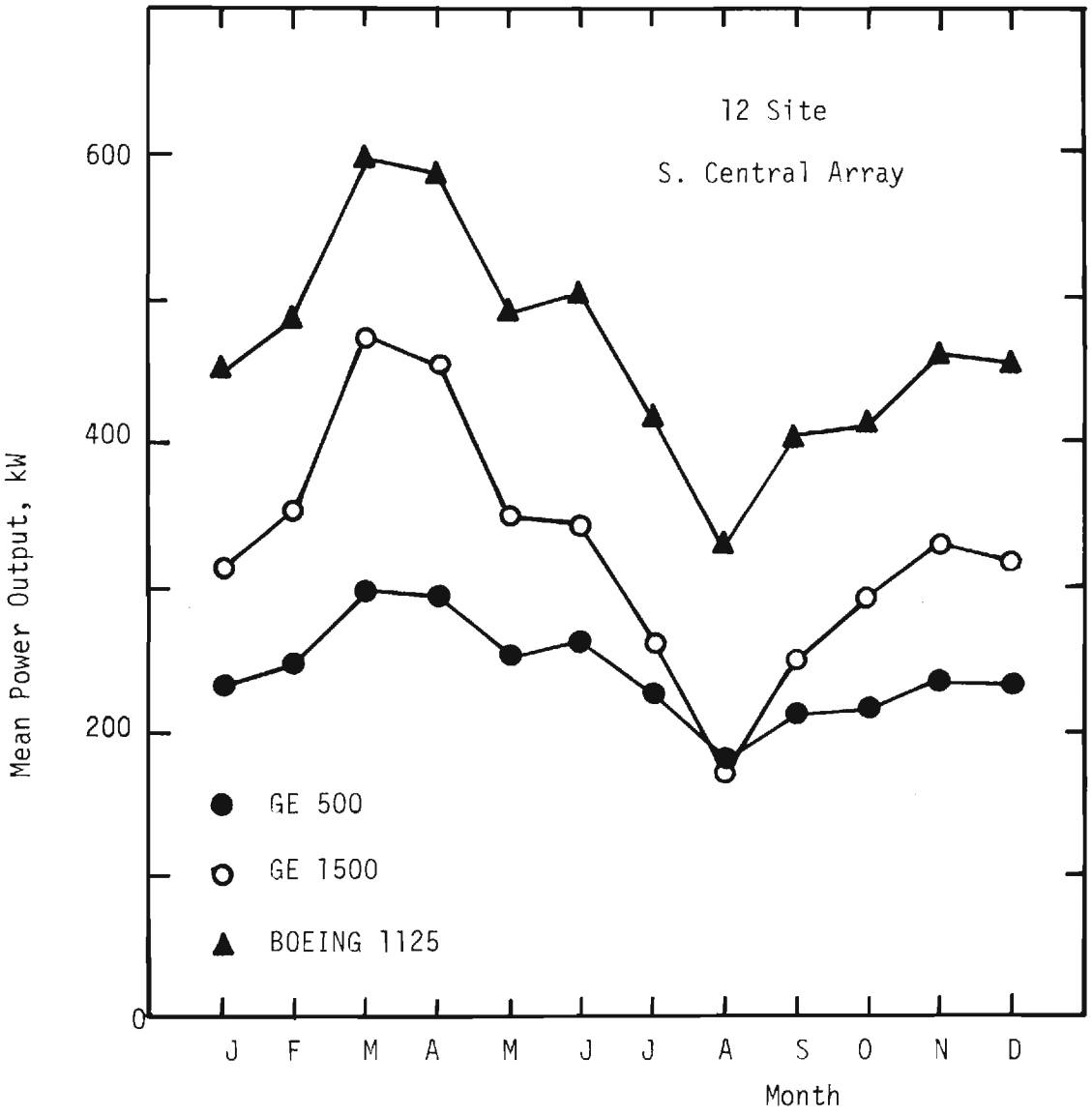

Figure 28 - Seasonal Variation of Monthly Mean Power Output for 12 Site S. Central Array.

of the set of five years. The bottom line of Tables 17 and 18 show annual average, standard deviation, maximum and minimum power in kW and also expressed as capacity factor (i.e. relative to the rated power of the wind turbine). Figures 27 and 28 show that the seasonal variations in mean output power follow in phase with the annual variation in monthly mean wind speed. Because of its higher cut-in speed and rated speed, the GE 1500 kW wind turbine is more sensitive to seasonal variations (varying seasonally from 0.55 to 1.45 times the annual mean) than the GE 500 kW and Boeing 1125 kW machines (which vary seasonally from 0.75 to 1.25 times the annual mean). Steadiest annual power output is provided by the Boeing 1125 kW wind turbine, which produces higher power levels than the 500 kW or 1500 kW machine, with less seasonal variation.

Figures 29 through 31 show, for each of the three wind turbines simulated, plots of: a) individual site monthly mean output power as a function of monthly mean speed, and b) array monthly mean output power as a function of array average monthly mean wind speed. The same linear relations as found in the New England - Middle Atlantic area (from zero power at 0.69 times cut-in speed to rated power at 1.27 times rated speed), also apply well to the data of Figures 29 - 31.

Cost Effectiveness as a Fuel Saver

From the annual mean power output, the cost effectiveness of the various wind turbine designs as a fuel saver can be evaluated, as was done for the New England - Middle Atlantic area in Table 7. Again the break-even wind turbine costs, in dollars per rated kilowatt were evaluated from Table 14.7 of Zimmer et al (1975) under the Condition 1 (pessimistic) and Condition 2 (optimistic) cases. Condition 1 assumes only proportional fuel replacement (in proportion to present mix of fuel usage), while Condition 2 assumes that

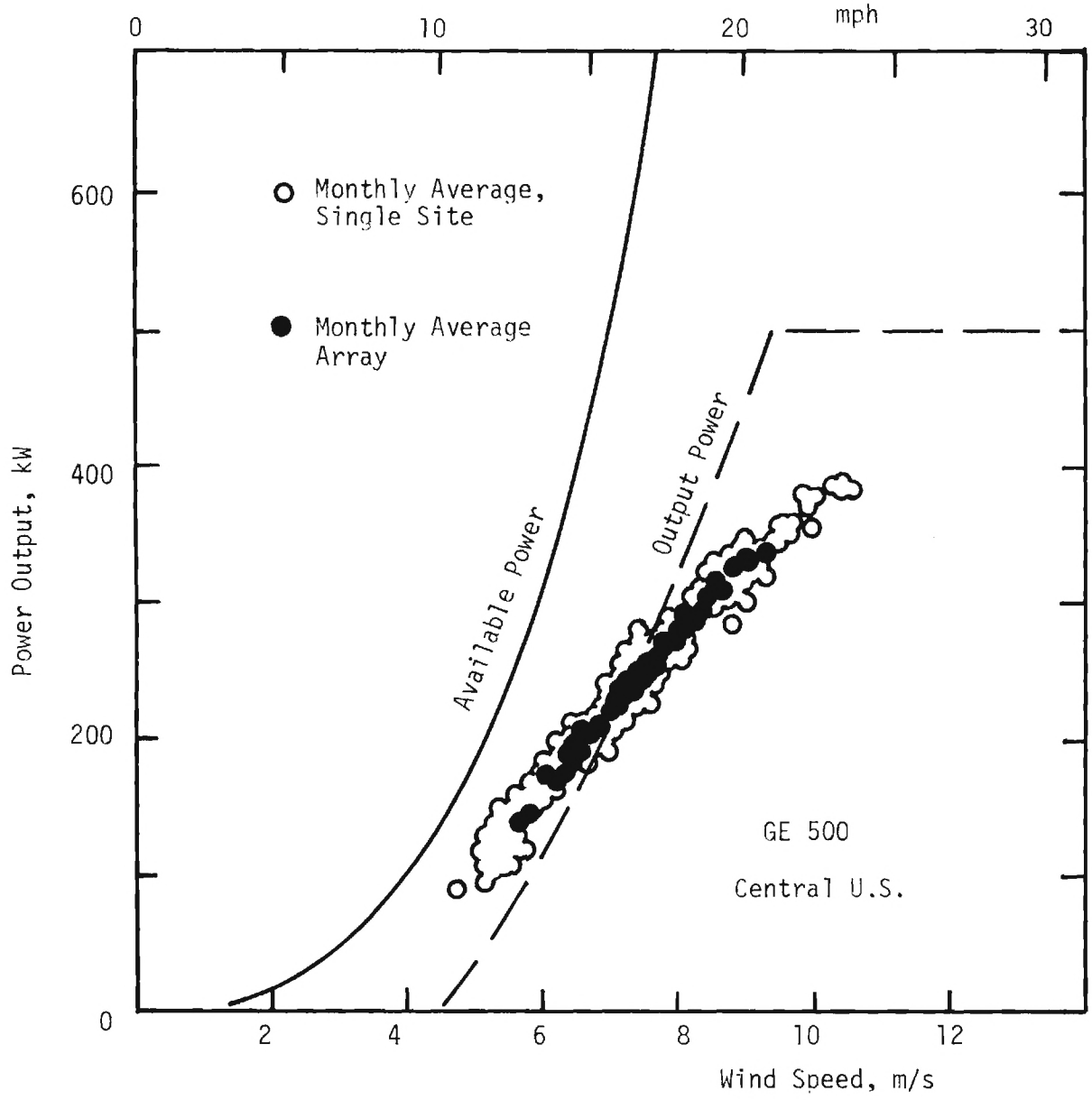

Figure 29 - Monthly Average Single Site and Array Output Power Versus Monthly Average Wind Speed for GE 500 kW Turbine in the Central U.S. Solid Line is Instantaneous Theoretically Available Power. Dashed Line is Instantaneous Output Power Versus Instantaneous Wind.

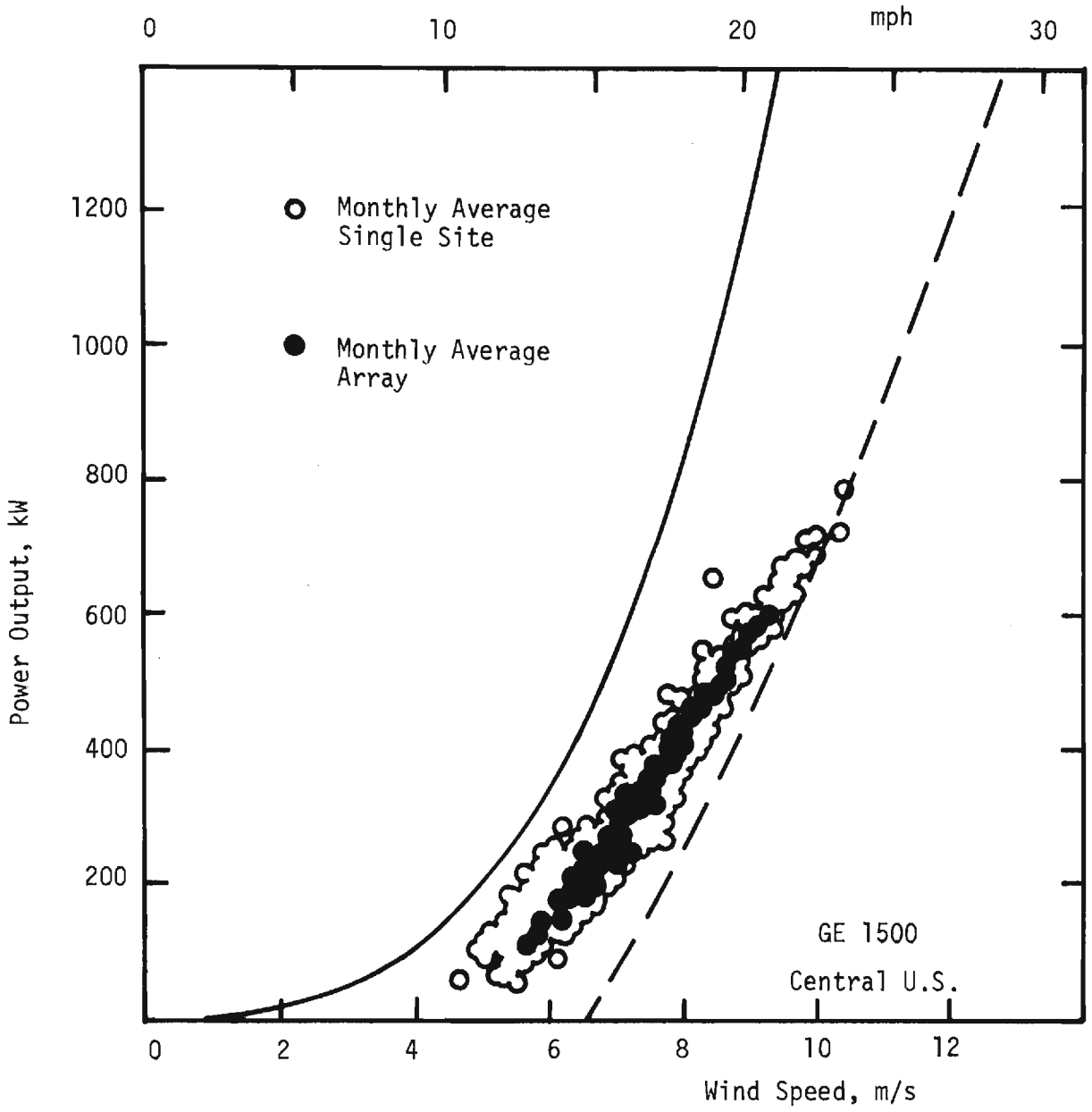

Figure 30 - As in Figure 29 for GE 1500 kW Wind Turbine.

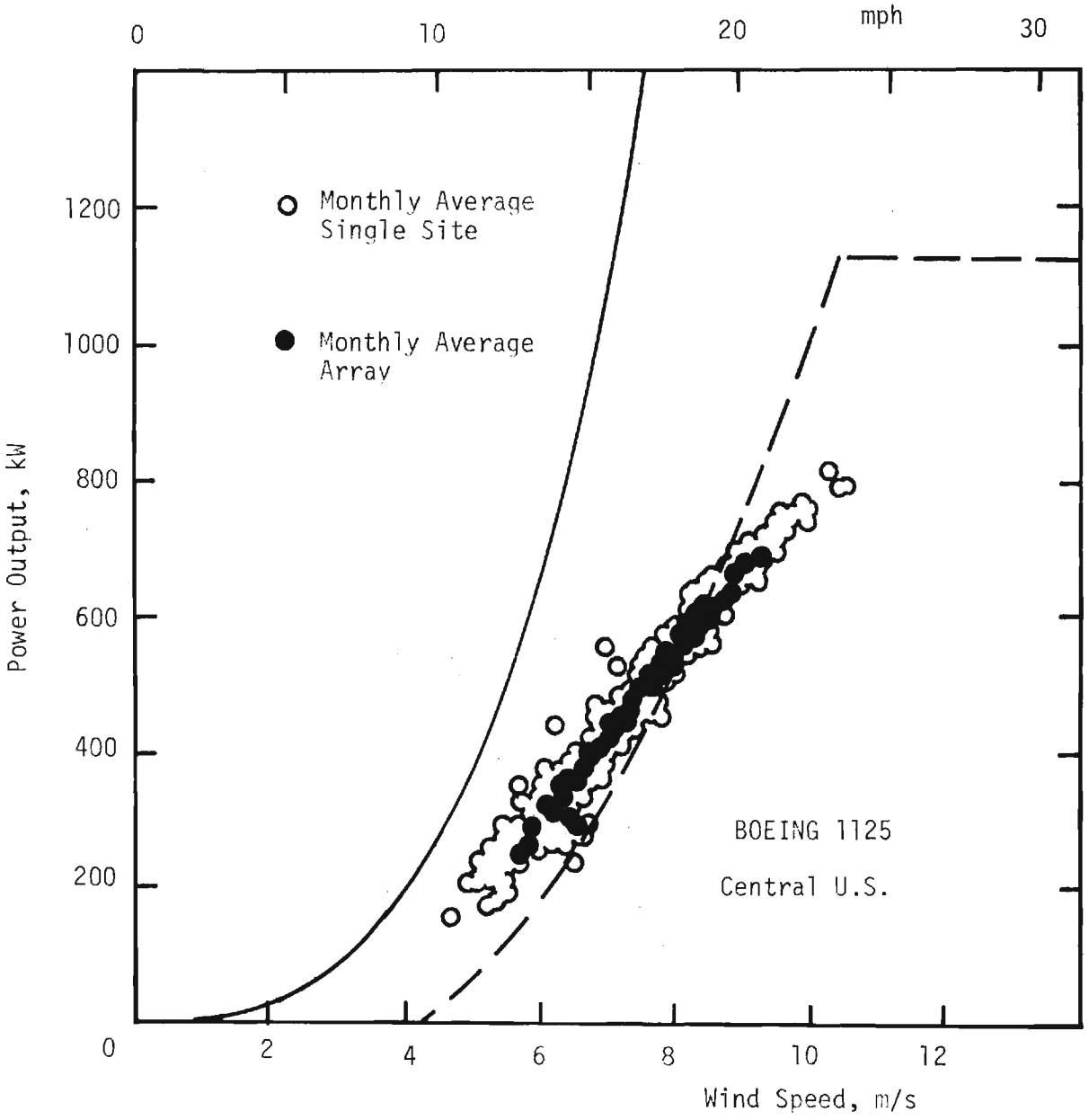

Figure 31 - As in Figure 29 for Boeing 1125 kW Wind Turbine.

wind energy replaces only the most expensive fuel. Since wind energy will be available some times when the most expensive fuel is not being used (i.e. off peak times), wind will have to replace less expensive fuels sometimes, so the true situation will fall somewhere between Condition 1 and Condition 2.

Table 19 shows, for the full 25 site Central U.S. array, the annual capacity factors, necessary break-even costs in $/kW (under Condition 1 and Condition 2), and the estimated actual production costs in $/kW for the three simulated wind turbines (General Electric, 1975; and Wiesner and Kisovec, 1976). The ratios of break-even to actual costs (which must be greater than one for cost-effectiveness) are an easy way to examine the relative cost-effectiveness of the three wind turbines under the two alternate conditions. Table 19 shows that none of the three wind turbines would be cost-effective in the Central U.S. under the pessimistic Condition 1. However, all three would be cost effective under the optimistic Condition 2. The difference between these results in Table 7 for New England and Table 19 for the Central U.S. is the high cost of fuel in New England. Thus, even though winds are better over a broader area in the Central U.S., it is not unambiguously clear that wind power is presently cost-effective there, when used as a fuel saver. The Boeing 1125 kW machine, with its high rated power at low cut-in and rated speed, comes the closest in the Central U.S. to being cost-effective under the pessimistic Condition 1. A higher technology single blade 1125 kW Boeing design (Wiesner and Kisovec, 1976) with estimated lower production costs (numbers shown in parenthesis in Table 19) would be even closer to cost-effectiveness than the two bladed Boeing 1125 kW design considered as the base unit in Table 19.

Wind Power Frequency (Reliability, with No Storage)

Frequency distributions of individual site output power or array output power were evaluated, as with the New England - Middle Atlantic area, by direct

TABLE 19

Estimated Cost-Effectiveness of Various Wind Turbines Based on Five Year Average Capacity Factors for 25 Site Central U.S. Array, as in Table 7.

Wind Turbine	GE 500	GE 1500	BOEING 1125
Annual Capacity Factor	0.48	0.22	0.41
Break-Even $/kW (Condition 1)	336	154	287
Break-Even $/kW (Condition 2)	1316	660	1139
Estimated Actual $/kW	974	449	617 (505)*
Ratio Necessary to Actual (Condition 1)	0.34	0.34	0.47 (0.57)*
Ratio Necessary to Actual (Condition 2)	1.35	1.47	1.85 (2.26)*

* Numbers in parentheses are for a higher technology single bladed rotor - the double bladed system is considered as the base unit.

counting up of simulated turbine output power values falling within various power intervals. Figures 32 through 34 show examples of the five year average January single site and array power output frequency distributions. Tables 20 and 21 give the observed cumulative frequencies of power levels within various power intervals for single sites and arrays, both for the 25 site Central U.S. array and the 12 site South Central array.

As discussed in Appendix B, the frequency distribution curves (as in Figures 32 - 34 or Tables 20 - 21) can be used to determine the improvement in power output reliability which can be achieved by dispersing the wind turbines into arrays. For example, Figure 34 shows, for the Boeing 1125 kW wind turbine, that a power output level of 200 kW per generator in the 25 site Central U.S. array is 90% reliable (10% cumulative frequency), whereas the single site power output level of 200 kW per generator is only 62% reliable (38% cumulative frequency). For 100 kW per generator power level, the 25 site Central U.S. array produces 99% reliability versus only 71% reliability for that power level in single site configuration.

Comparison of Figure 32 with Figure 14 and Figure 33 with Figure 15 illustrates the enhancement in reliability which can be achieved by increasing the number of sites in the array (from 7 in the Coastal array to 25 in the Central U.S. array) and decreasing the correlation by wider dispersal of the array (32% correlation in January for the Central U.S. array with $\bar{r}$ = 618 km, versus 64% in January for the Coastal array, with $\bar{r}$ = 198 km). For example, despite the fact that the January Coastal array produces more average power than the Central U.S. array (274 kW versus 242 kW for GE 500, 451 kW versus 334 kW for GE 1500), the Central U.S. array has significantly higher reliability for 100 kW per generator power levels than does the Coastal array

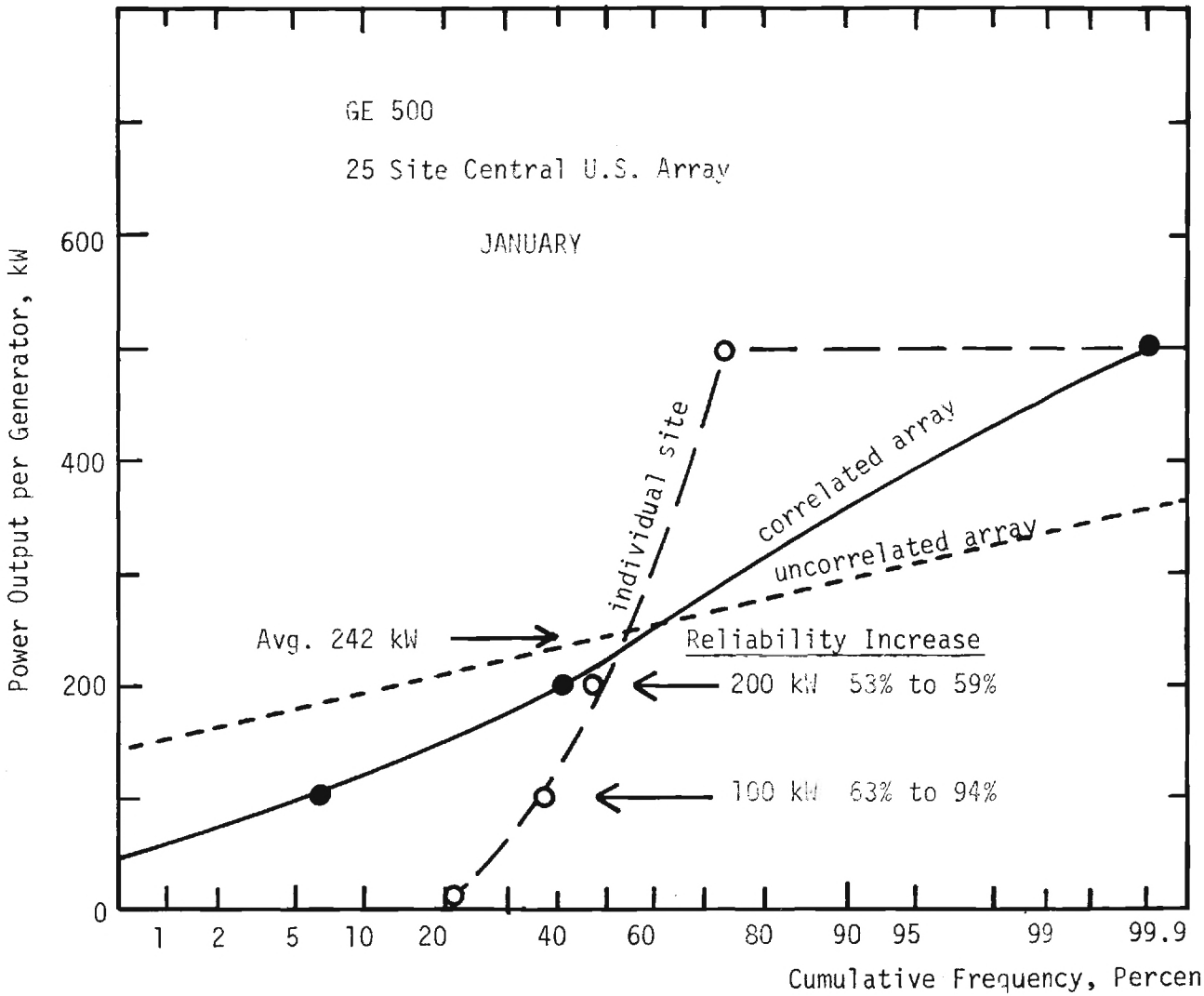

Figure 32 - Power Output Frequency Distribution for GE 500 kW Wind Turbines, 25 Site Central U.S. Array in January.

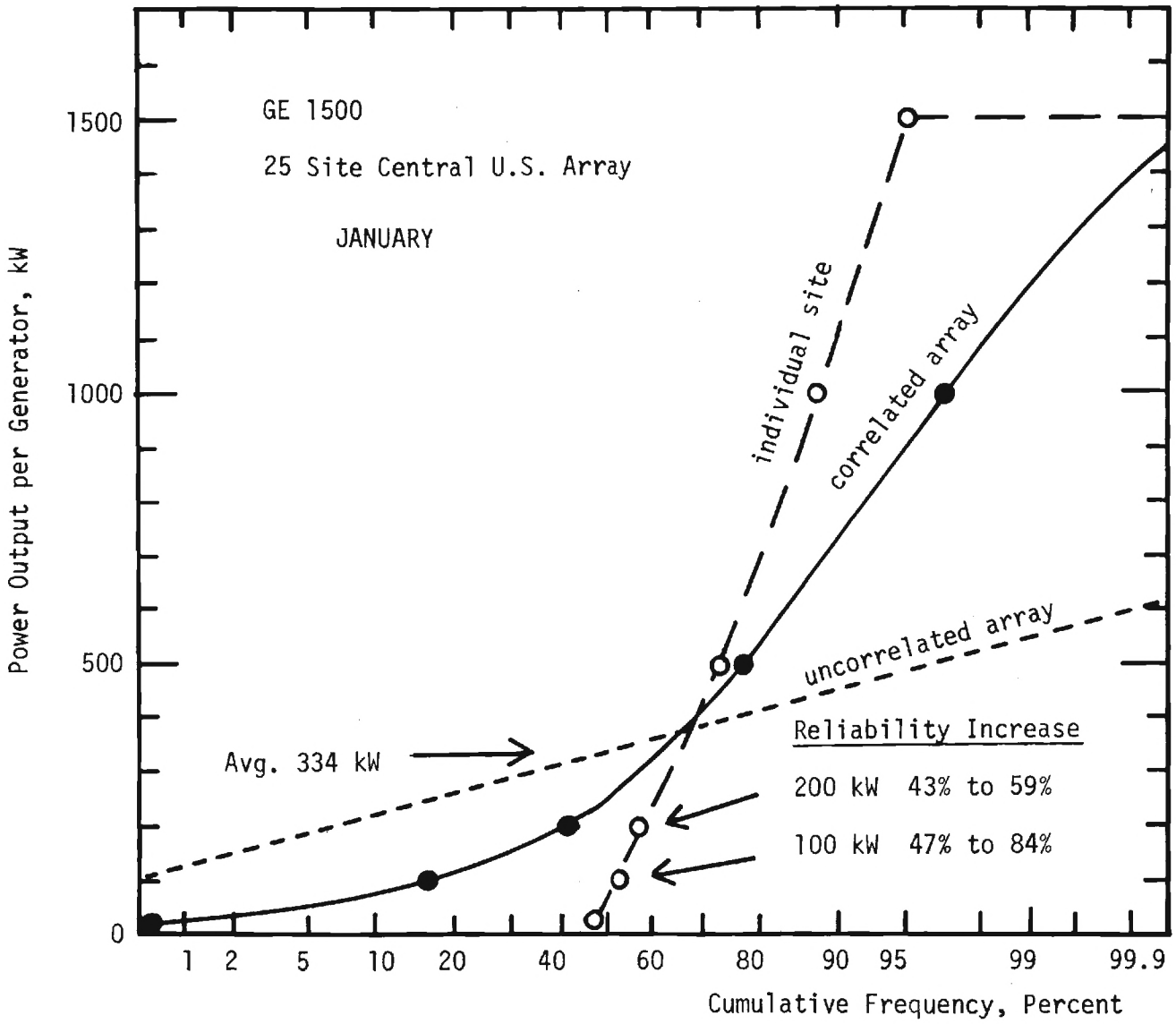

Figure 33 - Power Output Frequency Distribution for GE 1500 kW Wind Turbines, 25 Site Central U.S. Array in January.

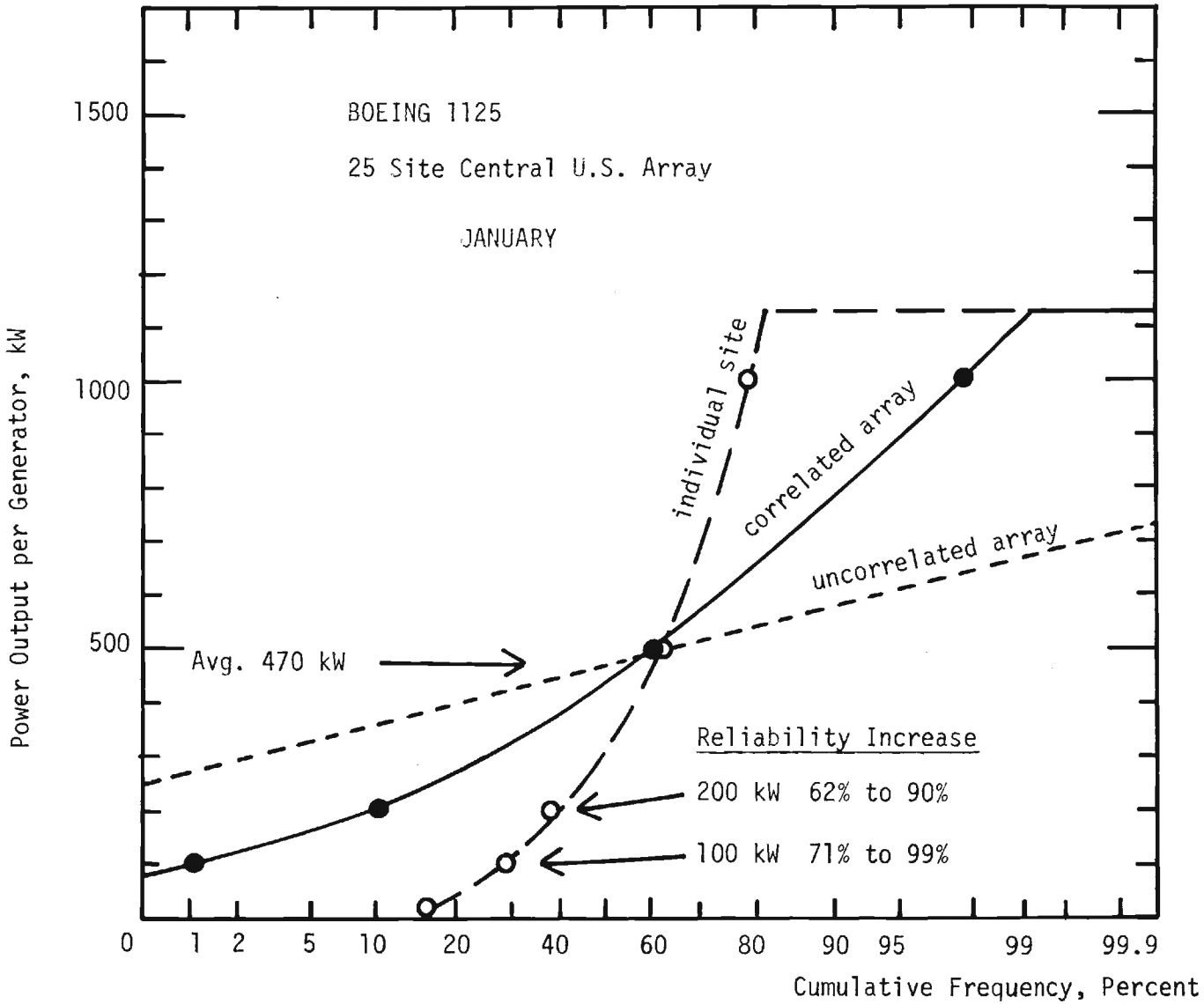

Figure 34 - Power Output Frequency Distribution for Boeing 1125 kW Wind Turbines, 25 Site Central U.S. Array in January.

TABLE 20

Five Year Average Power Output Frequency for 25 Site Full Array.
Cumulative Frequencies in Percent for Power Output Intervals Shown.

	Output Power, kW	JAN		APR		JUL		OCT	
		ARRAY	IND.	ARRAY	IND.	ARRAY	IND.	ARRAY	IND.
GE 500	0 - 10	0.0	21.1	0.0	14.7	0.0	22.1	0.0	25.3
	10 - 100	6.5	37.2	5.5	27.1	11.9	40.2	17.7	42.1
	100 - 200	41.0	47.4	22.7	36.1	46.7	52.3	47.3	52.6
	200 - 500	99.8	74.0	99.8	62.0	100.0	82.1	100.0	77.5
	≥ 500	100.0	100.0	100.0	100.0	---	100.0	---	100.0
GE 1500	0 - 10	0.6	46.7	0.8	35.6	0.9	51.5	2.7	52.0
	10 - 100	16.0	53.0	9.5	40.7	21.9	58.6	28.3	57.6
	100 - 200	41.0	56.7	22.0	44.4	49.7	63.1	47.3	61.2
	200 - 500	77.7	74.0	57.8	62.0	91.3	82.1	81.9	77.5
	500 - 1000	96.9	88.0	93.8	80.4	100.0	94.3	99.2	90.8
	1000 - 1500	100.0	95.2	100.0	91.6	---	98.7	100.0	97.2
	≥ 1500	---	100.0	---	100.0	---	100.0	---	100.0
BOEING 1125	0 - 10	0.0	16.0	0.0	10.5	0.0	15.9	0.0	19.1
	10 - 100	1.1	28.7	1.1	20.6	2.6	30.7	5.2	33.7
	100 - 200	10.2	37.8	6.9	27.7	15.7	41.0	23.0	42.7
	200 - 500	60.2	62.5	36.1	49.9	70.3	69.8	63.8	66.9
	500 - 1000	97.8	78.8	95.3	67.8	99.9	86.7	98.9	81.9
	≥ 1000	100.0	100.0	100.0	100.0	100.0	100.0	100.0	100.0

TABLE 21

Five Year Average Power Output Frequency for 12 Site South Central Array.
Cumulative Frequencies in Percent for Power Output Intervals Shown.

	Output Power, kW	JAN		APR		JUL		OCT	
		ARRAY	IND.	ARRAY	IND.	ARRAY	IND.	ARRAY	IND.
GE 500	0 - 10	0.0	21.6	0.0	13.5	0.2	17.1	0.2	23.8
	10 - 100	16.4	38.9	7.6	26.9	12.9	35.9	23.4	42.2
	100 - 200	45.2	49.0	25.2	36.0	43.7	48.6	50.0	52.6
	200 - 500	98.5	75.6	98.5	63.1	99.9	82.4	99.7	78.8
	$\geq$ 500	100.0	100.0	100.0	100.0	100.0	100.0	100.0	100.0
GE 1500	0 - 10	5.6	48.5	2.0	35.6	5.5	48.0	9.0	52.0
	10 - 100	26.6	55.0	14.3	41.1	27.9	56.1	35.4	58.1
	100 - 200	47.3	59.7	27.8	46.0	51.4	61.9	53.0	62.8
	200 - 500	78.2	75.6	58.7	63.1	88.6	82.4	81.5	78.8
	500 - 1000	95.6	88.3	92.3	81.1	99.9	95.1	98.6	91.5
	1000 - 1500	100.0	95.3	100.0	92.2	100.0	99.0	100.0	97.4
	$\geq$ 1500	---	100	---	100	---	100	---	100
BOEING 1125	0 - 10	0.0	17.6	0.0	10.2	0.2	13.3	0.1	19.2
	10 - 100	6.0	30.1	1.7	20.0	5.1	26.0	10.7	33.3
	100 - 200	19.6	38.9	9.8	26.9	16.0	35.9	27.0	42.2
	200 - 500	61.9	64.3	40.3	50.5	66.4	68.6	63.5	67.5
	500 - 1500	95.5	79.8	92.6	69.0	99.6	87.3	97.4	83.2
	$\geq$ 1000	100.0	100.0	100.0	100.0	100.0	100.0	100.0	100.0

(94% versus 83% for GE 500, 84% versus 75% for GE 1500 kW).

Return Times for Array Power (Reliability with Storage)

Table 22 shows the average, standard deviation, maximum and minimum return times in hours for the 25 site Central U.S. array for the months of January, April, July and October for array power output levels of 100 kW and 200 kW per generator. A return time is the time required after array power goes below the given power level until it returns above that level. The standard deviation of return time in Table 22 is the rms deviation of the individual year monthly mean return times for the five individual monthly time periods in the five year series. $\bar{T}_{MAX}$ is the average of the five maximum return times for the five individual monthly time periods in the five year series. σ_{MAX} is the rms deviation of the individual year monthly maximums about $\bar{T}_{MAX}$. T_{MAX} is the absolute maximum return time observed for any given month out of the five year data set.

Table 23 shows the observed frequency distribution (cumulative probability) for return times of various duration for the 25 site Central U.S. array. Figure 35 shows a sample of the data from Table 23 in graphical form. From Figure 35 it can be seen, by interpolation, that the GE 500 kW wind turbine, for example, would have 90% reliable 200 kW per generator power output if there were a storage system with about 20 hours of power storage (i.e. 4000 kW-hours storage capacity per generator, 200 kW x 20 hours).

Comparison of Power Reliability With and Without Storage

Power reliability data, without storage, from the power frequency distribution information (Table 20) can be combined with power reliability data, with storage, from the return time analysis (Table 23) to compare reliability with and without storage. These results for the 25 site Central U.S. array

TABLE 22

Average and Maximum Return Times for 25 Site Full Array and 12 Site South Central Array. $\bar{T}$ and σ are Mean Return Time and Standard Deviation in Hours. $\bar{T}_{MAX}$ and σ_{MAX} are Mean Maximum and Standard Deviation in Hours. T_{MAX} is Highest Maximum for 5 Year Data Set, in Hours.

			JANUARY					APRIL					JULY					OCTOBER				
			$\bar{T}$	σ	$\bar{T}_{MAX}$	σ_{MAX}	T_{MAX}	$\bar{T}$	σ	$\bar{T}_{MAX}$	σ_{MAX}	T_{MAX}	$\bar{T}$	σ	$\bar{T}_{MAX}$	σ_{MAX}	T_{MAX}	$\bar{T}$	σ	$\bar{T}_{MAX}$	σ_{MAX}	T_{MAX}
25 Site Full Array	100 kW/Gen	GE 500	6	1	13	6	18	6	2	11	1	12	6	1	13	1	15	9	2	18	2	21
		GE 1500	8	3	21	11	39	6	2	13	2	15	7	1	17	3	21	10	1	27	12	42
		Boeing 1125	2	2	4	4	9	3	3	3	3	6	4	2	7	4	12	6	1	13	3	15
	200 kW/Gen	GE 500	15	2	41	5	45	10	1	20	9	36	12	3	49	25	84	16	7	58	21	90
		GE 1500	13	3	40	6	45	9	2	19	6	30	12	2	50	20	84	18	3	63	19	90
		Boeing 1125	7	3	19	10	36	7	2	11	1	12	11	10	41	64	156	9	2	19	3	21
12 Site S. Central Array	100 kW/Gen	GE 500	8	3	23	11	42	5	1	11	5	18	6	1	15	4	21	10	2	24	7	36
		GE 1500	9	3	34	15	54	7	2	17	3	21	6	1	27	12	39	12	4	47	14	72
		Boeing 1125	7	2	13	5	18	6	2	9	7	21	5	2	7	3	12	6	2	11	4	15
	200 kW/Gen	GE 500	16	6	53	24	90	10	2	29	11	39	10	3	48	21	84	18	5	7	13	96
		GE 1500	15	5	56	25	90	10	3	37	17	60	12	3	45	10	60	20	5	94	28	132
		Boeing 1125	9	3	25	12	45	6	1	13	3	18	7	1	16	4	21	11	3	36	7	39

TABLE 23

Return Time Probability Distribution for 25 Site Full Array. Cumulative Frequencies are Given in Percent for Return Times Within Intervals Shown.

	Time Interval, Hours	GE 500				GE 1500				BOEING 1125			
		JAN	APR	JUL	OCT	JAN	APR	JUL	OCT	JAN	APR	JUL	OCT
100 kW Return Time	0 - 4	53.8	51.7	44.1	31.9	40.5	50.0	47.1	23.5	71.4	66.7	71.4	43.3
	4 - 8	71.8	62.1	67.6	47.8	66.2	69.2	66.4	42.9	85.7	100.0	85.7	70.0
	8 - 16	94.9	100.0	100.0	94.2	87.8	100.0	98.3	85.7	100.0	---	100.0	100.0
	16 - 32	100.0	---	---	100.0	98.6	---	100.0	98.0	---	---	---	---
	32 - 64	---	---	---	---	100.0	---	---	100.0	---	---	---	---
	64 - 128	---	---	---	---	---	---	---	---	---	---	---	---
200 kW Return Time	0 - 4	15.0	21.3	25.0	14.7	22.6	25.6	25.9	15.6	41.2	36.4	50.6	32.6
	4 - 8	34.0	35.0	41.7	24.2	40.9	45.1	42.2	29.2	66.7	54.5	67.4	52.3
	8 - 16	62.0	95.0	86.1	62.1	69.6	95.1	80.3	63.5	94.1	100.0	98.9	91.9
	16 - 32	89.0	98.8	95.1	85.3	93.9	100.0	93.2	84.4	98.0	---	100.0	100.0
	32 - 64	100.0	100.0	98.6	98.9	100.0	---	99.3	97.9	100.0	---	---	---
	64 - 128	---	---	100.0	100.0	---	---	100.0	100.0	---	---	---	---

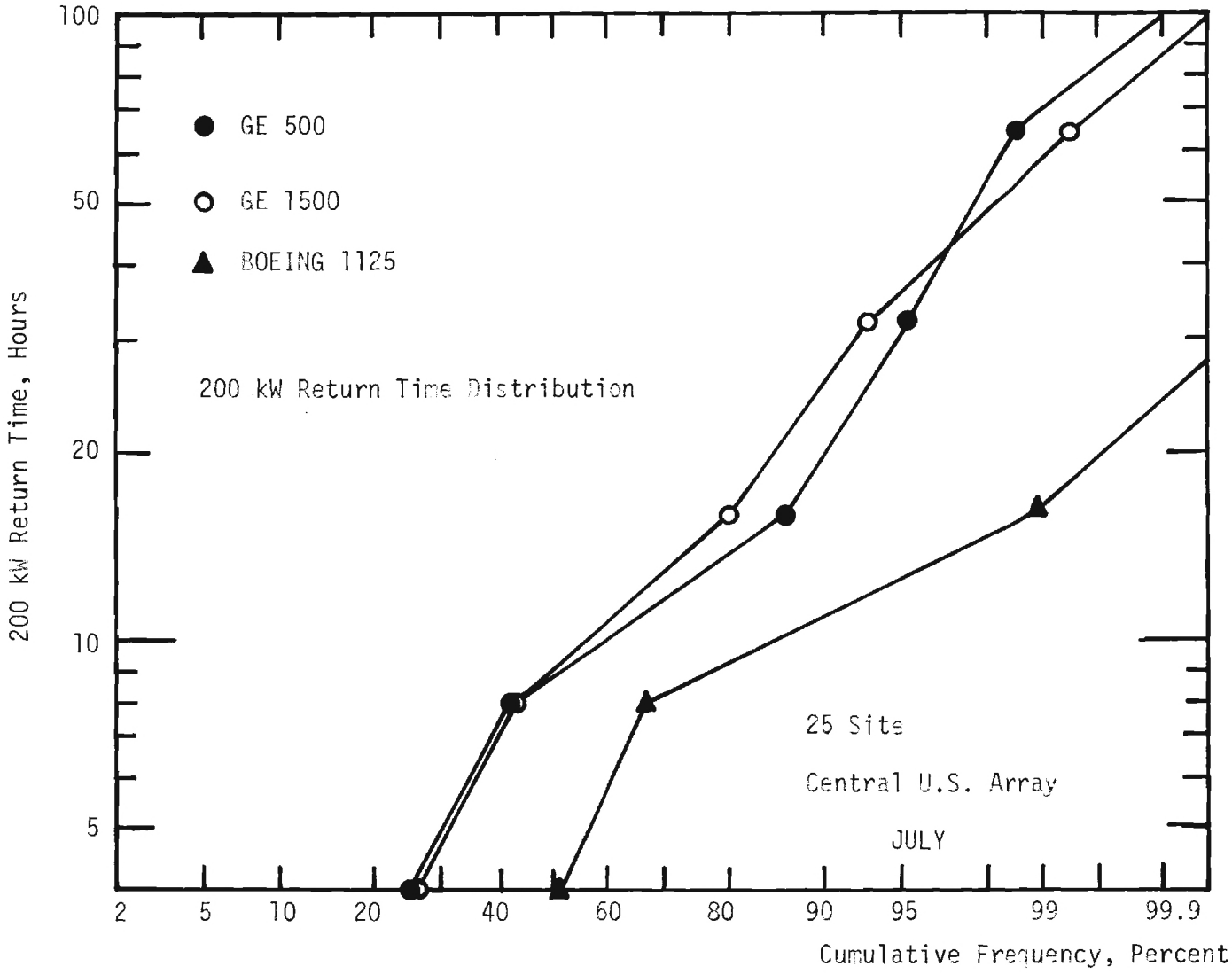

Figure 35 - Frequency Distribution of 200 kW Return Times for 25 Site Central U.S. Array in July.

are shown, for the months of January, April, July, and October, in Table 24. Comparison of reliability levels of 10 kW power per generator, without storage, in the single site and array configuration shows that this small level of power is virtually always available from the arrays.

For 100 kW and 200 kW per generator, Table 24 compares reliabilities in percent for individual sites and arrays without storage (T = 0), and the storage time, in hours, required to produce the given array power levels with 90%, 95%, and 99% reliability, Note that the good wind environment in the Central U.S. always produces improved reliability from the array configuration, even at the 200 kW per generator power level from the lower power 500 kW GE unit. Considerably less storage time is required in the Central U.S. to achieve given reliability than was needed for the Coastal New England array (c.f. Table 12). Best reliability is achieved with the Boeing 1125 kW wind turbine, for which, in the Central U.S. area, about 24 hours of storage or less would supply 99% reliable power at the level of 200 kW per generator.

4. DIURNAL VARIATIONS AND PEAK LOAD DISPLACEMENT

Although beyond the scope for detailed analysis under this study grant, some preliminary information on diurnal variations has been obtained, which indicates that significant peak load displacement might be possible with wind power, without resort to storage. These preliminary results are shown in Figures 36 through 39.

Figures 36 and 38 show five year average (1971-1975) January and July diurnal cycle winds for Boston (New England area) and Oklahoma City (Central U.S. area). These data were taken from monthly average winds by time of day, as published by NOAA in the Local Climatological Data for these two cities.

TABLE 24

Reliability of Power Levels of 10, 100, and 200 kW per Generator With and Without Storage, 25 Site Full Array or Individual Sites. T is Storage in Hours, R is Reliability in Percent. T = 0 Indicates No Storage.

		JANUARY						APRIL						JULY						OCTOBER					
		GE 500		GE 1500		BOEING 1125		GE 500		GE 1500		BOEING 1125		GE 500		GE 1500		BOEING 1125		GE 500		GE 1500		BOEING 1125	
		T hrs.	R %	T hrs.	R %	T hrs.	R %	T hrs.	R %	T hrs.	R %	T hrs.	R %	T hrs.	R %	T hrs.	R %	T hrs.	R %	T hrs.	R %	T hrs.	R %	T hrs.	R %
10 kW/Gen	IND.	0	79	0	53	0	84	0	85	0	64	0	90	0	78	0	49	0	84	0	75	0	48	0	81
	ARRAY	0	100	0	99	0	100	0	100	0	99	0	100	0	100	0	99	0	100	0	100	0	99	0	100
100 kW/Gen	IND.	0	63	0	47	0	71	0	73	0	59	0	79	0	60	0	41	0	69	0	58	0	42	0	66
	↑	0	94	0	84	0	99	0	95	0	91	0	99	0	88	0	78	0	97	0	82	0	72	0	95
	A	13	90	17	90	9	90	10	90	10	90	5	90	10	90	11	90	9	90	14	90	19	90	10	90
	R	16	95	22	95	10	95	11	95	11	95	5	95	11	95	13	95	10	95	16	95	24	95	11	95
	↓	21	99	35	99	12	99	13	99	13	99	6	99	13	99	18	99	12	99	22	99	39	99	13	99
200 kW/Gen	IND.	0	53	0	43	0	62	0	64	0	56	0	72	0	48	0	37	0	59	0	47	0	39	0	57
	↑	0	59	0	59	0	90	0	77	0	78	0	93	0	53	0	50	0	84	0	53	0	53	0	77
	A	33	90	27	90	13	90	14	90	14	90	10	90	20	90	25	90	11	90	36	90	38	90	15	90
	R	37	95	34	95	18	95	16	95	16	95	11	95	32	95	36	95	13	95	45	95	49	95	18	95
	↓	46	99	54	99	37	99	34	99	21	99	13	99	69	99	58	99	16	99	66	99	78	99	24	99

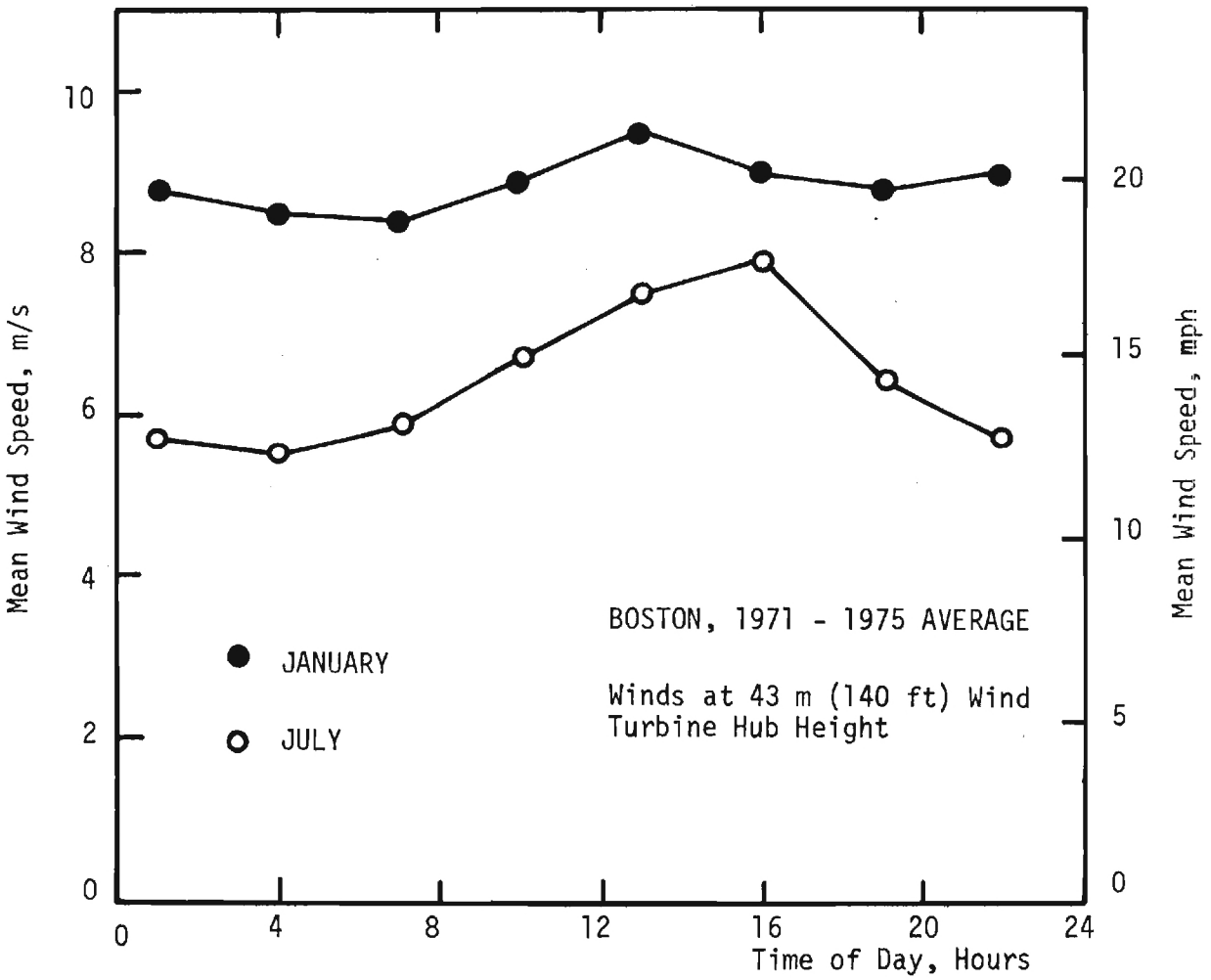

Figure 36 - Five Year (1971-1975) Average Diurnal Cycle Winds for Boston in January and July. Winds are Adjusted to 43 m (140 ft) Wind Turbine Hub Height by Methods Described in Appendix A.

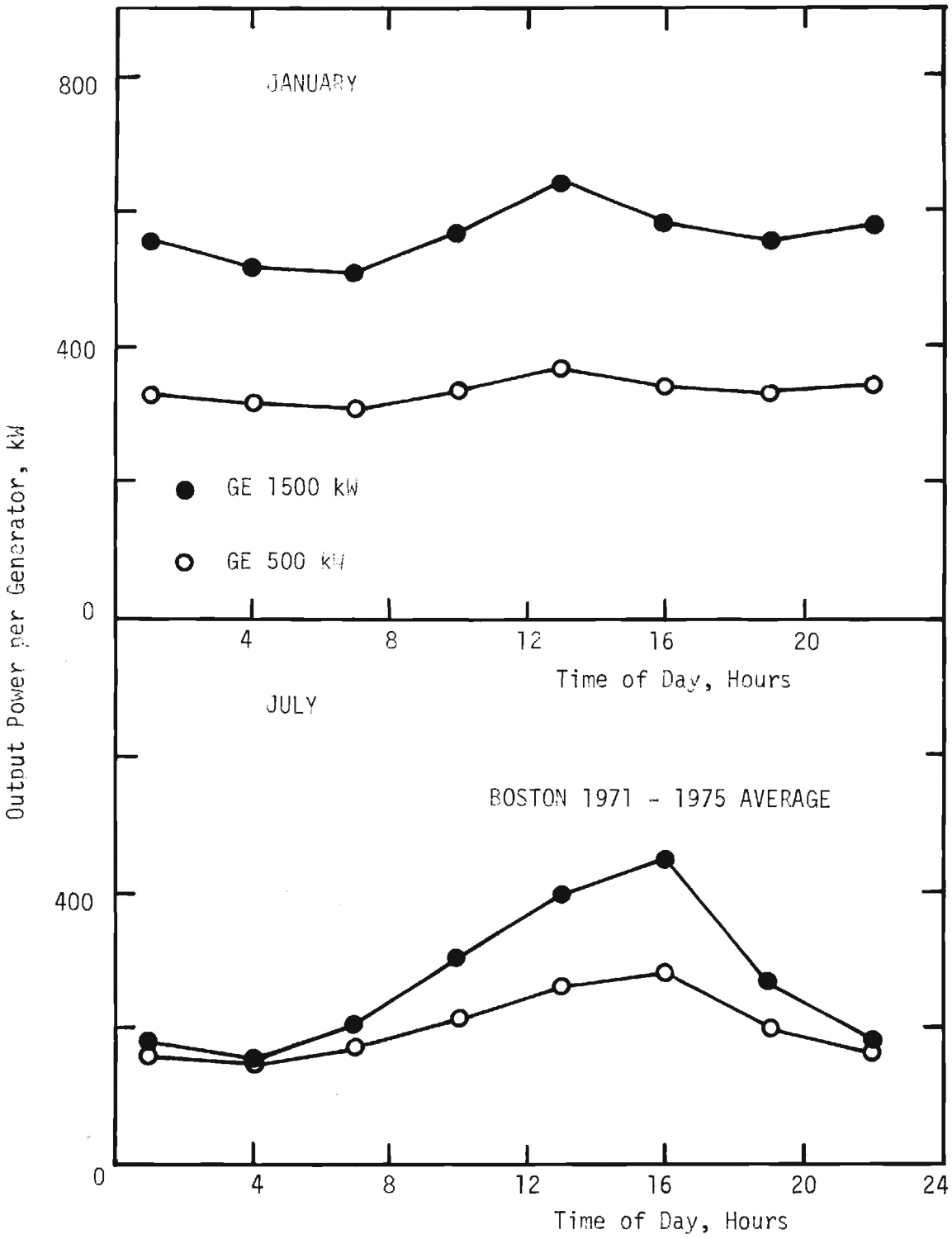

Figure 37 - Mean Power Output for GE 500 kW and GE 1500 kW Wind Turbines Versus Time of Day in January and July (Boston), based on Wind Data from Figure 36 and Power Versus Wind Speed Relations from Figures 10 and 11.

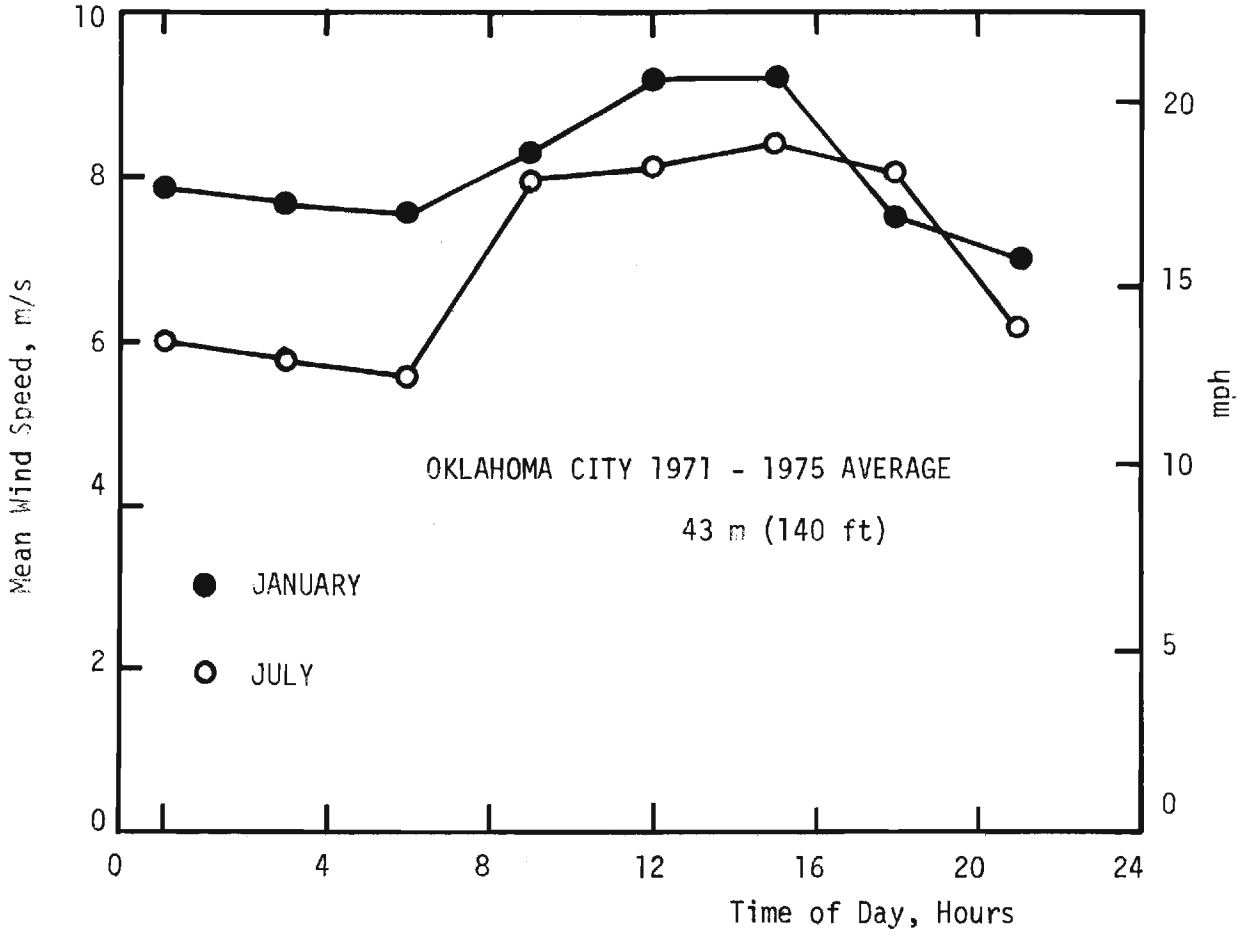

Figure 38 - Five Year (1971-1975) Average Diurnal Cycle Winds for Oklahoma City in January and July. Winds Adjusted to 43 m (140 ft) Wind Turbine Height.

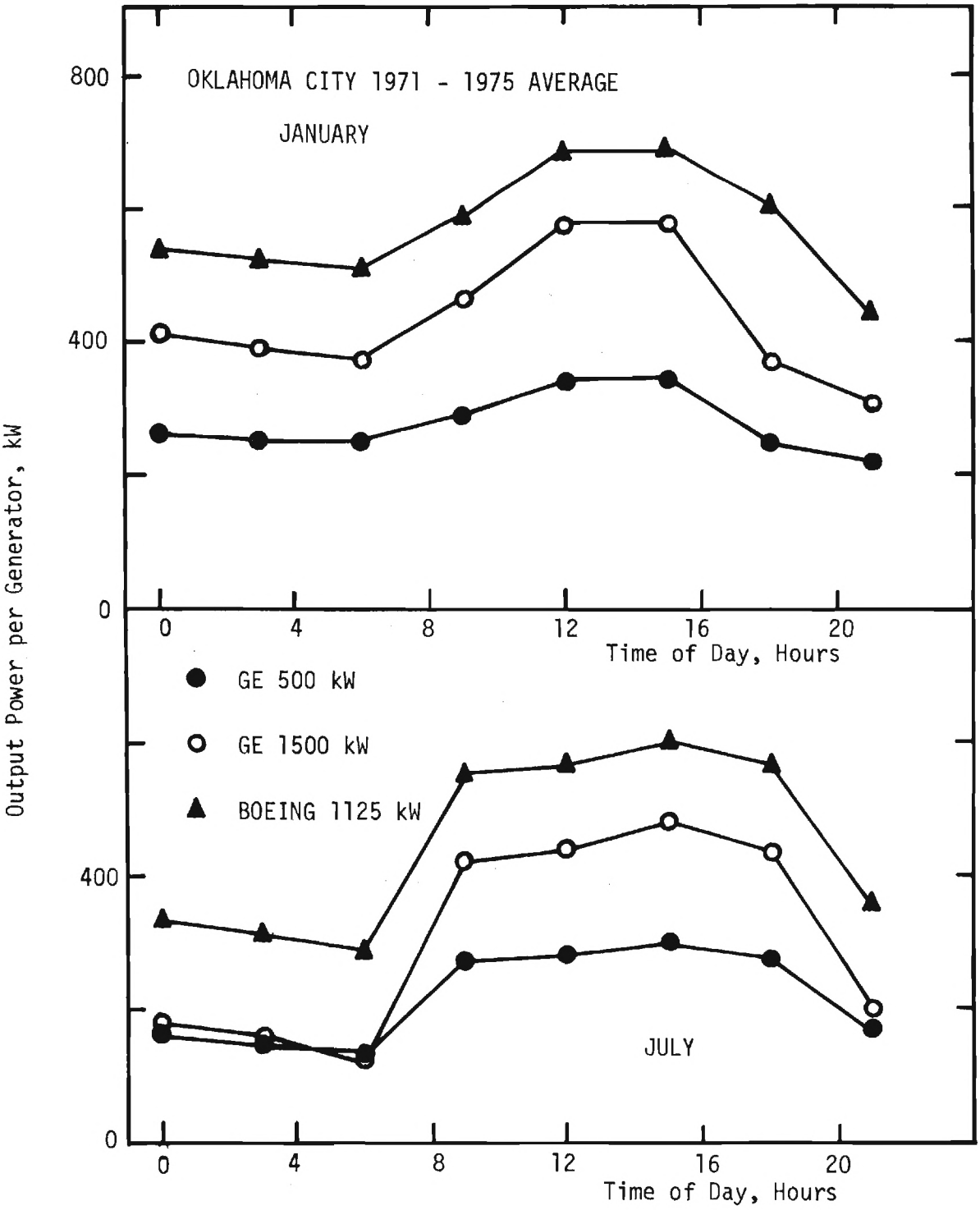

Figure 39 - Mean Power Output for GE 500 kW, GE 1500 kW, and Boeing 1125 kW Wind Turbines Versus Time of Day in January and July (Oklahoma City), Based on Wind Data from Figure 38 and Power Versus Wind Speed Relations from Figures 29-31.

Winds were adjusted from anemometer height to 43 m (140 ft) simulated wind turbine hub height by the methods described in Appendix A. Figures 37 and 39 show estimated January and July diurnal cycle mean power output from GE 500 kW, GE 1500 kW and Boeing 1125 kW wind turbines for these two cities. These data were evaluated by taking the diurnal cycle mean winds (Figure 36 or 38) and using them in the linear relationships for power versus mean wind which approximates the data of Figures 10 and 11 (Boston) or Figures 29 - 31 (Oklahoma City).

Figures 36 and 38 confirm the results of the time autocorrelation analysis (Figures 3, 4, 21, 22, and 23), which indicate little diurnal influence in winter and strong diurnal influence in summer. Figure 36 shows the diurnal winds for Boston in January vary daily from 94% to 107% of the daily average, while the July daily winds vary from 86% to 123% of the July daily mean. Similarly Figure 38 shows that diurnal winds in Oklahoma City vary from 87% to 114% of the daily mean in January but from 80% to 119% of the daily mean in July. These diurnal wind variations are reflected in the diurnal power variations in Figures 37 and 39, both of which show strong afternoon peaks in power output during summer (July), which coincide with the summertime peak load due to air conditioning demand. In contrast the wintertime (January) wind power is both higher on the average, and steadier over the diurnal cycle.

Best performance is again provided by the Boeing 1125 kW wind turbine which produces highest mean and peak afternoon power levels, but (because of its lower cut-in and rated speeds) does not suffer the low nighttime values of the GE 1500 kW wind turbine.

The strong summertime afternoon wind power output, corresponding in

time to the air conditioning peak demand, means that significant peak load displacement can be achieved with wind power, without resort to storage. In effect, because of the correspondence between available wind and peak load, reliabilities of wind power for summertime peak load displacement are better than the average basis given in Tables 12 and 24 would indicate. Also, in terms of cost effectiveness as a fuel saver, the summertime correspondence of available wind with peak load means that Condition 2 (most expensive fuel replacement) will be more nearly correct than Condition 1 (only proportional fuel replacement), so the cost effectiveness of the wind turbines studied would likely be better than the average basis of Tables 7 and 19 would indicate.

These conclusions regarding diurnal variations are, of course, tentative because of the preliminary nature of their data and analysis method. Diurnal variations and the resultant implications on peak load displacement, power reliability, and cost-effectiveness will be studied in detail during continued research under ERDA sponsorship.

5. CONCLUSIONS AND RECOMMENDATIONS

Conclusions

While interpreting the results presented here, one should keep in mind the caveats outlined in the Disclaimer (page ix), namely: 1) the machines simulated here have not actually been built and hence the performance and cost data used here cannot be guaranteed, and 2) the airport wind environment data used in this study are not necessarily representative of either the actual operating environment which will be selected for real wind turbines or the wind environment for which the machine designs were optimized. Keeping these points in mind, one can make the following conclusions from the study results reported here:

Wind Turbine Performance - Good performance of wind turbines such as the 500 kW and 1500 kW units studied in this report can be expected in the Coastal area of New England and throughout the Central U.S. area studied. In these areas, 500 kW units could be expected to average 240 kW annually with monthly averages varying between about 180 kW and 290 kW. Since the 1500 kW units simulated in this study have operating characteristics equivalent

to the design specifications of the ERDA Mod 1 unit, the 1500 kW ERDA Mod 1 unit could produce an annual average of about 330 kW, with monthly averages varying between about 190 kW and 480 kW.

Improved Performance - Further improvements in power output performance might be achieved by going to designs with lower cut-in and rated speeds (hence larger blade diameters) than the 1500 kW ERDA Mod 1 design. Studies of an 1125 kW design of this type indicated that, in the Central U.S., an annual average power of about 460 kW could be achieved, with monthly averages ranging between about 330 kW and 590 kW.

Cost Effectiveness as Fuel Saver - Despite comparable wind regimes in Coastal New England and in the Central U.S., wind power would be more cost-effective as a fuel saver in the New England area, because of the higher costs of fuels used in this region. Details on how cost effective wind power will be as a fuel saver depends on the reliability with which wind energy can replace the expensive peak load fuels (c.f. Tables 7 and 19).

Array Power Reliability - Dispersal of wind turbines into large (500 - 1000 km diameter) arrays enhances the reliability (and hence cost-effectiveness) with which they can produce power. For large arrays made up of several sites, each site of which may be a wind energy "farm" with several wind turbines, the array output reliability can be enhanced by decreasing the average inter-site correlation or by increasing the number of quasi-independent array sites (see Appendix B). Reliability increases also depend on the wind turbine design and seasonal variations, but for example, in April, for the 25 site Central U.S. array, 200 kW generator power output can be increased to about 80% by the use of arrays of GE 500 or 1500 kW units, versus about 60% reliability if all the wind turbines were at a single location. Under similar circumstances, 200 kW per generator power levels from the Boeing 1125 kW unit would be increased to about 90% (from about 70%) by going to the array configuration (c.f. Table 24).

Spatial and Locational Effects - Spatial cross correlation studies of various size arrays show that correlation decreases steadily with array size, but array sites remain positively correlated out to separations of at least 1000 km.

Certain mountain or rolling terrain sites showed unusually low correlations, with neighboring sites, but not consistently for all months. If array sites could be selected which had low inter-site correlations, this would improve the reliability of array power output.

Reliability with Storage - Depending on season, about 24 to 48 hours of storage would be required to bring the reliability of 200 kW per generator from the 1500 kW ERDA Mod 1 unit up to 95% (c.f. Tables 12 and 24). From 12 to 18 hours of storage would be adequate to achieve 95% reliable 200 kW per generator power levels with the 1125 kW design studied, and about 24 hours of storage would produce almost 99% reliable 200 kW per generator power levels from the 1125 kW unit.

Diurnal Wind and Load Demand Cycles - Analyses of diurnal cycles of mean winds from New England and Central U.S. (c.f. Figures 36 and 38) indicate that high wind power is available during summertime afternoons, corresponding to summertime air conditioning load demands. This correspondence of available wind power with peak demands in the summer may mean that even better peak load displacement, reliability, and cost-effectiveness as a fuel saver might be achieved than indicated by the diurnally averaged results in this report.

Time Autocorrelation Analysis - The strong diurnal cycle in summertime winds was also indicated by the time autocorrelation studies (c.f. Figures 4, 22, and 23). In contrast, the diurnal cycle has little influence in winter months (c.f. Figures 3 and 21). The time autocorrelation analyses show that 3 hour spacing of wind data is adequate to resolve the important diurnal and synoptic scale influences on the winds (at least in a statistical sense).

Mean Power versus Wind Speed - Mean monthly output power versus monthly mean wind speed for the various wind turbines studied was found to be represented

well (at least as an approximate relationship) by a linear function going from zero power at about 0.69 times the cut-in speed to rated power at about 1.27 times the rated speed (c.f. Figures 10-13 and 27-29). Although variance of the wind speed about the mean is another important factor (Justus, Hargraves, and Yalcin, 1976), this relationship of mean power to mean speed could be useful for first order estimates.

Recommendations

The research results reported here have, of course, only partially answered the questions raised or met the goals outlined in the Introduction. Further study along the lines outlined below is recommended:

Diurnal Analysis - More complete diurnal analysis than reported in Section 4, with mean power output and array power reliability evaluated versus time of day from hourly (or 3 hour) time series data.

Correlation of Available Wind Power with Load Demand - The high wind power available in summertime afternoons (c.f. Section 4) indicates good correlation of summertime available wind power with air conditioning load demand. Correlations with cooling degree days (summer) and heating degree days (winter) would provide additional data on the relationship between available wind power and electric utility demand. Direct correlation with utility load data would be even better. From such studies, the reliability with which expensive peak load fuels can be replaced would be better determined.

Improved Energy Storage Analysis - Time series analysis of energy storage charge and discharge cycles would provide better information on storage requirements than the return time analysis presented here. Such an analysis would be performed by assuming some desired continuous or cyclic power demand on the wind generators, with the storage system being charged when array power exceeded the requirement and discharged when it fell short of the requirements. An accurate

assessment of the reliability provided by storage could thus be made, for various storage capacities, by performing a time series simulation of the storage status (i.e. amount of kW hours available in storage). This method would be more accurate than the return time analysis because an extended period during which storage is required could begin with the storage already partially exhausted, instead of fully charged (as the return time analysis implies).

Correlation of Available Wind Power with Available Solar Power - It is expexted that available wind power and solar power may be in positive correlation with one another on some time scales and during some seasons, and negatively correlated on other time scales and during other seasons. Under the hypothesis that an ideal alternate energy system - both on an individual home scale and on a utility power production scale - may be combined solar and wind, it is recommended that the interrelationship of these two energy forms be investigated. The high wind power availability in summertime afternoons, discussed in Section 4, would indicate positive correlation, on a diurnal time scale, between sun and wind energy forms during this season. However, stronger winds are likely to occur during frontal passages (cloudy weather) during winter - so during this season sun and wind energy systems would complement each other. These relationships are likely to depend on geography also - being different, for example, at coastal sites than at inland sites.

Simple Relations Between Mean Wind Speed and Mean Wind Power - Further development of the method to relate monthly mean wind to monthly mean power (e.g. Figures 10-13 and 29-31) is recommended. This type of method will be useful for first

order estimates of potential wind power output from prospective sites. However, the general relationship between the mean power versus mean wind curve and the wind turbine characteristics (e.g. cut-in and rated speed) is not yet completely understood.

Improvement of Instantaneous Power Output Model - The instantaneous power output from a wind turbine is presently being modeled by a curve such as shown in Figure A-1 or analytically be equation (A-8). In contrast to the smooth curve of Figure A-1, the actual power output versus instantaneous wind has considerable scatter, as shown by Figure 40. This scatter is contributed to by a number of factors, some electromechanical (e.g. fluctuations in blade pitch control or in generator output regulation) and some meteorological (e.g. density variations, wind gusts, shear and direction shifts). Detailed comparisons of meteorological data with actual wind turbine performance are recommended so that relation A-8 may be modified to incorporate explicitly these meteorological factors as much as possible. In a similar vein, meteorological tower data should be more extensively studied in order to improve, if possible, the height variation technique (equations A-1 through A-4) currently being used (e.g. to account for atmospheric stability and surface roughness influence).

Development of Synoptic Wind Power Forecast Techniques - For large arrays of wind turbines, such as visualized in this study, to be effective at peak load displacement, their available wind power output must be predicted at least 24 hours in advance (for utility load scheduling and utility interconnect power purchasing arrangements). The time autocorrelation studies reported here indicate almost no correlation at a time displacement of 24 hours in winter, and only about 30% correlation over 24 hours during summer (when the strongest diurnal influences are felt). Two concepts of wind power forecasting should be investigated: 1) utilization of, and improvement in, the National Weather

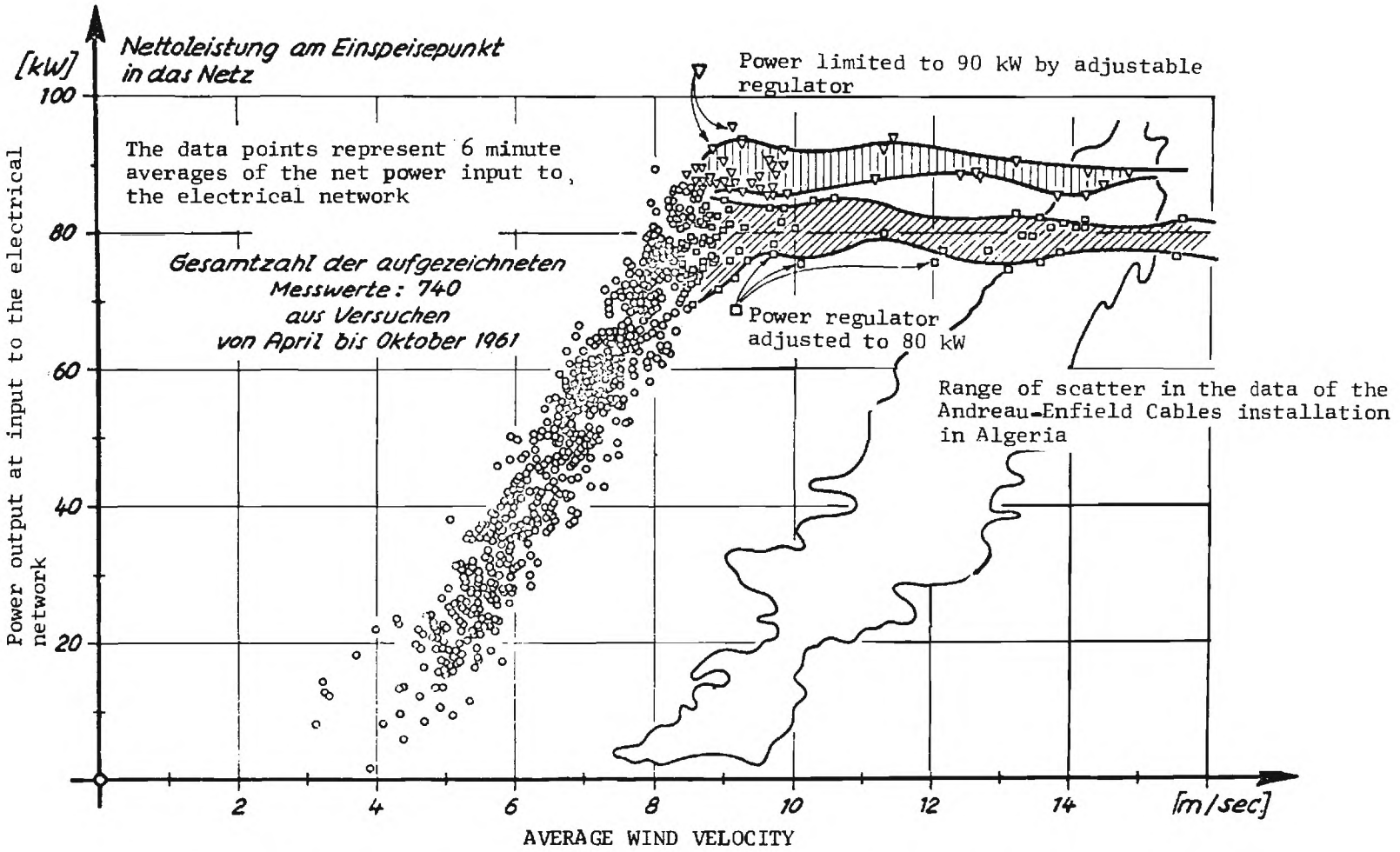

Figure 40 - The power output of the Hutter-Allgaier 100 kW wind-driven generator plant as a function of the average wind speed and a comparison with the performance of the 100 kW Andreau-Enfield-Cables wind generator.

Service wind speed forecast data (especially through techniques such as the Model Output Statistics method), and 2) development of an advective wind regime model - assuming a weather system and its associated winds are just advected with the mean wind (so that current measured data at upwind sites can be used to forecast future winds at sites downwind).

Only a few of these recommended studies will be carried out under the proposed follow up work to be sponsored by ERDA. Complete implementation of these recommendations must await further study efforts by the present investigators or by others.

REFERENCES

Ballester, M. (1961): "Speculative Methods in Wind Surveying", paper W7 at U.N. New Sources of Energy Conference, Rome, August, 1961, Conference Proceedings 1964, pp. 49-59.

Buell, C. E. (1960): "The Structure of Two-Point Wind Correlations in the Atmosphere", J. Geophys. Res., 65, 3353-3366.

Buell, C. E. (1972): "Correlation Functions for Wind and Geopotential on Isobaric Surfaces", J. Appl. Meteorol., 11, 51-59.

General Electric (1975): "Final Presentation - Wind Turbine Generator Study Contract NAS-319403", July 17.

Honeywell (1976): "The Application of Wind Power Systems to the Service Area of the Minnesota Power and Light Company", Quarterly Report No. 2, COO-2618-2, January.

Justus, C. G. and Amir Mikhail (1976): "Height Variations of Wind Speed and Wind Distributions Statistics", Geophy. Res. Letters, 3, 261-264.

Justus, C. G., W. R. Hargraves, and Ali Yalcin (1976): "Nationwide Assessment of Potential Output from Wind Powered Generators", J. Appl. Meteorol., 15, 673-678.

Kaman,(1975): "Wind Generator System Final Design Review", July 16.

Panchev, S. and M. Syrakova (1975): "Space-Time Statistical Macrostructure of the Geopotential Field at 500 mb", GARP Report No. 8 on Numerical Experimentation, pp. 19-21.

Seaman, R. S. and I. M. Draudins(1975): "Statistics on the Simultaneous Variation of Wind in Time and Space - Australian Region, 20,000 and 40,000 Ft", Australian Numerical Meteorology Research Centre, Tech. Rept. No. 1.

Wiesner, W. and A. Kisovec (1976): "Design Characteristics and Cost of an Advanced Technology Wind Turbine Generator for Minnesota Wind Spectra", Boeing Vertol Report D210-11051-2, March.

Zimmer, R. P., C. G. Justus, R. M. Mason, S. L. Robinette, P. G. Sassone, and W. A. Schaffer (1975): "Benefit-Cost Methodology Study with Example Application of the Use of Wind Generators", NASA CR-134864, July.

APPENDIX A

ANALYSIS METHODS

Wind Data

Wind speeds used in the study are the routinely measured (manual observation) one minute average wind speeds at National Weather Service airport locations. The one minute average winds are read once per hour, on the hour. Only every third observation is digitized onto tape at most sites, however. Thus the input data are one minute average wind speeds spaced once per three hours (8 observations per day). Time autocorrelation results (discussed in the main text) provide justification for the adequancy of this three hour spacing for resolving the significant diurnal variations. For purpose of most statistics, the sample interval of 8 per day can be considered a quasi-random sampling method which provides approximately 240 samples per month.

If wind speed values were not available or were outside reasonable limits for a particular time, values from the preceding and subsequent time were used in linear interpolation to fill in the missing or bad value. Two conservative missing or bad data were similarly filled in by interpolation, but if three or more consecutive missing or bad data were found at a particular site, that site was deleted from the analysis for the month in which the problem occured.

Wind speeds were measured at anemometer heights which varied from station to station and, in some cases, changed during the five year period of study at a given site. In order to put all of the wind data on a common basis which would be most applicable to the wind power study, winds were projected from anemometer height Z_a to a common hub height Z_h by the relation

$$V_h = V_a \, (Z_h/Z_a)^n \qquad \text{(A-1)}$$

where, from Justus and Mikhail (1976), the exponent n was considered to be variable with the measured wind speed V_a at the anemometer height, through the relationship

$$n = a + b \ln V_a \tag{A-2}$$

where the coefficients a and b are given by

$$a = 0.37/[1 - 0.0881 \ln (Z_a/10)] \tag{A-3}$$

$$b = -0.0881/[1 - 0.0881 \ln (Z_a/10)] . \tag{A-4}$$

For values of constants as given in equations (A-2) through (A-4) the speed V_a must be in m/s and the anemometer height Z_a must be in meters.

Wind Speed Statistics

Two types of statistics of the wind speed data were analyzed and presented in this report: time autocorrelation and spatial cross correlations. These statistics were evaluated after height correction to the common hub height, as described above. The time autocorrelation $f(\Delta t)$ of the wind speed deviations $v(t)$ from the monthly speed V_m (i.e. $v(t) = V(t) - V_m$) is given by

$$f(\Delta t) = \langle v(t)\, v(t + \Delta t)\rangle / \langle v^2 \rangle \tag{A-5}$$

where the angle brackets denote a time average over the monthly record. The spatial cross correlation $f(r)$ of the speed deviations from the monthly mean, is given by

$$f(r) = \langle v(\underset{\sim}{x}, t)\, v(\underset{\sim}{x} + \underset{\sim}{r}, t)\rangle / [\langle v^2(\underset{\sim}{x})\rangle \langle v^2(\underset{\sim}{x} + \underset{\sim}{r})\rangle]^{1/2} \tag{A-6}$$

where $v(\underset{\sim}{x}, t)$ is the wind speed departure from monthly mean at one site (location $\underset{\sim}{x}$), $v(\underset{\sim}{x} + \underset{\sim}{r}, t)$ is the wind speed departure from monthly mean at the other

site (distance between sites = r), and, again, angle brackets denote a time average over the month. Of course, a space-time correlation function (correlating $v(\underset{\sim}{x}, t)$ with $v(\underset{\sim}{x} + \underset{\sim}{r}, t + \Delta t)$) could have been studied, but this was considered beyond the scope of this initial year study. Note, therefore, that there is no time dependence (i.e. $\Delta t = 0$ only) in the spatial cross correlation A6, the time dependence in $v(\underset{\sim}{x}, t)$ being averaged out by the monthly average process.

Wind Turbine Power Output Statistics

Several preliminary designs for 500 kW to 1500 kW rated power wind turbine systems were used in the simulations for this study. Each wind turbine was assumed to have a power output curve similar to the one illustrated for the GE 500 kW wind turbine shown in Figure A-1. This curve is assumed to start at zero output power at the hub height cut-in speed V_0, increase to the rated power at the hub height rated speed V_1 then remain constant at rated power up to the hub height cut-out speed V_2 at which point the system is shut down for safety at high winds. For comparison with the actual power output curve, Figure A-1 shows the theoretically available power flux through the rotor swept area for the GE 500 kW wind turbine. This theoretically available power P_o as a function of wind speed V is given by

$$P_o = 0.5\ \rho\ V^3\ A \qquad \text{(A-7)}$$

where ρ is the air density (assumed to be 1.225 kg/m^3 in Figure A-1) and A is the rotor swept area ($\pi d^2/4$, where d is the rotor swept diameter). Table A-1 shows values of the cut-in speed, cut-out speed, rated speed, rotor swept diameter and hub height for each of the wind turbines used in the studies reported here. Although the Kaman 500 kW and the two Boeing units were designed for different hub heights, they were assumed in the study comparisons to be at a hub height of 42.7 m (140 ft), in order to put them at the same height as the GE and other Kaman units.

At a given time the one minute average wind speed V, adjusted to 42.7 m

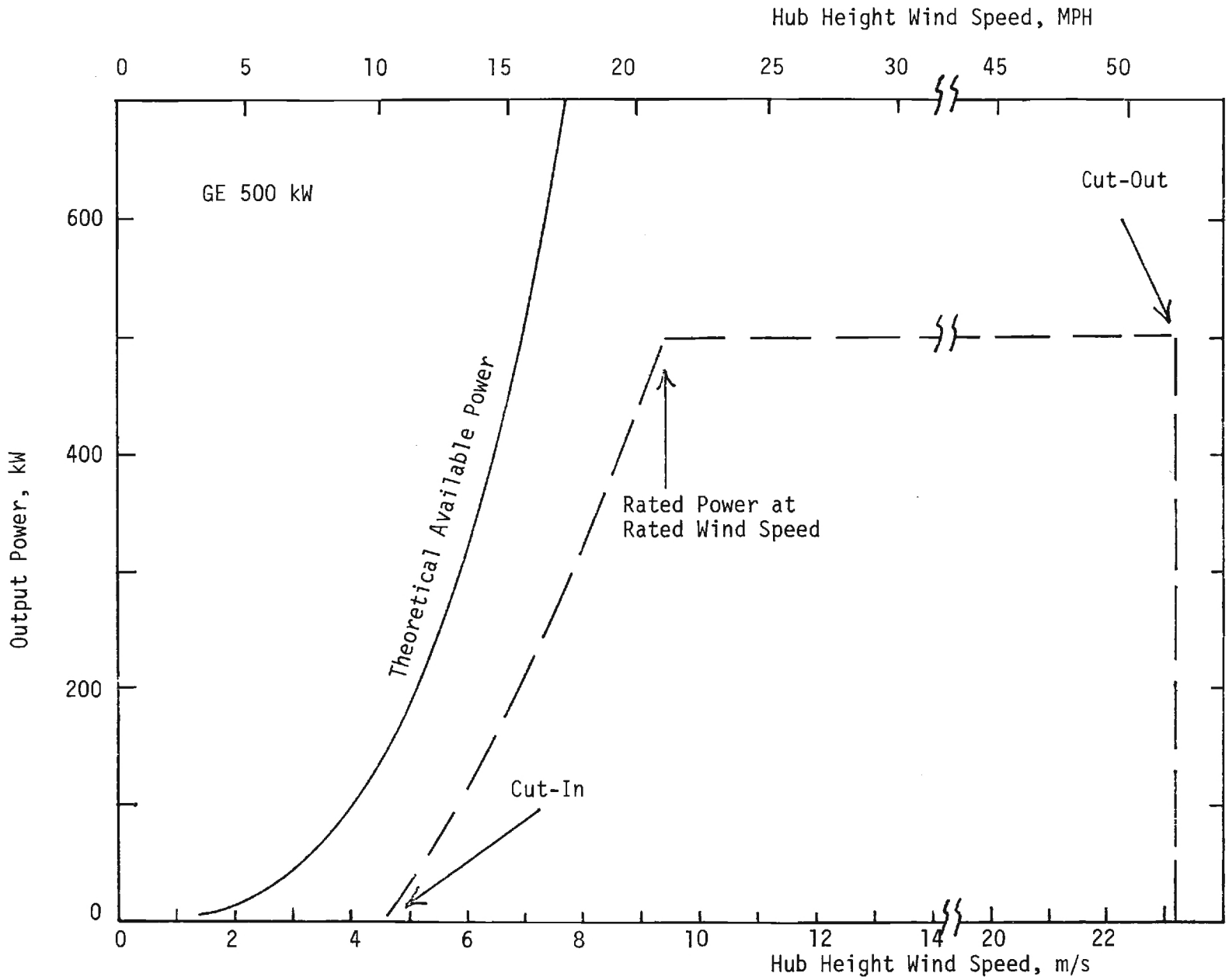

Figure A-1: Assumed Power Output Curve for the GE 500 kW Rated Power Wind Turbine.

(140 ft) hub height, is used as the argument of an analytical expression P(V) to determine output power for a given wind turbine. The analytical expression P(V) for the given generator is given by

$$P(V) = \begin{cases} 0 & V \leq V_o \\ A + BV + CV^2 & V_o < V \leq V_1 \\ P_r & V_1 < V \leq V_2 \\ 0 & V > V_2 \end{cases} \qquad \text{(A-8)}$$

where V_o is the hub height cut-in speed, V_1 is the hub height rated speed, V_2 is the hub height cut-out speed, P_r is the rated power and the coefficients A, B and C are determined by solution of the following set of simultaneous conditions

$$\begin{aligned} A + BV_o + CV_o^2 &= 0 \\ A + BV_1 + CV_1^2 &= P_r \\ A + BV_c + CV_c^2 &= P_r\,(V_c/V_1)^3 \end{aligned} \qquad \text{(A-9)}$$

where $V_c = (V_o + V_1)/2$. General solutions for A, B and C from (A-9) are given by Zimmer et al. (1975).

At a given time the array output $\bar{P}$ is computed by averaging over the set of National Weather Service sites assumed to make up the array.

$$\bar{P} = \sum_i P\,(V_i)/n \qquad \text{(A-10)}$$

where $P(V_i)$ is the analytical expression (A-8) evaluated at observed speed V_i (adjusted to hub height) at site i, and there are n sites in the array. This output per generator would be the same if one assumed n sites with one generator per site or, more realistically, assumed n sites with a "farm" of x generators at each site (x being the same at all sites).

Various statistics such as mean, standard deviation, probability distri-

TABLE A1

Characteristics of the Wind Turbines Used in the Site Array Analyses. Data Values Obtained for GE (1975), Kaman (1975), Wayne Wiesner, private communication (Boeing 1000 kW), and Wiesner and Kisovic (1976), (Boeing 1125 kW).

Company	GE	GE	Kaman	Kaman	Boeing	Boeing
Rated Power (kW)	500	1500	500	1500	1000	1125
Rated Wind Speed at 9 m (30 ft)						
(m/s)	7.3	10.1	9.2	11.2	7.1	7.6
(mph)	16.3	22.5	20.5	25.0	15.9	17.1
Rated Wind Speed at Hub Height						
(m/s)	9.4	13.1	11.7	14.6	10.3	10.4
(mph)	21.0	29.3	26.2	32.7	23.0	23.3
Cut-In Speed at 9 m (30 ft)						
(m/s)	3.5	5.1	4.0	5.4	3.4	3.1
(mph)	7.9	11.4	9.0	12.0	7.6	6.9
Cut-In Speed at Hub Height						
(m/s)	4.6	6.6	5.1	7.0	4.9	4.2
(mph)	10.3	14.8	11.4	15.7	11.0	9.4
Cut-Out Speed at 9 m (30 ft)						
(m/s)	17.9	22.3	13.4	20.1	9.3	19.7
(mph)	40.0	50.0	30.0	45.0	20.7	44.0
Cut-Out Speed at Hub Height						
(m/s)	23.2	28.8	17.1	26.1	13.4	26.8
(mph)	51.9	64.4	38.3	58.4	30.0	60.0
Rotor Swept Diam.						
(m)	55.8	57.9	45.7	54.9	80.8	80.8
(ft)	183	190	150	180	265	265
Tower Height						
(m)	42.7	42.7	38.1*	42.7	50.3*	57.0*
(ft)	140	140	125*	140	165*	187*

* Design tower height, 42.7 m (140 ft) used in these studies, for consistency.

bution, etc. are computed for the average individual site situation (all values of $P(V_i)$ for each site i for all times, i.e. about 240 n values per month) and for array average situation (values of $\bar{P}$ for all times, i.e. about 240 values per month). Such statistics as probability distributions are evaluated by direct counting of values of $P(V_i)$ or $\bar{P}$ within various intervals - no reliance is made on any assumed analytical wind speed distributions. Analyses were performed for each month of a five year time series, then results were reported as five year average by averaging corresponding monthly data over the five yearly sets of results.

Return Time Statistics

One important result of this study is the comparison of array power output statistics versus individual site power output statistics, to determine how much increase in output power reliability can be achieved (without storage) by going to dispersed arrays of wind turbines. In order to assess the additional reliability which could be achieved by storage, the array power output return times were evaluated for selected values of return power. The return time $t_R(P)$ for a given return power P is defined as the time required for the array power output to return above the level P after once going below that value. Return powers were expressed as power per generator. Thus, for an array of n generators, the array return power would be n times P. By evaluation of all return times over the duration of a month the monthly mean and probability distribution of return times were evaluated. The averaging was continued over corresponding months of the five year record to compute the overall average return times and the average return time probability distributions.

If a storage system is designed to provide P kW per array generator for t_S hours (i.e for n generators, the total storage in kW-hours is n Pt_S), and if an array power return time $t_R(P)$ is found to have, say, a 90% cumulative prob-

ability then 90% of the time when the array output power goes below nP the available kW hours of storage would not be exhausted before the array power returns above nP again (assuming the storage started fully charged with nPt_S kW hours). Thus a 90% cumulative probability for $t_R(P) = t_S$ means roughly that the storage time t_S will provide array power P per array generator with a reliability of 90%. For more accurate assessment of reliability achieved by various storage, a time series simulation of the storage status (i.e. amount of kW hours available) must be performed. This is because a long period of time when storage is required could begin with the storage already partially exhausted, instead of fully charged.

APPENDIX B

SOME ASPECTS OF STATISTICS OF ARRAYS OF WIND TURBINES

"Binomial" Wind Turbine Arrays

Consider, as a simple illustration, an array of, say 100, wind turbines with rated power of 1000 kW each. Suppose, for purpose of illustration, that these generators act in such a way as to produce zero power if the winds are below "cut-in" and to produce the full rated 1000 kW if the winds are above cut-in. Moreover, assume that the probability of winds being above cut-in is 50%. Hence each wind turbine is binomial in its output power probabilities (50% probability for "off", zero output; 50% probability for "on", 1000 kW output). Consider first the case in which all 100 of the wind turbines are located on the same "wind farm" (a relatively small area over which the winds can be considered completely 100% correlated), such that if one turbine is "on" then all turbines are "on". In this case the array power output probability is 50% for all wind turbines off, 50% for all wind turbines on. Expressed in terms of power output per generator, this case would produce 50% probability of 0 kW per generator and 50% probability for 1000 kW per generator. This situation would correspond to the cumulative probability curve A in Figure B-1.

Next consider the case of the same 100 wind turbines (each of which can still be either "on" or "off"), spread into an array, with 25 turbines each at four different locations. Consider the 25 wind turbines at a given "wind farm" to be 100% correlated with the other wind turbines at the same farm, but consider the separate wind farms to be entirely uncorrelated with each other. In this case, in accordance with the binomial distribution statistics

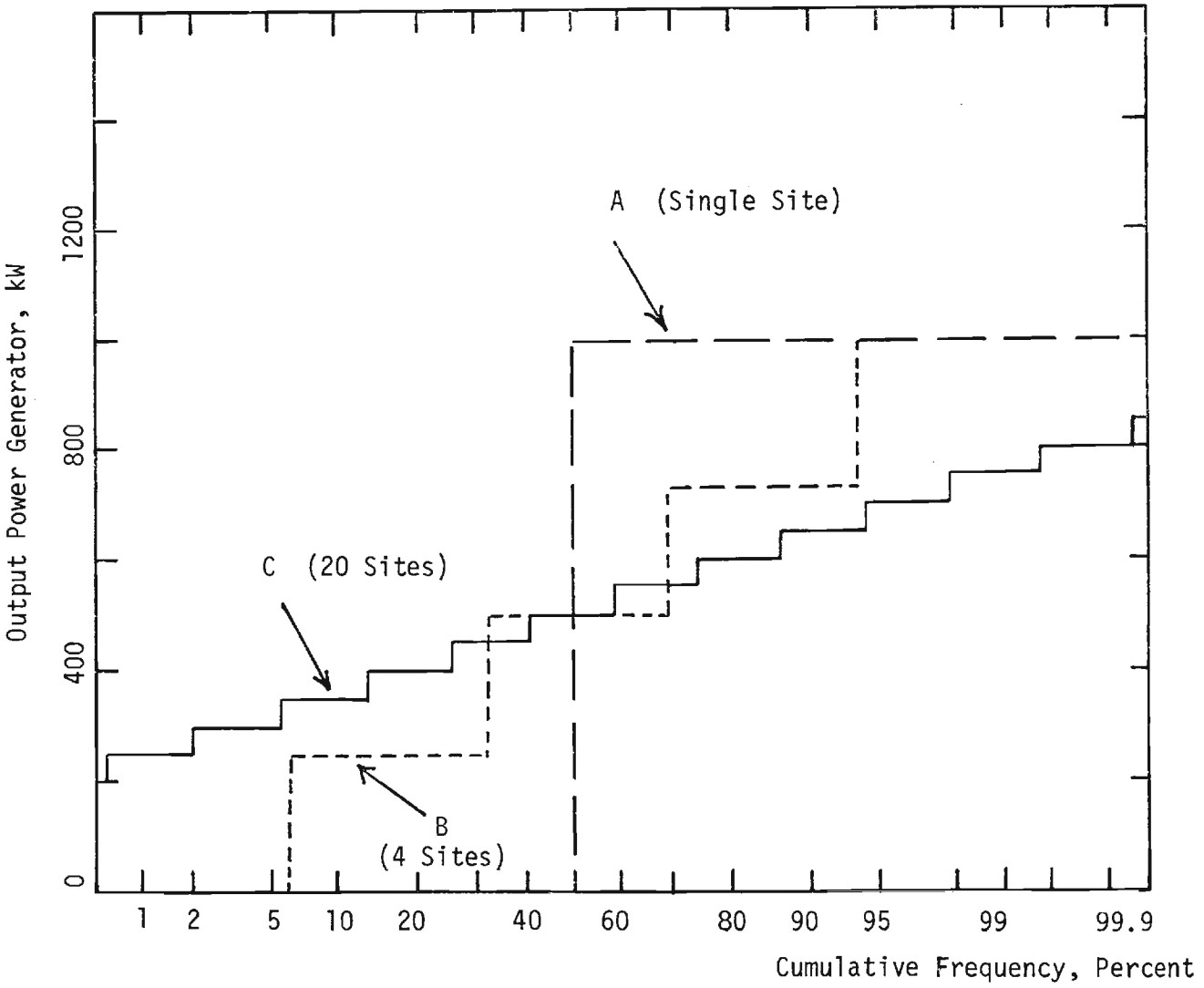

Figure B-1: Power Output Frequency Distribution for Hypothetical 1000 kW "Binomial" Wind Turbines (50% "on", and 50% "off"), at single Site and in 4 and 20 Site Uncorrelated Arrays.

for 50% success probability (e.g. the statistics of "heads" on independent coin tosses), the probability of none of the wind farms being on is $1/2^4$ = 1/16 = 6.25%; the probability for one wind farm (25 turbines) being on is $4/2^4$ = 1/4 = 25%; the probability for two farms (50 turbines) being on at the same time is 6/16 = 37.5%; the probability for three being on simultaneously (75 turbines in operation) is also 25%; and the probability of all four farms being on (all 100 turbines operating) is 1/16 = 6.25%. With only one farm (25 generators) out of the whole array (100 generators) operating, the array output per generator would be (1/4)(1000 kW) = 250 kW; with two farms in operation the array output per generator would be 500 kW; with three farms 750 kW per generator, and with all four farms operating the array output would be 1000 kW per generator. Thus the above probability would plot as the cumulative frequency curve B in Figure B-1. This curve comes from 6.25% cumulative probability for 0 kW per generator (no turbines in operation); 31.25% cumulative (= 6.25% + 25%) probability for 250 kW per generator (25 turbines, 1 farm, in operation); 68.75% cumulative (= 31.25% + 37.5%) for 500 kW per generator (50 turbines, 2 farms, in operation); 93.75% cumulative (= 68.75% + 25%) for 750 kW per generator (75 turbines, 3 farms, in operation); and, of course, 100% cumulative (= 93.75% + 6.25%) for 1000 kW per generator (all 100 turbines, all four farms, in operation).

Next consider the case of the same 100 wind turbines arranged in 20 "wind farms" with 5 turbines at each farm. Again assume all units at a given farm are 100% correlated, but no correlation between farms. Again, by application of the binomial statistics, the probability can be evaluated for having only one farm operate ($1/2^{20}$ probability), of having two farms operating, etc. From this process the cumulative probability distribution curve C in Figure B-1 is generated.

Note the general progression from curve A to curve C in Figure B-1. Curve A (single site, 100% correlated) is a step function with only one step. Curve B (four separate sites, uncorrelated with each other) is a step function (steps "rising" to the right) with four steps of steep slope (rapid "rise" of the steps). Curve C (20 separate sites, uncorrelated with each other) has many slowly rising steps, with considerably less slope. If the steps of Curve C were smoothed into a straight line, it would represent a Gaussian cumulative probability with a mean of 500 kW per generator and a standard deviation of about 100 kW. Notice that for these hypothetical "binomial" wind turbines, all of the various arrays have 50% cumulative probability at the arithmetic mean power output. This is because the binomial distribution is symmetric about its mean value (equally likely high values and low values).

"Gaussian" Wind Turbine Arrays

Next consider the somewhat more realistic case of wind turbines which have some probability of being off (zero output), some probability of being at full (rated) output, and have a Gaussian probability distribution for any power values between zero and rated power. The solid curve in Figure B-2 represents such a wind turbine. For the particular example of Figure B-2 an individual wind turbine (solid curve) has a 4.75% chance of zero output, a 4.75% chance of 1000 kW (full rated power) output, and a Gaussian distribution (mean = 500 kW, standard deviation 300 kW) of power output between 0 and 1000 kW. If, again, we consider a large "farm" of 100 such wind turbines all 100% correlated with each other, the same solid distribution curve of Figure B-2 would represent the array power output per generator.

If we consider, again, the 100 unit array spread into 4 uncorrelated "farms" of 25 units each, with each farm still 100% correlated, then to a good approximation the distribution of output power per generator would be a

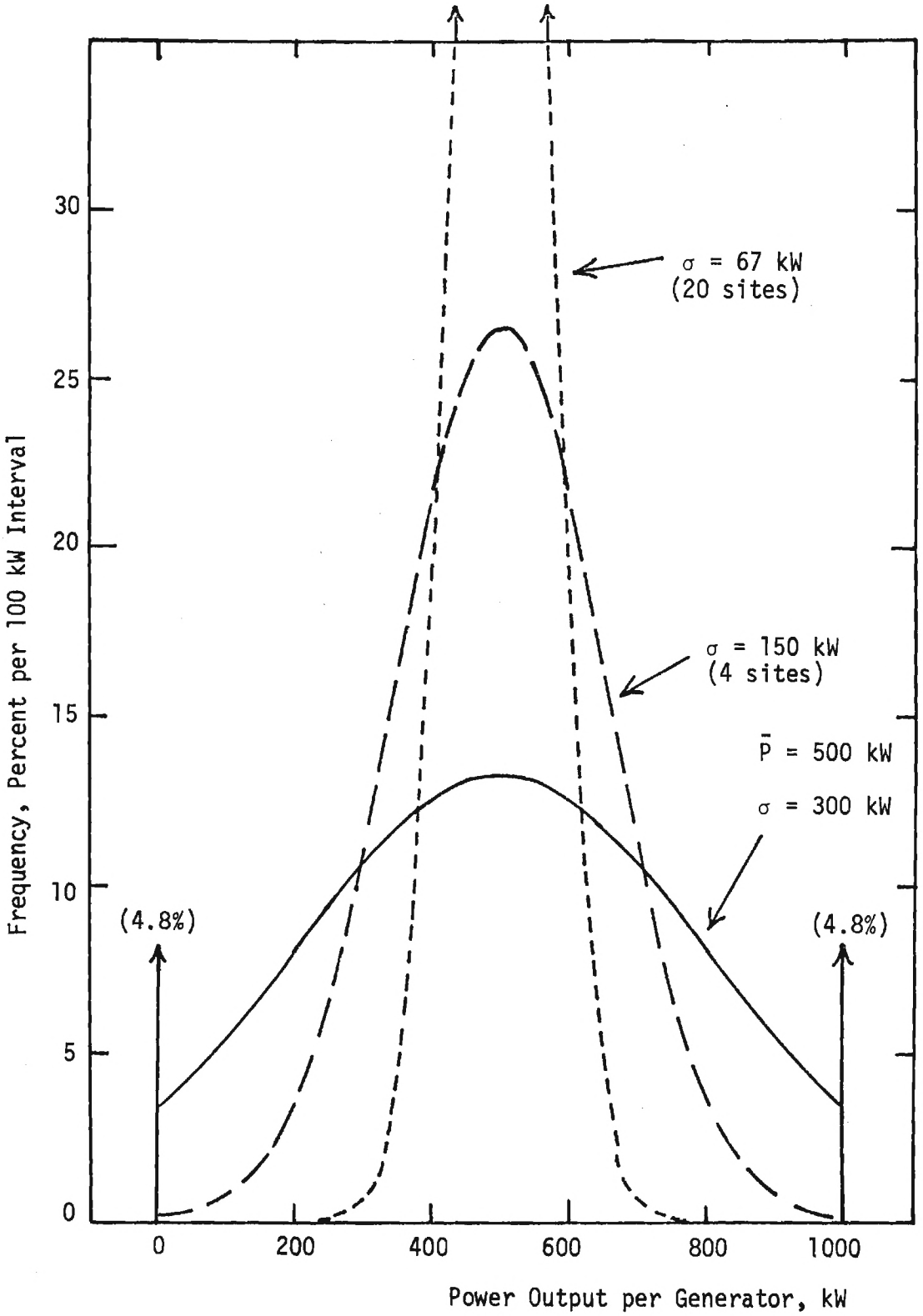

Figure B-2: Frequency Distribution of Arrays of 1000 kW "Gaussian" Wind Turbines at Single Site, and in 4 and 20 Uncorrelated Site Arrays.

Gaussian with mean 500 kW and a standard deviation of $300/\sqrt{4}$ = 150 kW, illustrated as the dashed curve in Figure B-2. The reason for this is found in the statistics of independent normal variates - namely, if X_i (i = 1 to n) is a set of normal random variates with corresponding means $\bar{X}_i$ and standard deviations σ_i. Then the variate

$$Y = \sum_{i=1}^{n} a_i X_i \qquad \text{(B-1)}$$

(where a_i is some weighting factor) is also a normal random variate. The mean value of Y is related to the means of the X_i's by

$$\bar{Y} = \sum_{i=1}^{n} a_i \bar{X}_i \qquad \text{(B-2)}$$

and the standard deviation of Y is related to the standard deviations of the X_i's by

$$\sigma_y^2 = \sum_{i=1}^{n} a_i^2 \sigma_i^2 \qquad \text{(B-3)}$$

Thus if X_i is power per generator for an array of m generators at each of n different sites and $a_i = 1/n$, then Y will be the array output per generator, and for n = 4, m = 25, $\bar{X}_i = 500$, $\sigma_i = 300$, the mean array power output per generator, $\bar{Y}$, would be

$$\bar{Y} = \sum_{i=1}^{4} \frac{500}{4} = 500$$

and the standard deviation in array power output per generator would be

$$\sigma_y = \left[\sum_{i=1}^{4} (300)^2/16\right]^{1/2} = 300/\sqrt{4} = 150$$

For general n, σ_y would just be $\sigma_y = \sigma_i/\sqrt{n}$.

For the "Gaussian" wind turbines considered here, the power output per

generator is not completely Gaussian, since the "tails" are truncated at 0 and rated power. However, these differences are minor and can reasonably be ignored. Thus for an array of n independent sites with m generators per site, each generator having mean power $\bar{P}$ and standard deviation σ, the array power per generator would have an average value also equal to $\bar{P}$ and a standard deviation of $\sigma_n = \sigma/\sqrt{n}$. If we generalized to n sites, each site with a different number of generators m_i (total number of generators $M = \Sigma\, m_i$), and each site having a different mean power per generator $\bar{P}_i$ and standard deviation σ_i, then the weighting factors in B-2 would be $a_i = m_i/(nM)$. Hence the mean array output power per generator would be

$$\bar{P} = \sum_{i=1}^{n} m_i P_i / M \qquad \text{(B-4)}$$

or, the mean total array output would be $\Sigma\, m_i P_i$, array power per generator times the total number of generators M, and the standard deviation of array power output per generator would be

$$\sigma_M = \left[\sum_{i=1}^{n} m_i^2\, \sigma_i^2 / M^2 \right]^{1/2} \qquad \text{(B-5)}$$

If we next consider the array of 100 wind turbines in an array of 20 uncorrelated sites with farms of 5 wind turbines at each site, the distribution of array output power per generator would be as illustrated by the dashed curve in Figure B-2. This is a Gaussian curve with a mean of 500 kW per generator and a standard deviation of $300/\sqrt{20} = 67$ kW. From Figure B-2 it is apparent that the larger the number of independent sites, the narrower the distribution of array output power, centered about the mean power which is the same for the array as for the individual wind turbines.

Figure B-3 shows the array power output distributions plotted as cumulative frequency. The solid curve (mean = 500 kW, σ = 300 kW) is for all

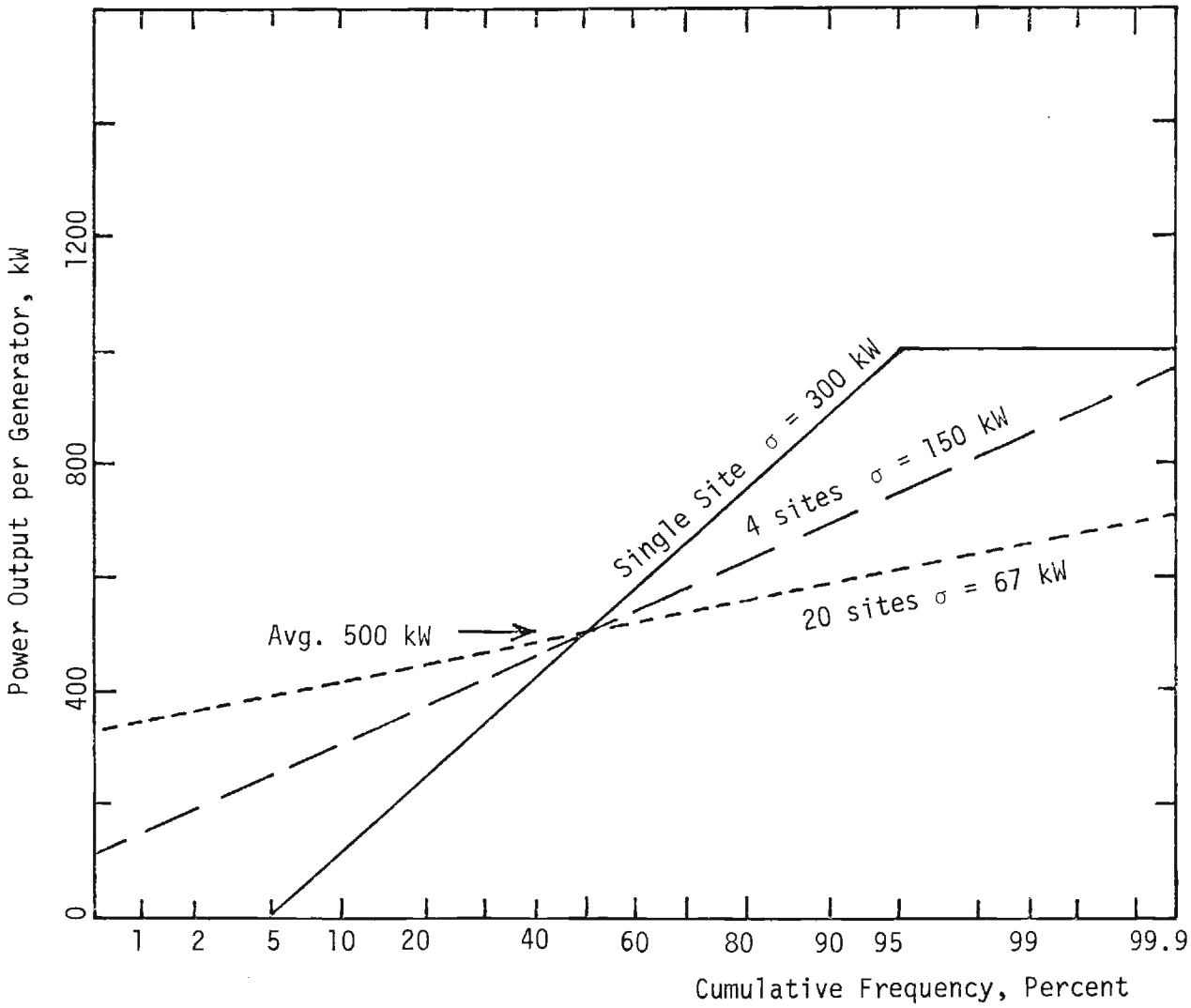

Figure B-3: As in Figure B-2 but Expressed as Cumulative Frequency Distribution.

100 units at one site. The dashed curve (mean = 500 kW, σ = 150 kW) is for farms of 25 units each at four uncorrelated sites. The dotted curve (mean = 500 kW, σ = 67 kW) is for farms of 5 each at 20 uncorrelated sites. Notice the similarity between Figure B-3 for the "Gaussian" wind turbines and Figure B-1 for the "Binomial" wind turbines, which were either on (1000 kW) or off (zero output). Notice that in Figure B-3 the mean power per generator of 500 kW occurs at the 50% point on all curves, because of the symmetry of the distributions in Figure B-2 about the mean.

Realistic Wind Turbines

Actual wind turbine output would be neither "Binomial" nor "Gaussian", but might look something like the solid curve in Figure B-4, which has a certain percentage occurrence of zero output (9%), a different frequency of rated (1000 kW) output (17%) and a skewed distribution of frequencies for power values between 0 and 1000 kW. The particular solid curve shown in Figure B-4 still has a mean of 500 kW per generator and a standard deviation (rms deviation from the mean) of 300 kW. Since the realistic generator individual unit power output is not too drastically different from Gaussian, the array power output can still be considered Gaussian, with mean and standard deviation as in equations (B-4) and (B-5). Frequency distributions of 4 uncorrelated sites with 25 units at each site (dashed curve) and 20 uncorrelated sites with 5 units at each site (dotted curve) are also illustrated in Figure B-4. Figure B-5 shows the corresponding cumulative frequency curves for these cases. Notice that the only difference between Figure B-5 and B-3, then, is the non-linear nature of the single site curve with a mean value which occurs at a cumulative frequency not equal to 50%, because of the skewed nature of the distribution about the mean (solid curve, Figure (B-4)).

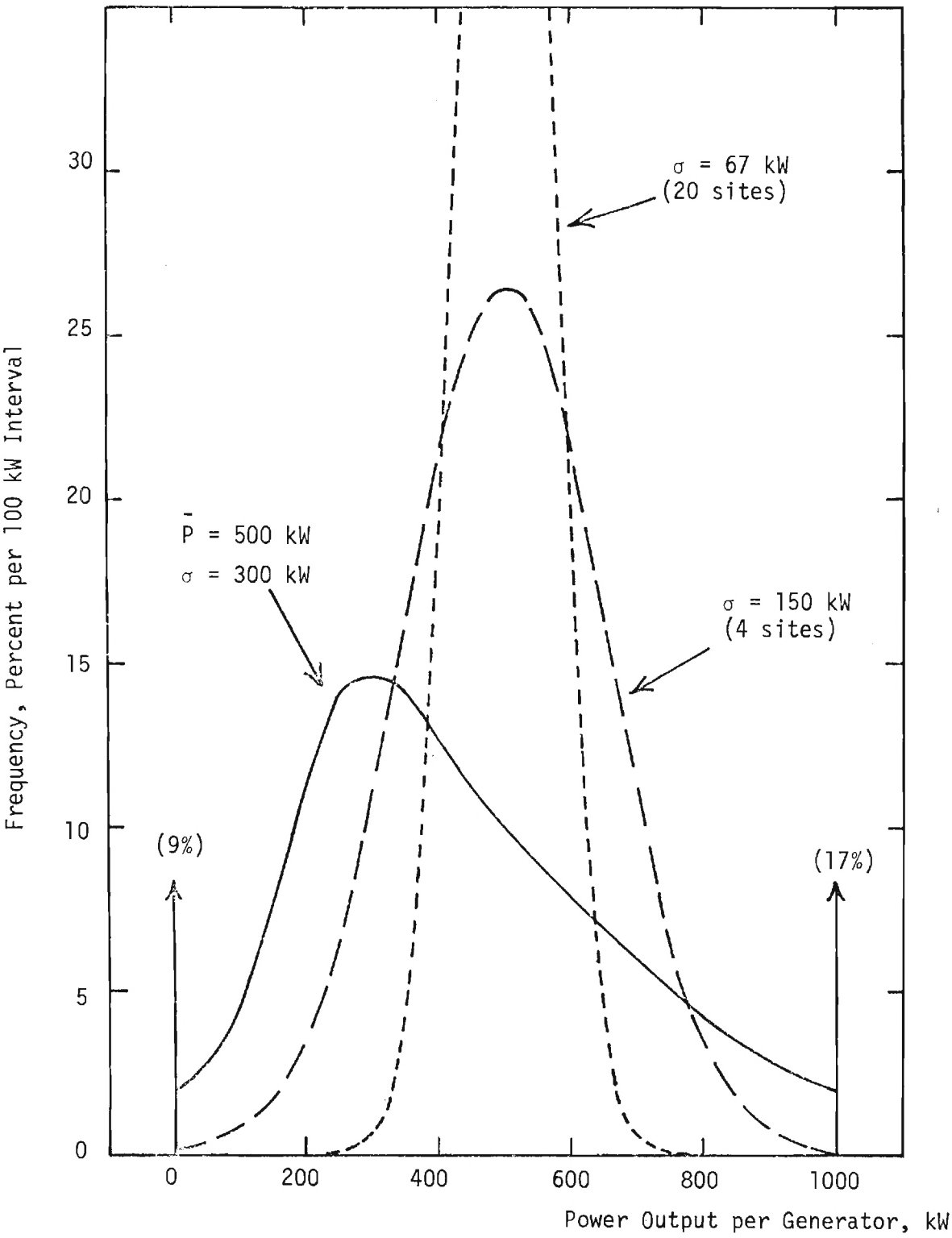

Figure B-4: Frequency Distribution of Arrays of Realistic 1000 kW Wind Turbines at Single Site, and in 4 and 20 Uncorrelated Site Arrays.

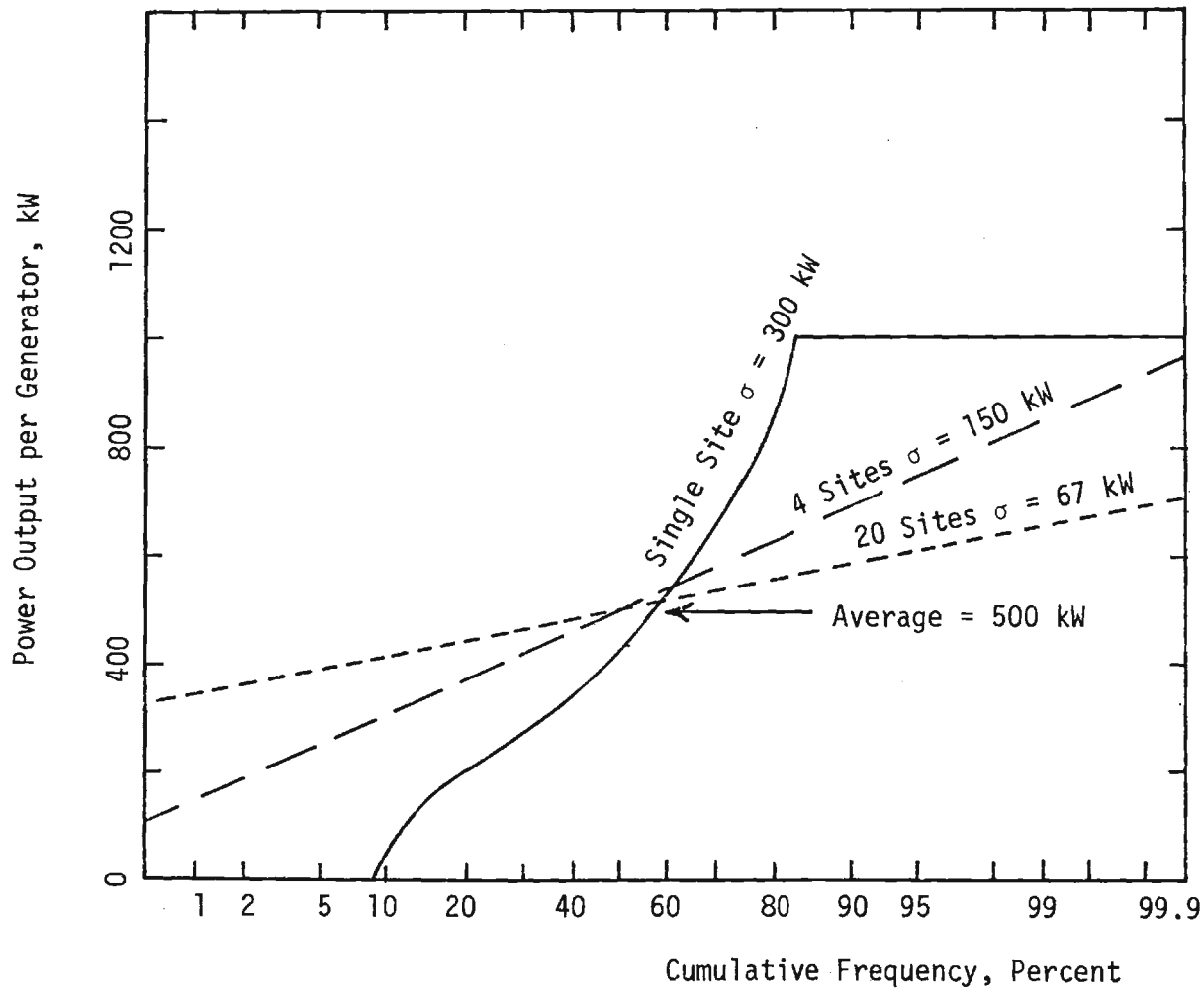

Figure B-5: As in Figure B-4 but Expressed as Cumulative Frequency Distribution.

Correlated Arrays

All of the above discussions are based on independent random variates (power output) for sites which are uncorrelated. In actual fact winds at sites separated by as much as several hundred kilometers are not uncorrelated. Therefore, the power outputs from separate array sites cannot be combined as independent variates. Instead, as discussed in the main body of the report, the correlated array power output distribution falls somewhere between that for the single site (100% correlation) and the array of uncorrelated (independent) sites.

In summary, the array averaging process does not increase the total energy production (array average power per generator is the same as average individual power per generator), but it does increase the reliability of power levels below that average. For example: Figure B-1 shows 250 kW per generator increased from 68% reliability (32% cumulative frequency) to 98% reliability (2% cumulative frequency) by going from four sites to 20 sites; Figure B-3 shows single site reliability for 250 kW per generator as 80% while for four site and 20 site arrays it has 95% and 99.99% reliability, respectively. While the array smooths out the lulls and makes powers somewhat below the average occur with higher probability, the array averaging also smooths out the peaks, and makes powers significantly higher than average also occur less frequently. This is due to the narrowing of the distributions (dashed and dotted curves in Figures B-2 and B-4) about the average power.